ISSN 1349-1121
JAXA-RM-11-010E

JAXA Research and Development Memorandum

Sonic Boom Data from D-SEND#1

Yusuke NAKA

February 2012

Japan Aerospace Exploration Agency

Contents

Sonic Boom Data from D-SEND#1*

Yusuke NAKA*1

ABSTRACT

JAXA conducted D-SEND#1 Test in May 2011, whose main objective was to demonstrate the low-sonic-boom aircraft design concept by measuring sonic booms created by two types of test bodies designed with and without the concept. D-SEND#1 was successful, and distinct sonic boom signatures from the differently shaped test bodies were captured as designed. The collected sonic boom data is reported in this study. The data were collected at several microphone locations: at multiple (three or four) altitudes up to about 1000 m above the ground, on the ground surface, and in a small house.

Keywords: supersonic flight, sonic boom, measurement, D-SEND#1

1. INTRODUCTION

As part of D-SEND (acronym for Drop test for Simplified Evaluation of Non-symmetrically Distributed sonic boom) Project, JAXA conducted D-SEND#1 [1] in May 2011 at Esrange Space Center in northern Sweden. The schema of D-SEND#1 is shown in Fig. 1-1. During the D-SEND#1 campaign period, drop tests were conducted twice in the same manner. In each test, two axisymmetric bodies having different cross-sectional distributions and lengths, but the same maximum diameter were lifted by a stratospheric balloon and released to start free-fall. During the drop, the descending speeds of the test bodies exceeded the speed of sound, producing sonic booms. The shapes of the two test bodies, named N-Wave Model (NWM) and Low-Boom Model (LBM), were designed so as to generate different shapes of overpressure time histories of sonic booms; NWM creates a traditional N-wave, while LBM produces a shaped, "low-boom" signature. The measured sonic boom data are reported in this paper.

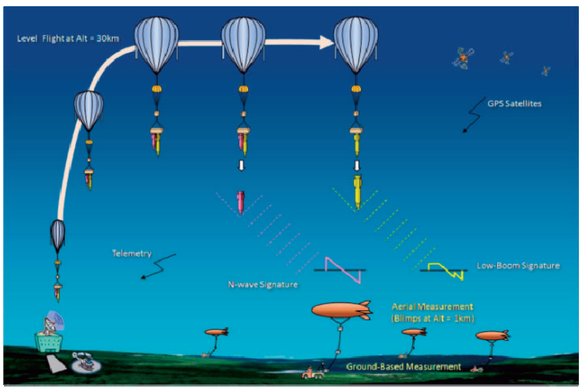

Fig. 1-1 Schema of D-SEND#1

* Received 12 December 2011

*1 D-SEND Project Team, Aviation Program Group

2. SONIC BOOM MEASUREMENT

2.1. Acoustic Measurement System

Similar specifications as in general sonic boom measurement with larger airplanes were required for the acoustic measurement system used in D-SEND#1. One of the most important specifications for sonic boom measurement system is the low-frequency response. The measurement system was designed so as to have the lower cut-off frequency of 0.2 Hz or lower.

In this regard, low-frequency microphones GRAS 40AZ-S1 and 40AZ-S2 were used for aerial and ground measurement, respectively. These microphones have the same specifications with the lower cut-off frequency of 0.09 Hz, but different shapes. 40AZ-S1 is straight in its form, while 40AZ-S2 has an L-shaped low-frequency adapter between the microphone capsule and the pre-amplifier. The latter is suitable for measurement on the ground surface with flush-mount setup.

As an AD converter, National Instruments NI 9234 was used. It has a lower limit of 0.5 Hz when AC coupling is selected. The AC coupling must be turned on to provide IEPE power to the microphones. In order to meet the low-frequency requirement, a filter to compensate the low-frequency response of the AD converter was used. This filter was applied in real time in the measurement software described below. Data were sampled with 51,200 Hz of rate and with 24-bit resolution.

A laptop PC was incorporated with the microphones and the AD converter to construct an acoustic measurement system. The system was controlled via in-house software developed by using NI LabVIEW and installed in the laptop PC. The measured data were stored also on the laptop PC.

Details of the whole measurement system, including the remote control and monitor functions, are beyond the scope of this report, and is planned to be described in a separate report.

2.2. Measurement Points

D-SEND#1 was conducted in the rocket impact area located north of Esrange Space Center. The impact area, in which the test bodies were allowed to be dropped, is similar to a diamond in its shape, roughly 70 km wide and 100 km long, as illustrated in Fig. 2-1.

Within the test range, four locations had been chosen as sonic boom measurement

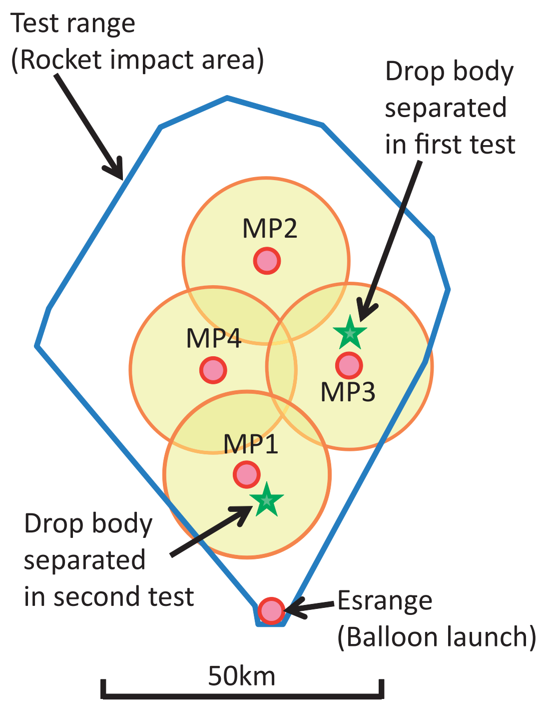

Fig. 2-1 Test range and sonic boom measurement points (MP's)

points (MP's). Since the trajectory of the balloon conveying the drop bodies depended significantly on the wind condition at the time of the test, and hence the capability of controlling it was limited, it was difficult to determine the location for separating the drop bodies from the balloon in the planning phase of the test, which was several months before the campaign. Therefore, we decided to prepare and make sonic boom measurements at multiple sites at the same time. The locations of the MP's (MP1 through MP4) were selected so that sonic booms reached at least one of the four MP's if the drop bodies were separated in the pre-determined area which covered the most of the test range. The separation area was the union of circles centered at each MP and radius of 15 km, indicated by the shaded area in Fig. 2-1. The radius of the circle was determined by the maximum distance at which the desired level of sonic boom waveforms were able to be measured.

2.3. Aerial Measurement

It is known that sonic boom waveforms are distorted by atmospheric turbulence in the planetary boundary layer [2], which is usually up to one to two kilometers from the ground surface. In order to reduce the distortion due to turbulence, aerial measurement was conducted in addition to ground measurement. For the aerial measurement, the microphones were raised up to about 1000 m above the ground by using a tethered blimp. Originally, four microphones were planned to be setup at three different altitudes at each MP: two at 1000 m, one each at 750 m and 500 m. At each measurement altitude, a standalone measurement system, i.e., a microphone, an AD converter, and a laptop PC, were located as shown in Fig. 2-2. These systems were controlled remotely from the ground (under the blimp) and in the control room located in Esrange.

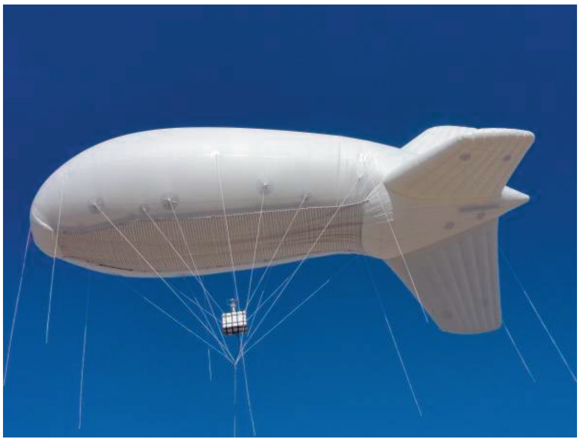

(a) System at 1000m alt.

(b) System at 750m alt.

Fig. 2-2 Aerial measurement system setup

2.4. Ground Measurement

At each MP, sonic booms were also measured on the ground surface. The microphones were installed with flush-mount setup on aluminum boards with 1 m sides. Sand was installed beneath the boards to reduce the vibration. In the original configuration, three microphones were distributed at each MP. The microphones were located about 3 to 5 m apart from each other. The typical setup is shown in Fig. 2-3.

2.5. Indoor Measurement

Indoor sonic boom measurement was conducted only at MP1, where a small house about 15-m wide by 8-m deep, shown in Fig. 2-4 (a), was available. Three microphones were installed inside a room as shown in Fig. 2-4 (b).

Fig. 2-3 Ground microphone setup

2.6. Microphone Configuration

2.6.1. First Drop Test

In the first drop test, the sonic boom measurement systems (microphones) were distributed as the default setting. Four aerial and three ground microphones were installed at all of the four MP's. At MP1, additional microphones were setup for indoor measurement as described in Sec 2.5.

(a) External view

(b) Microphone setup

Fig. 2-4 Indoor measurement setup

2.6.2. Second Drop Test

In the second drop test, acoustic measurement devices were distributed unevenly among the three of the four measurement sites, namely MP1, MP2, and MP4. The microphones originally planned to be used at MP3 was distributed to MP1 and MP4. Since the trajectory of the stratospheric balloon predicted a few days before the test passed close to MP1, seven out of eight microphones originally assigned to MP3 were moved to MP1. One of the seven additional microphones were used in the aerial measurement at 250 m of altitude, and the rest were setup in the ground measurement. The other microphone (one out of eight) was installed at 250 m above the ground at MP4.

In addition, some of the microphones assigned to MP2 were moved to MP1 and Esrange Space Center during the preparation on the test day, although this had not been planned beforehand. A blimp problem occurred while preparing the measurement system at MP2, and the aerial measurement became infeasible. Therefore, two of the four microphones initially prepared for the aerial measurement at MP2 were used at MP1, and the remaining two were setup at Esrange, where a chance of sonic boom arrival had been predicted from the propagation analysis right before the test. The result of such rearrangement of microphones is summarized in Table 2-1. Please note that indoor measurement was also conducted at MP1, where a suitable small house was located.

3. MEASUERED SONIC BOOM DATA

In D-SEND#1, each microphone located at the MP where sonic booms reached collected a multiple number of sonic boom signatures. This is due to the change of the speeds of the test bodies with time, which affects the direction and path of the sonic boom propagation as schematically shown in Fig. 3-1. Typically, sonic booms produced at two different altitudes arrived at each of the microphones. In addition, direct and ground-reflected booms were captured in the aerial measurement microphones. As a result, 34 waveforms (22 aerial and 12 ground) were collected in the first drop test, and 96 (40 aerial, 44 ground, and 12 indoor) in the second test.

Among the sonic boom waveforms generated at different altitudes and propagated along different paths, the pressure time histories of the direct waves generated at lower altitude are the signatures to be used for validating the low-boom design concept.

3.1. First Drop Test (MP3)

In the first drop test, sonic booms generated from the drop bodies reached MP3. No sonic boom signatures were measured at the other MP's.

Table 2-1 Microphone arrangement in second drop test

	Aerial	Ground	Indoor
MP1	5	10	3
MP2	0	3	0
MP3	0	0	0
MP4	5	3	0
Esrange	0	2	0

All the waveforms recorded at all of the microphone altitudes at MP3 are shown in Fig. 3-2. As explained above, each microphone captured multiple sonic boom signatures. Indicated by the broken lines in Fig. 3-2 are the traces of the booms generated at two different altitudes. Note that since the sonic booms propagated with certain oblique angles with respect to the aerial microphone alignment, waveforms on the same broken line in Fig. 3-2 propagated on different (but almost parallel) paths.

As seen in Fig. 3-2, The two drop bodies were separated from the balloon with a 10-second interval. LBM was released first, followed by NWM.

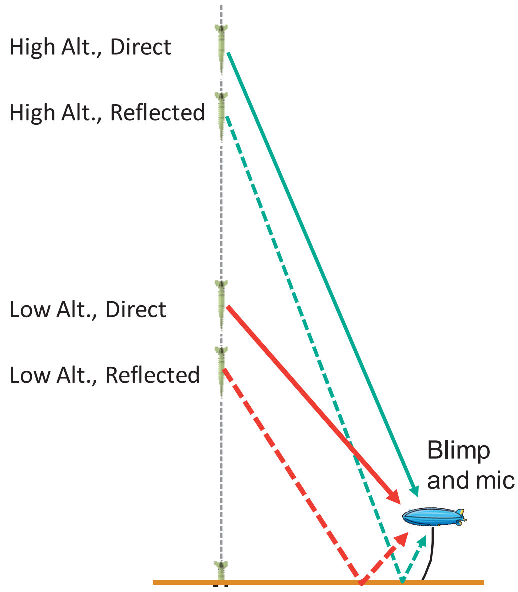

Fig. 3-1 Multiple paths to a microphone

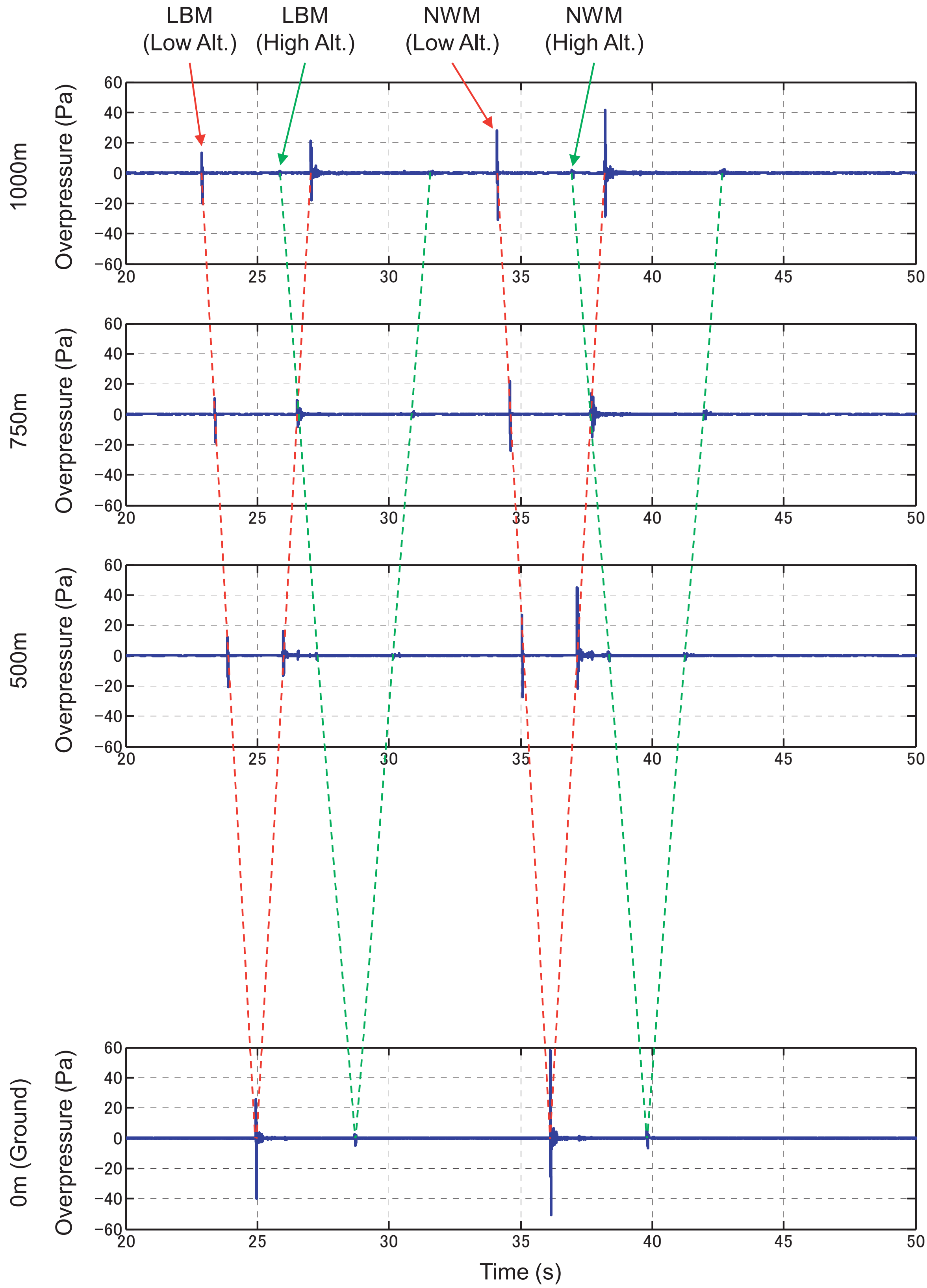

Fig. 3-2 Waveforms measured at MP3 in the first drop test

3.1.1. Aerial Measurement

At MP3 in the first drop test, aerial measurement was successful at all of the measurement altitudes (1000, 750, and 500 m), although one of the two microphones installed at 1000 m did not work at the time of sonic boom arrival and measurement failed.

Fig. 3-3 shows the signatures generated at low altitude and directly reached at the microphones and measured by the aerial microphones. At all altitudes, waveforms from two drop bodies have significant discrepancy. NWM created an N-wave, while LBM produced a flat-top low-boom signature as designed. The low-boom signature has about a half of the maximum overpressure in the front shock, and the magnitude of the rear shock was also reduced by distributing a small shock about 10 ms before the rear shock. This observation strongly supports the validity of demonstrating low-boom design concept by using a scaled model, such as the silent supersonic concept model (S3CM) that will be used in D-SEND#2.

By comparing the data measured on the ground, which are shown in Sec 3.1.2, aerial data have “clean” waveforms with less effects of turbulence. The only major distortions are found in the waveforms recorded at 1000 m of altitude. There are “bumps” about 10 ms after the front and rear shocks. It is inferred that these are observed as a result of the interaction of the booms with the blimp, as the microphone was installed about 10 m below the blimp whose dimensions are about 5 m in diameter and about 15 m in length. However, such distortion was not clearly observed in ABBA Test#1 with almost the same microphone and blimp configuration[3]. Therefore, it is suspected that slight differences in relative positions of the microphone and blimp with respect to the

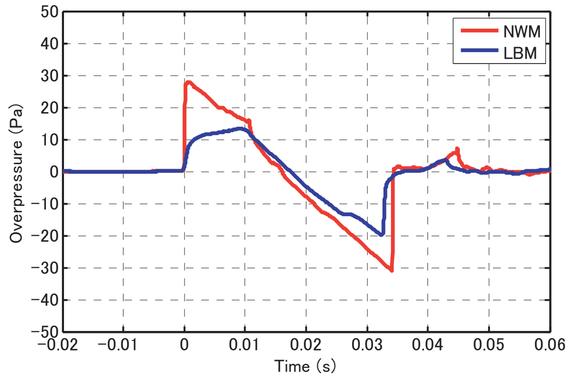

(a) 1000 m

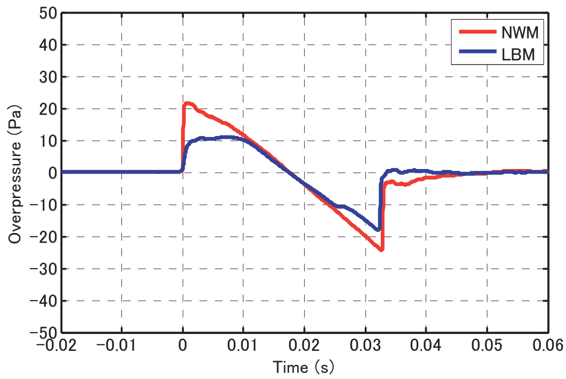

(b) 750 m

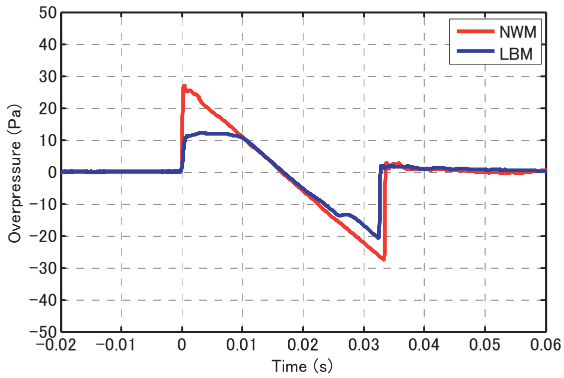

(c) 500 m

Fig. 3-3 NWM and LBM aerial data in first drop test direction of the sonic boom propagation might be influential. Detailed cause and mechanism of the distortion are currently under investigation.

All of the measured aerial signatures in the first drop test are shown in Fig. 3-4 through Fig. 3-9. In each panel of these figures, the left figure shows the overall waveform including the pressure disturbance after the main sonic boom signature, and the right one shows the zoomed view. Abscissa axes are time relative to the start of the signature, defined as the time when the overpressure reaches 10 % of the maximum value. However, in some signatures, especially ones generated at high altitude or ones reflected at the ground, the relative time of zero does not necessarily correspond to the start time of the signature, because of the slow growth of the overpressure right before the main boom signature.

At 750 m, the reflected waves generated at the lower altitude and the direct waves coming from the higher altitude reach the microphone almost at the same time as seen in Fig. 3-2. Therefore, the recorded waveforms (panels (b) and (c) in Fig. 3-6 and Fig. 3-7) are superposition of the two signatures.

Other than the direct waves from the lower altitudes, the waveforms significantly differ from N-shape and flat-top signatures. Also found is the considerable level of pressure fluctuation after the main boom signature in the reflected data. Such fluctuation could be related to the so-called “post-boom noise” observed in the ground measurement data [4].

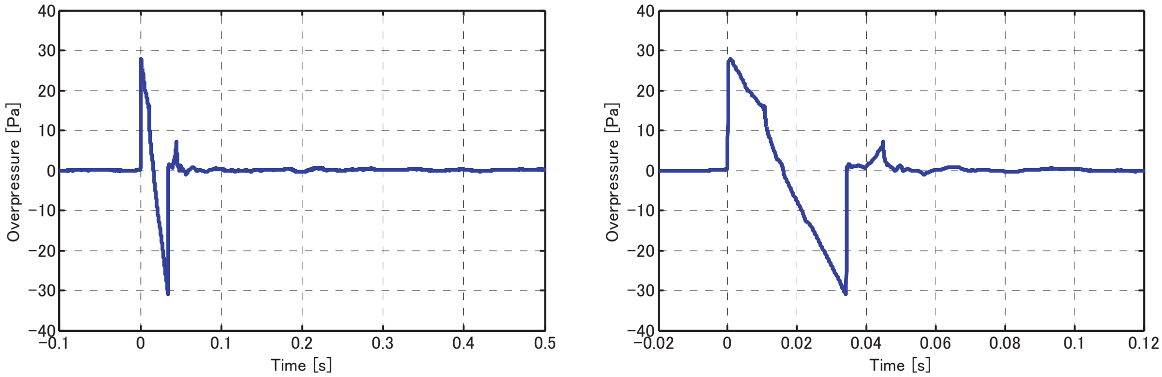

(a) Low Altitude, Direct

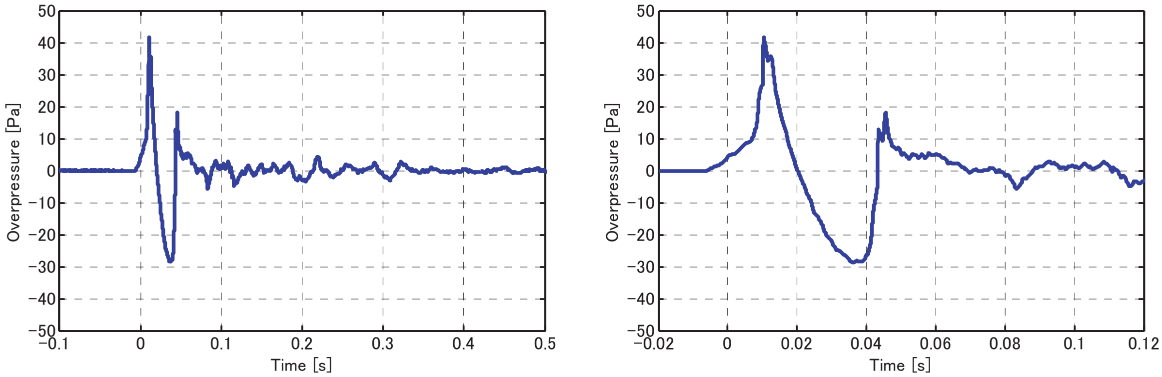

(b) Low Altitude, Reflected

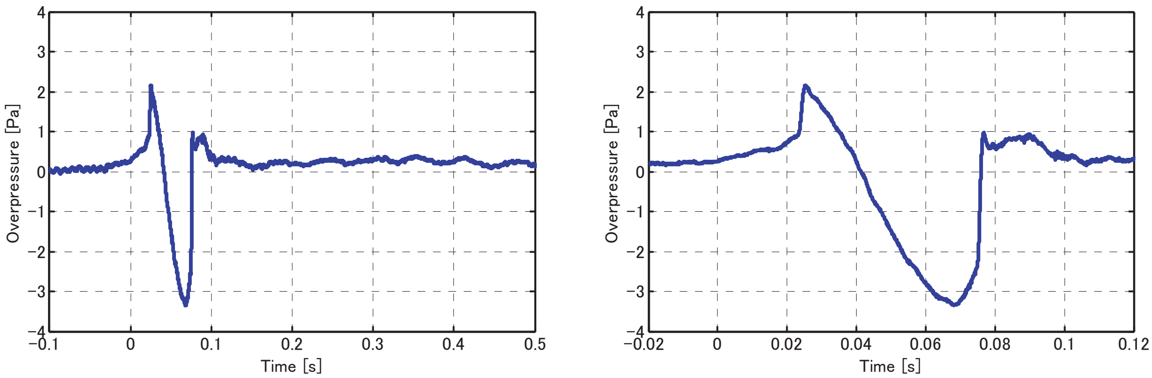

(c) High Altitude, Direct

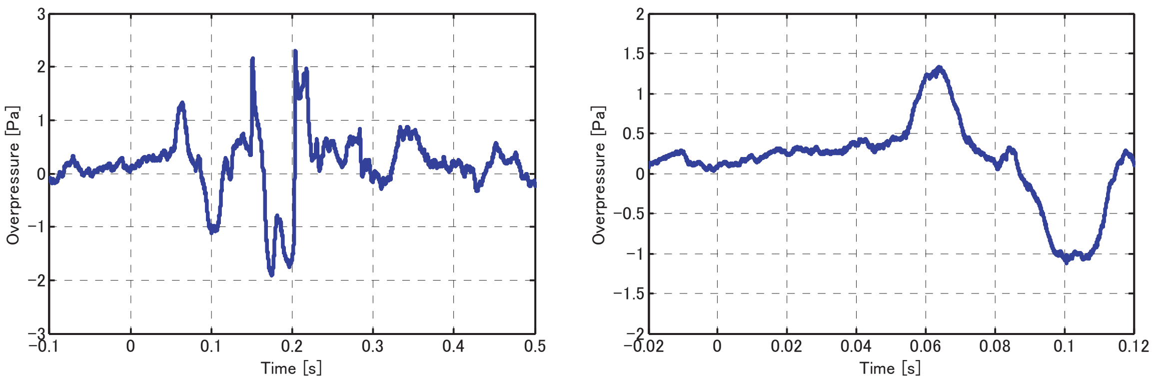

(d) High Altitude, Reflected

Fig. 3-4 Sonic booms in first drop test (MP3, Aerial 1000m Ch1, NWM)

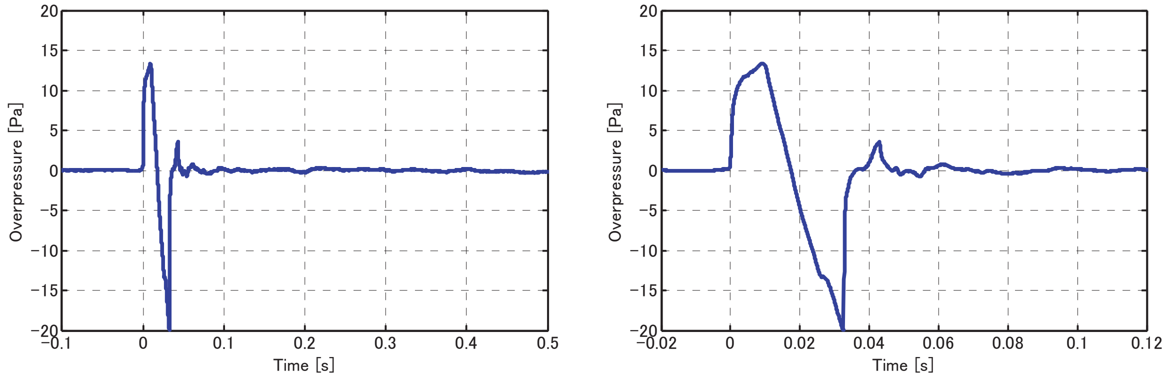

(a) Low Altitude, Direct

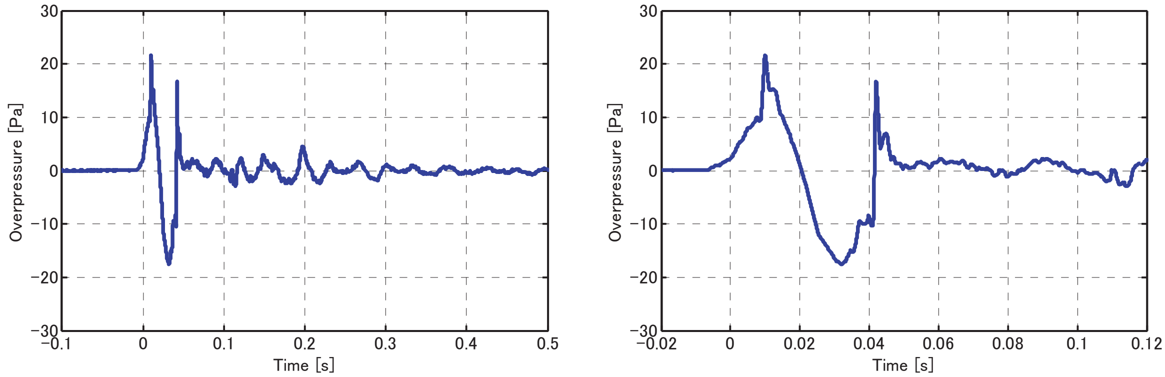

(b) Low Altitude, Reflected

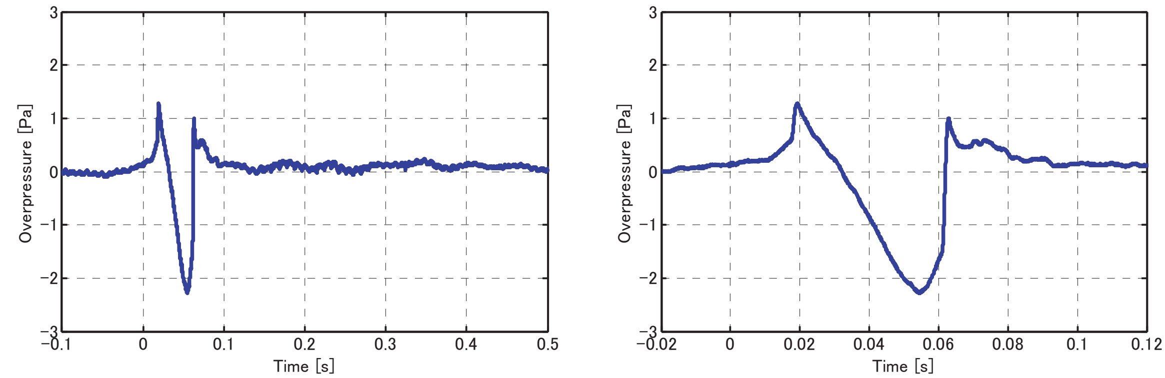

(c) High Altitude, Direct

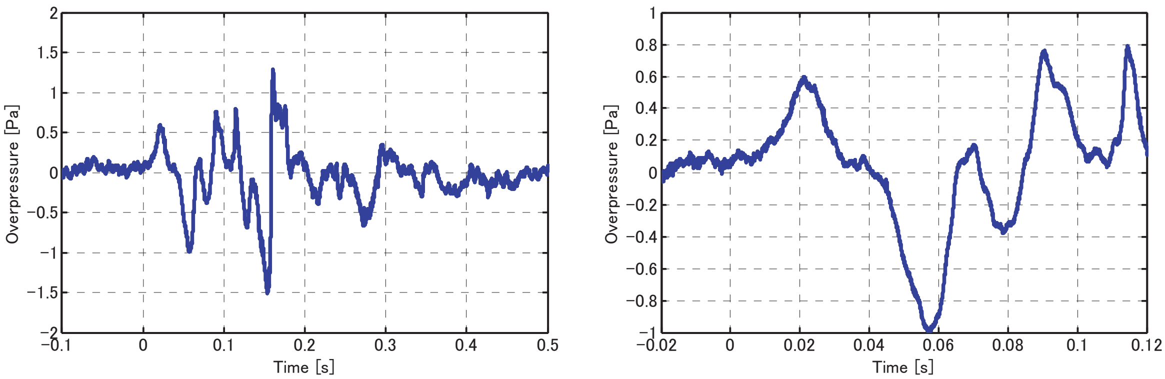

(d) High Altitude, Reflected

Fig. 3-5 Sonic booms in first drop test (MP3, Aerial 1000m Ch1, LBM)

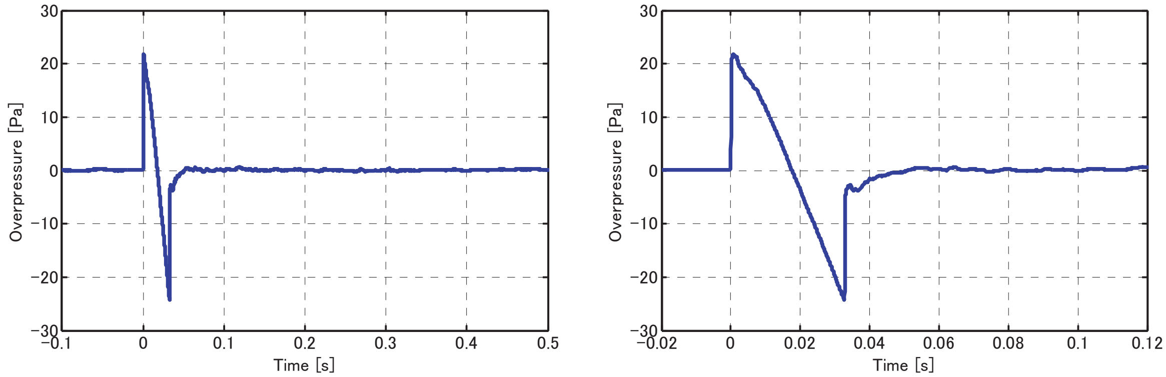

(a) Low Altitude, Direct

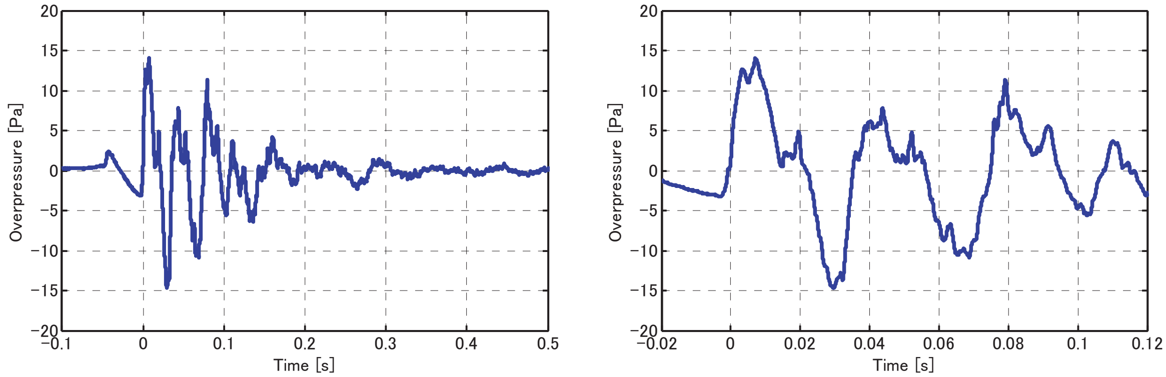

(b) Low Altitude, Reflected and (c) High Altitude, Direct

(Two waveforms are overlapped.)

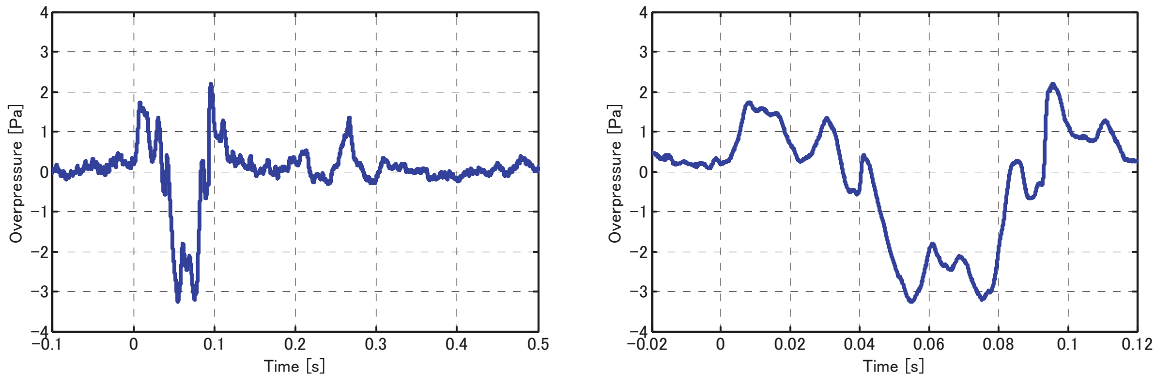

(d) High Altitude, Reflected

Fig. 3-6 Sonic booms in first drop test (MP3, Aerial 750m Ch1, NWM)

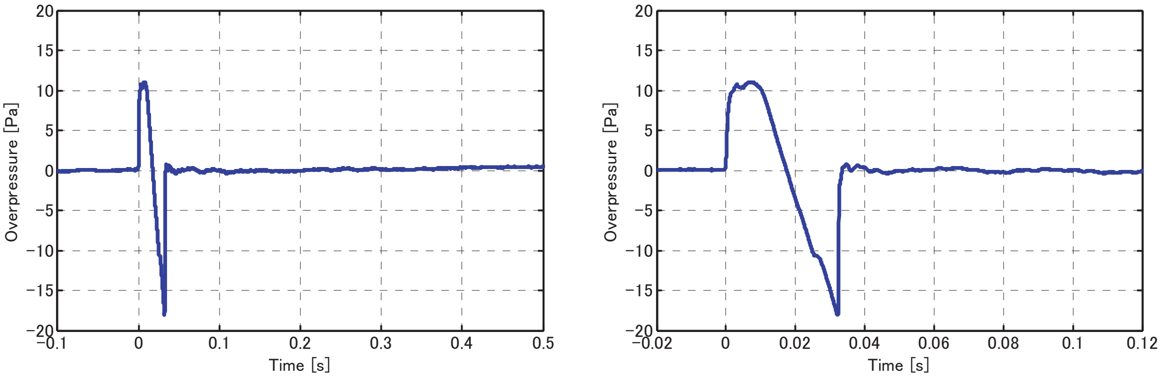

(a) Low Altitude, Direct

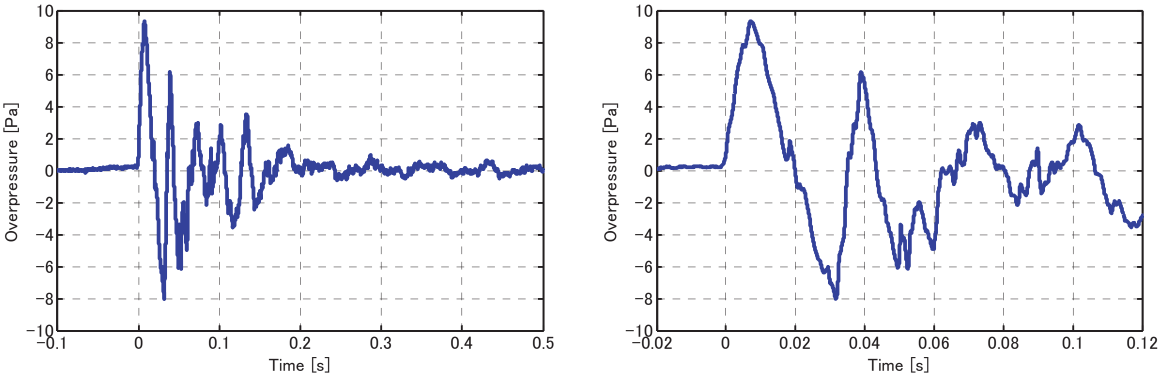

(b) Low Altitude, Reflected and (c) High Altitude, Direct

(Two waveforms are overlapped.)

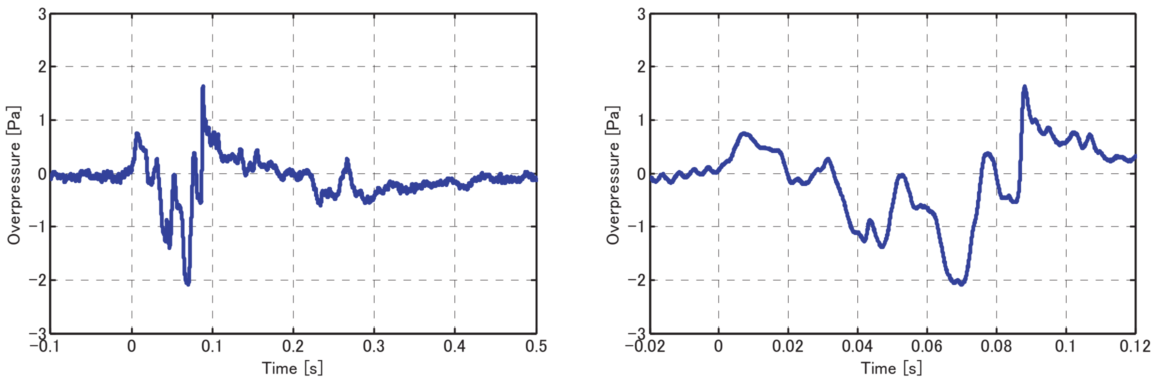

(d) High Altitude, Reflected

Fig. 3-7 Sonic booms in first drop test (MP3, Aerial 750m Ch1, LBM)

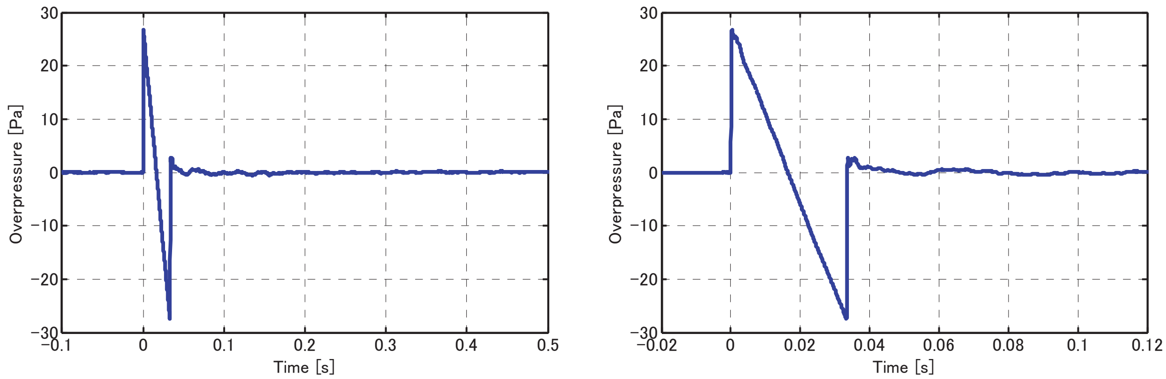

(a) Low Altitude, Direct

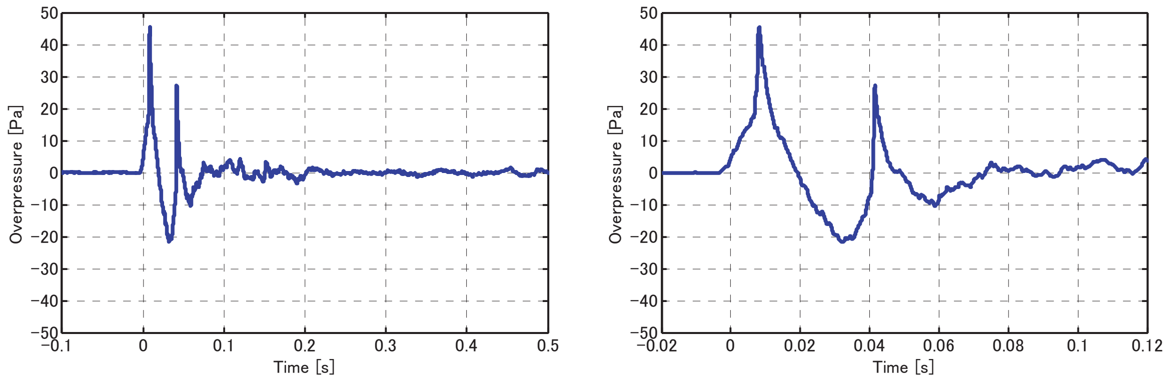

(b) Low Altitude, Reflected

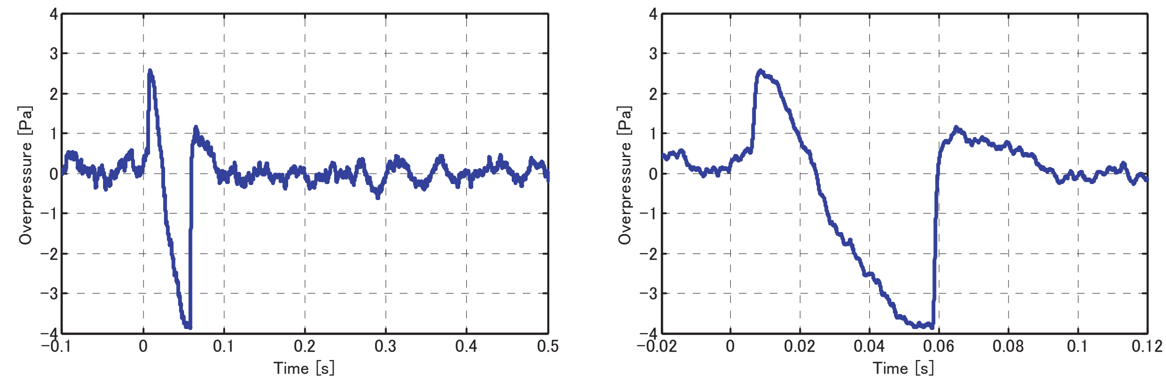

(c) High Altitude, Direct

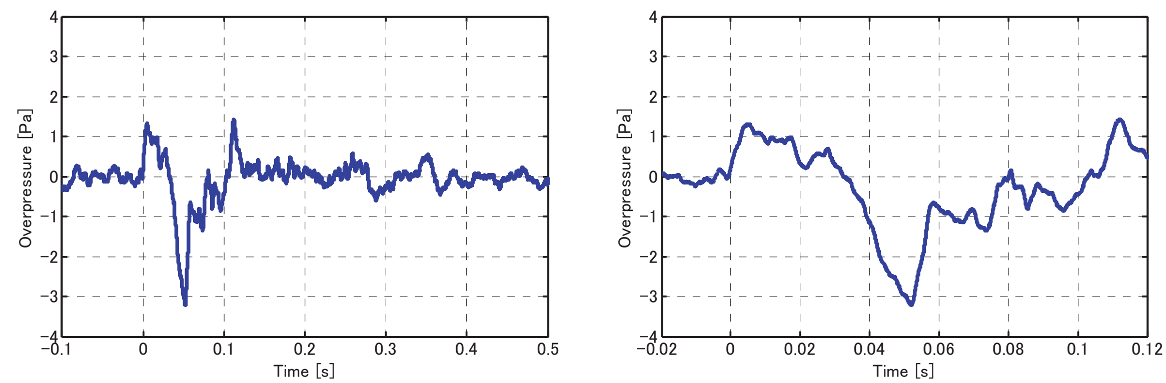

(d) High Altitude, Reflected

Fig. 3-8 Sonic booms in first drop test (MP3, Aerial 500m Ch1, NWM)

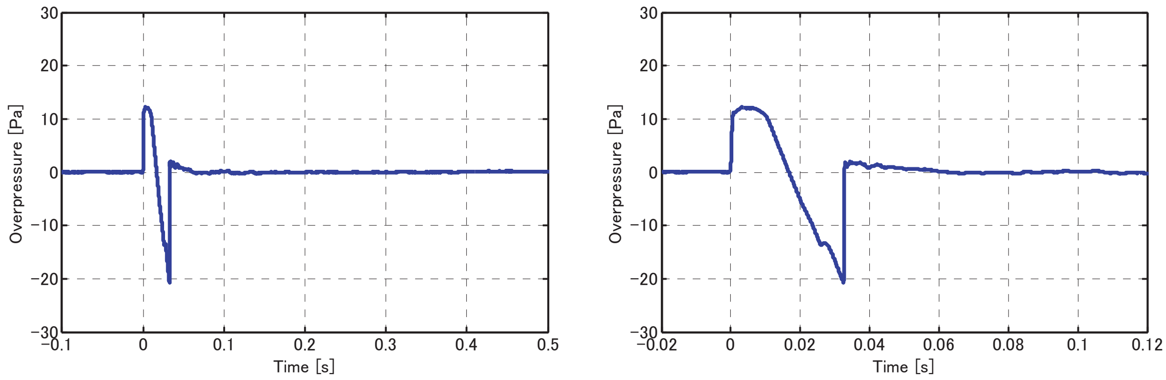

(a) Low Altitude, Direct

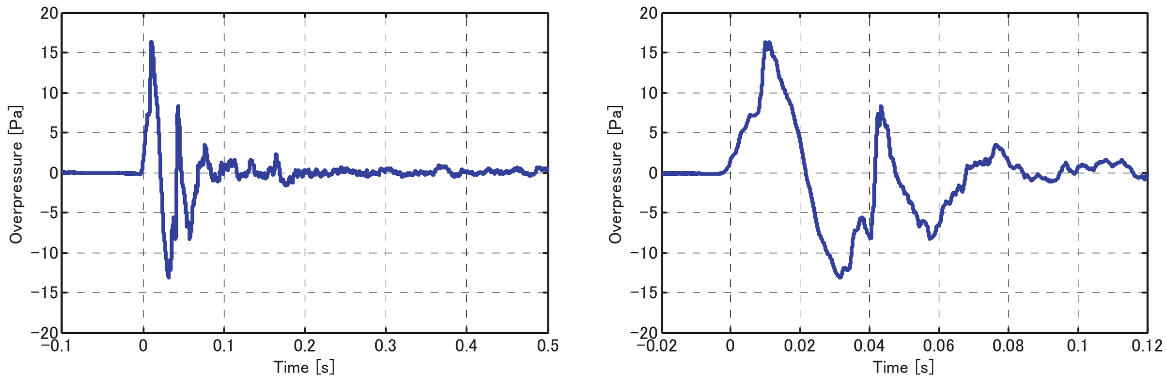

(b) Low Altitude, Reflected

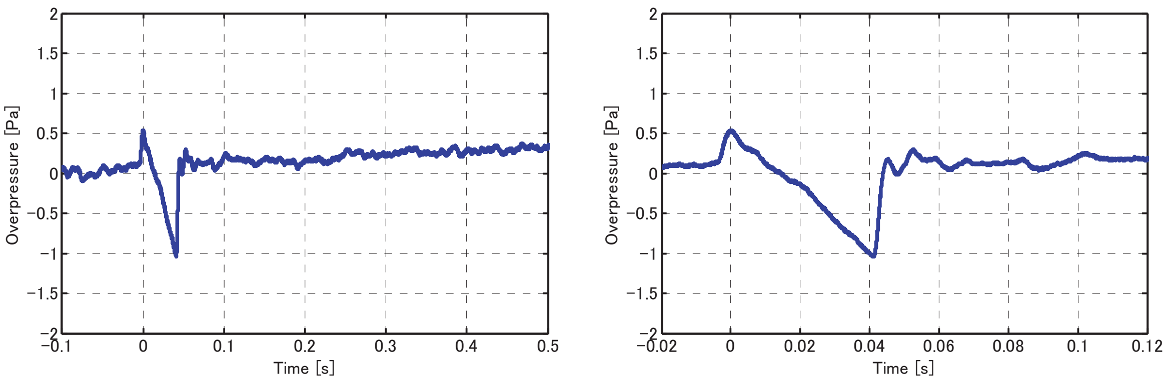

(c) High Altitude, Direct

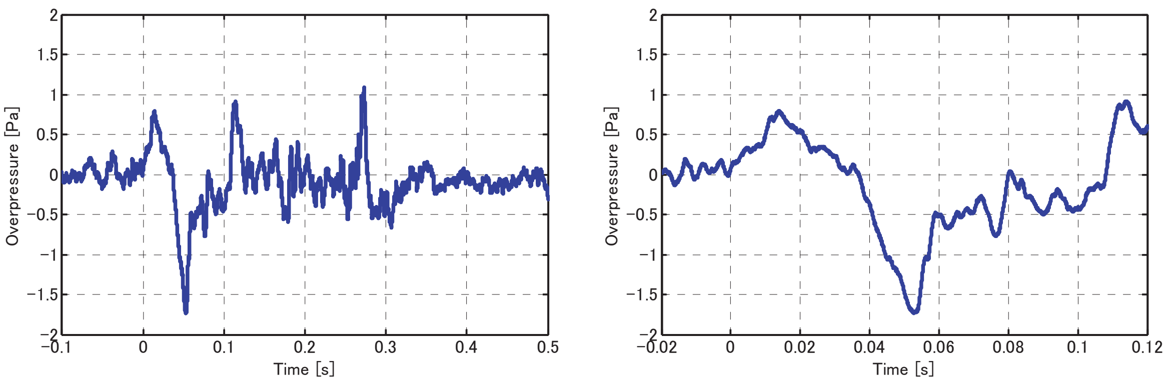

(d) High Altitude, Reflected

Fig. 3-9 Sonic booms in first drop test (MP3, Aerial 500m Ch1, LBM)

3.1.2. Ground Measurement

Ground measurement at MP3 in the first drop test was successful for all of the three microphone channels. Recorded sonic boom signatures produced at the designed flight condition (at the lower altitude) are shown in Fig. 3-10. Compared to the aerial data in the previous subsection, the waveforms are distorted due to turbulence and also possibly to interaction with the ground surface and objects on the ground, such as diffraction and scattering. The manner of distortion differs among channels, in spite of the fact that the microphones were located only about 5 m apart from each other. The N-wave in Ch 2 has sharp peaks at the end of both of the front and rear shocks, while that in Ch 3 has rounded waveforms.

Despite the distortion, the N-shape and low-boom signatures are still clearly recognizable.

All the direct and reflected sonic boom waveforms produced at the two different altitudes and recorded on the ground surface at MP3 are shown in Fig. 3-11 through Fig. 3-16. In these figures, post-boom noises are observed in all data. Since no engine was mounted on the drop bodies, the hypothesis that the main cause of post-boom noise is the engine noise is declined. Rather, it is implied that post-boom noise is closely related to the interactions of sonic booms with ground surface and objects on the ground, as mentioned in Sec 3.1.1.

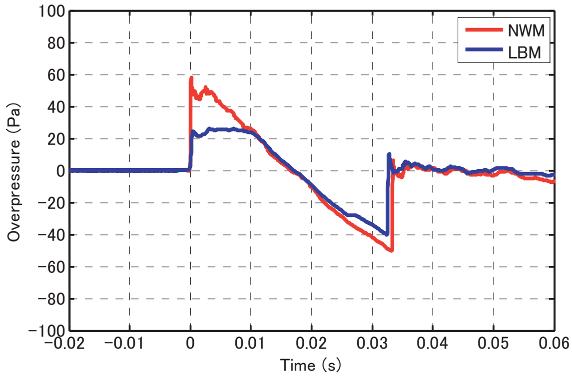

(a) Ch 1

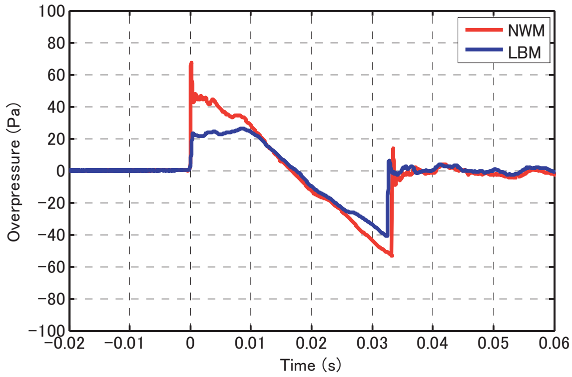

(b) Ch 2

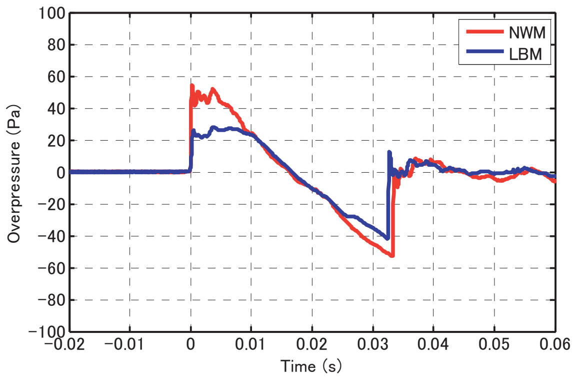

(c) Ch 3

Fig. 3-10 NWM and LBM ground data in first drop test

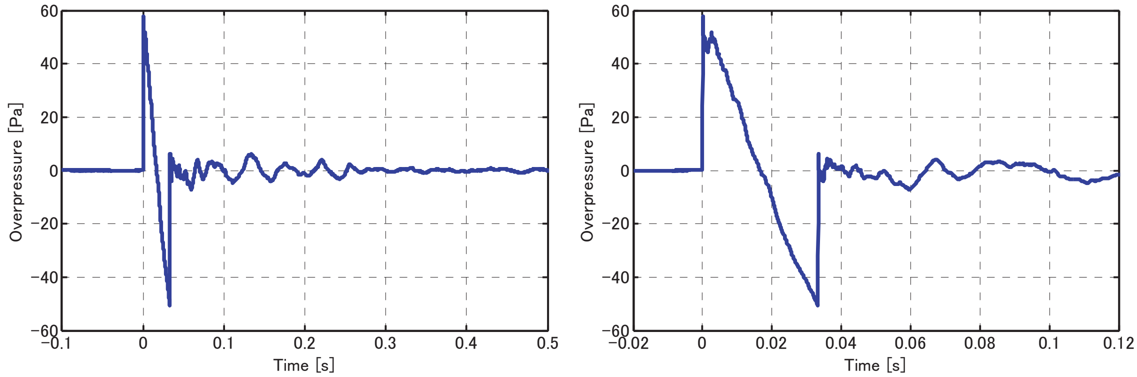

(a) Low Altitude

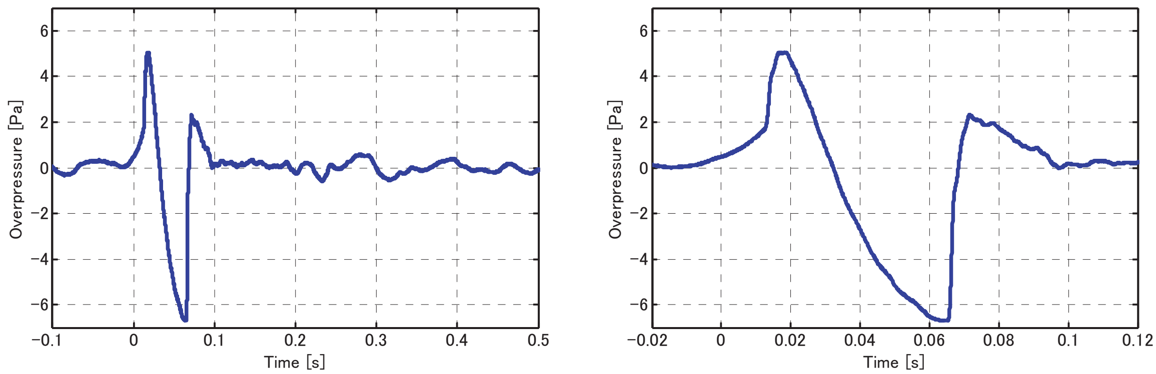

(b) High Altitude

Fig. 3-11 Sonic booms in first drop test (MP3, Ground Ch1, NWM)

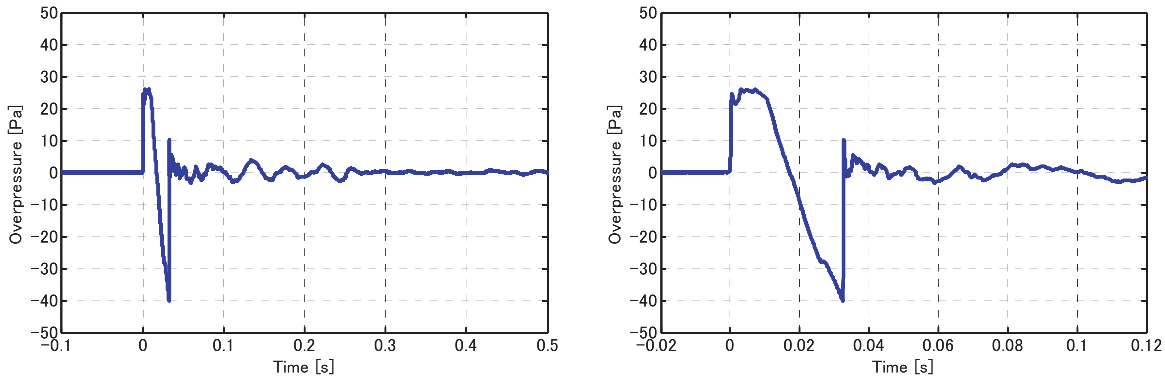

(a) Low Altitude

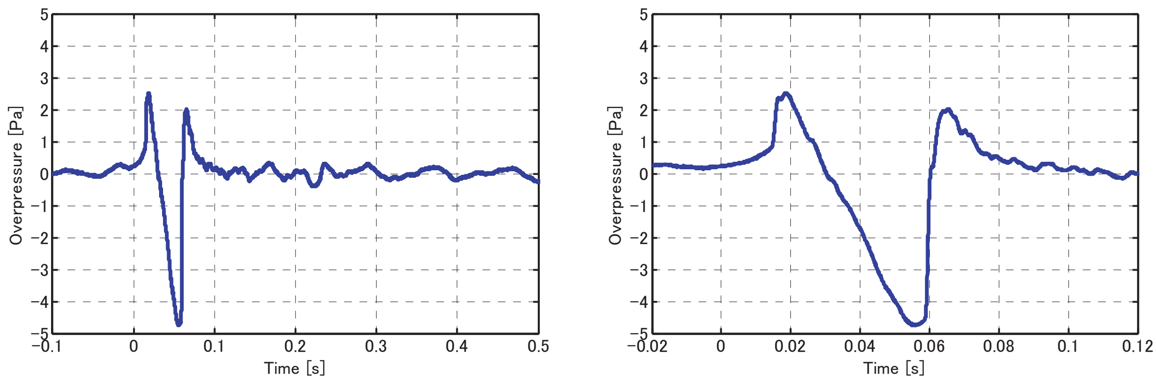

(b) High Altitude

Fig. 3-12 Sonic booms in first drop test (MP3, Ground Ch1, LBM)

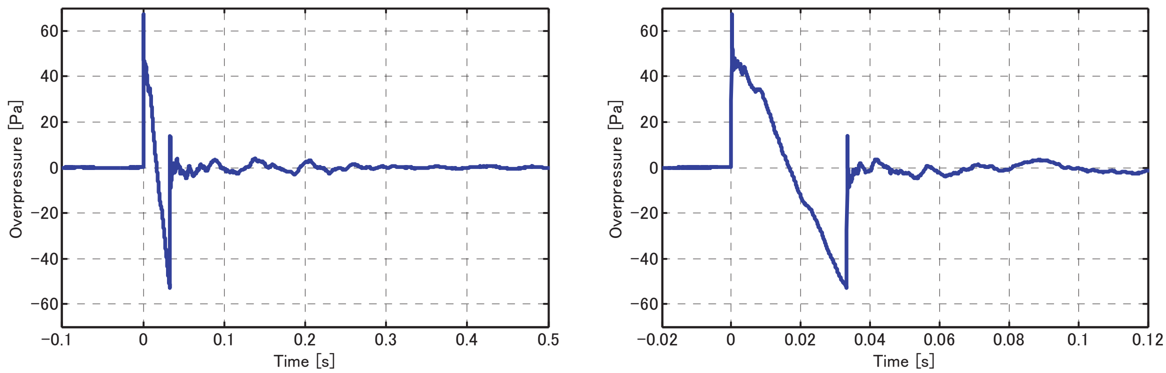

(a) Low Altitude

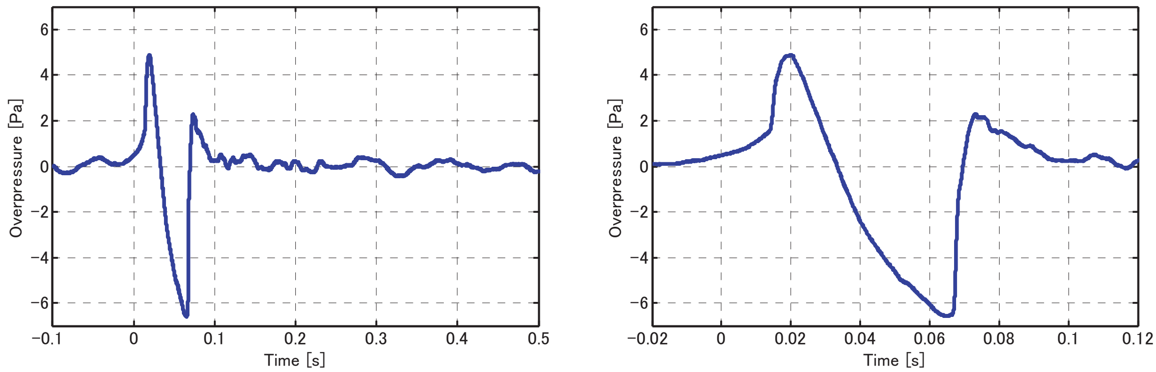

(b) High Altitude

Fig. 3-13 Sonic booms in first drop test (MP3, Ground Ch2, NWM)

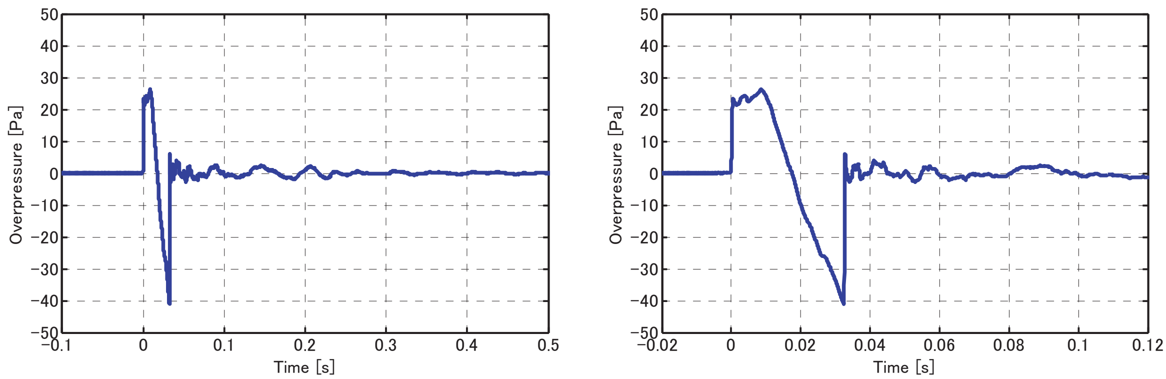

(a) Low Altitude

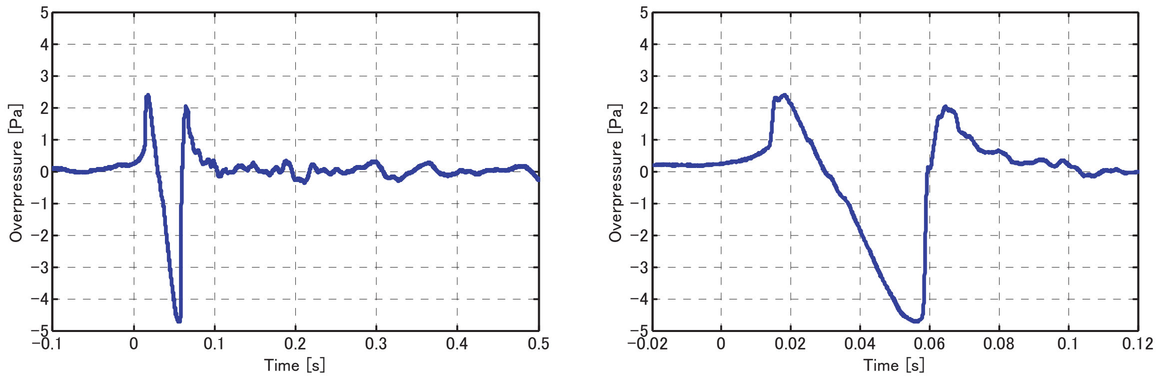

(b) High Altitude

Fig. 3-14 Sonic booms in first drop test (MP3, Ground Ch2, LBM)

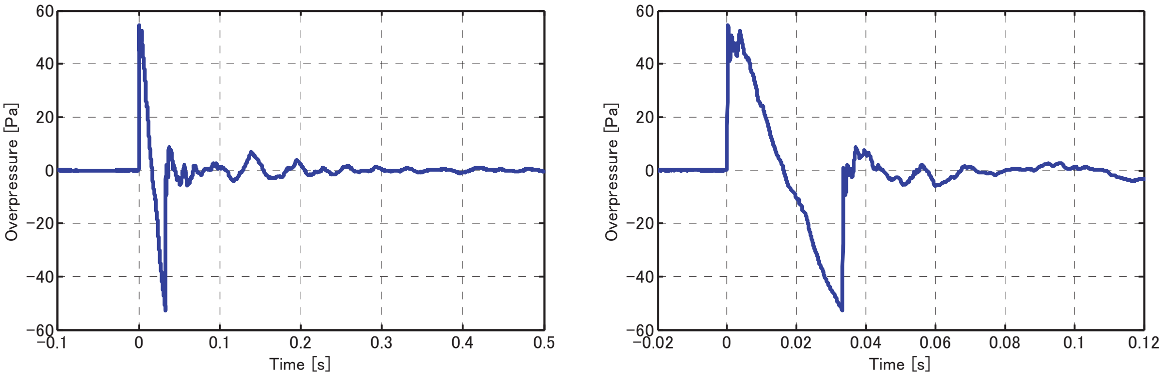

(a) Low Altitude

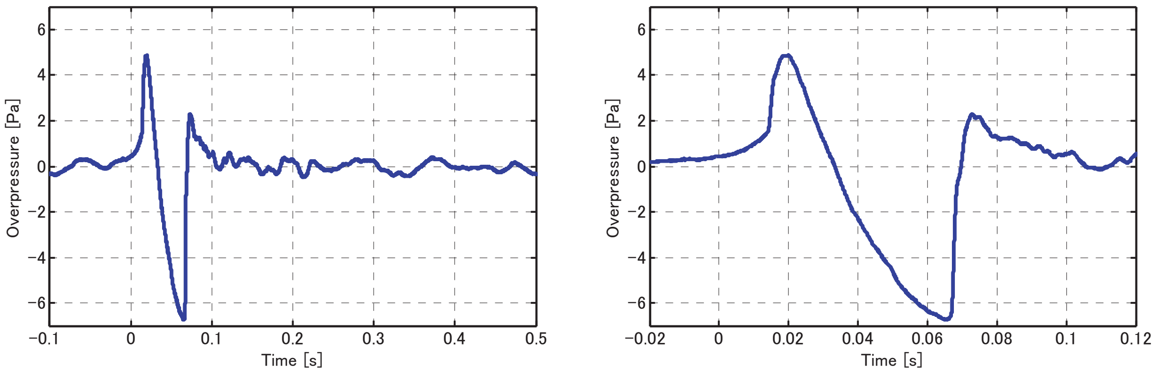

(b) High Altitude

Fig. 3-15 Sonic booms in first drop test (MP3, Ground Ch3 NWM)

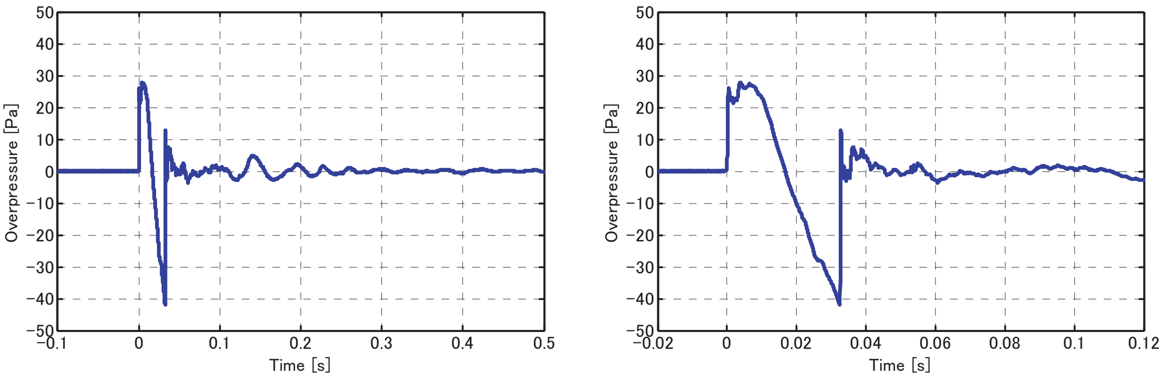

(a) Low Altitude

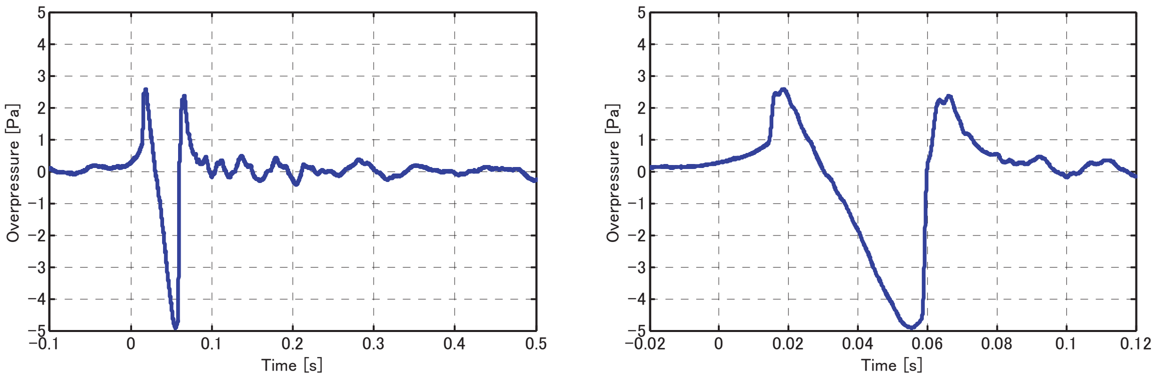

(b) High Altitude

Fig. 3-16 Sonic booms in first drop test (MP3, Ground Ch3, LBM)

3.2. Second Drop Test (MP1)

In the second drop test, sonic booms were measured at MP1 and Esrange. Data obtained at MP1 are shown in this section, and those at Esrange in Sec 3.3.

As described in Sec 2.6.2, more microphones than the initial plan were distributed at MP1 where it had been predicted that sonic booms would most likely arrive. For the aerial measurement, five microphones were used. Two of them were located at an altitude of 1000 m, and the others were distributed at 750, 500, and 250 m.

As with the first drop test, more than one sonic boom signatures were captured by each microphone. Overview of the waveforms at all of the measurement altitudes is shown in Fig. 3-17 and Fig. 3-18 for NWM and LBM, respectively. In the second drop test, NWM was released from the stratospheric balloon first, followed by LBM with roughly one minute of interval. The starting time of the abscissa axis in Fig. 3-17 corresponds to 7:36:35 AM local time, and that in Fig. 3-18 is 7:37:45 AM.

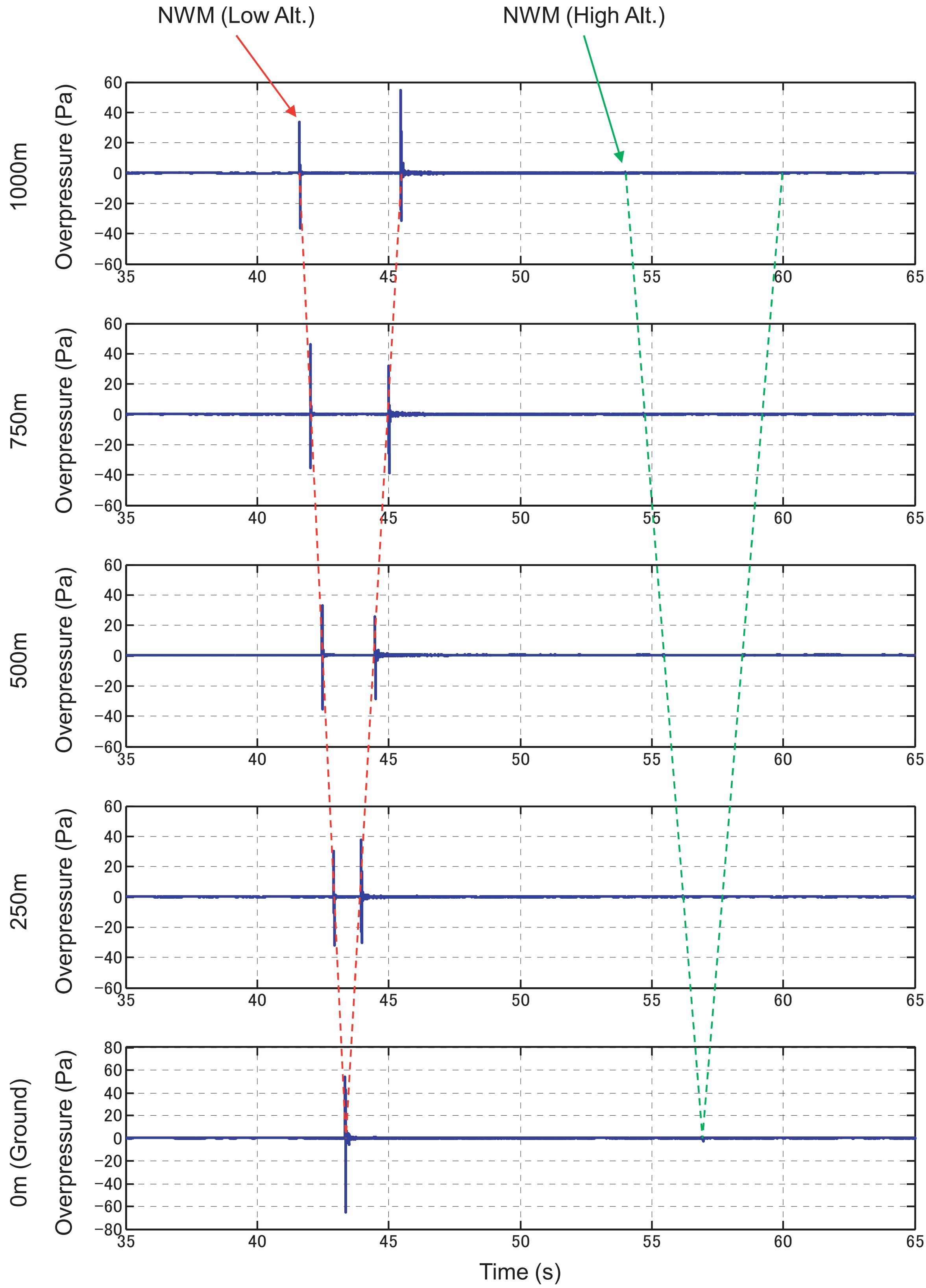

Fig. 3-17 Waveforms from NWM measured at MP1 in the second drop test

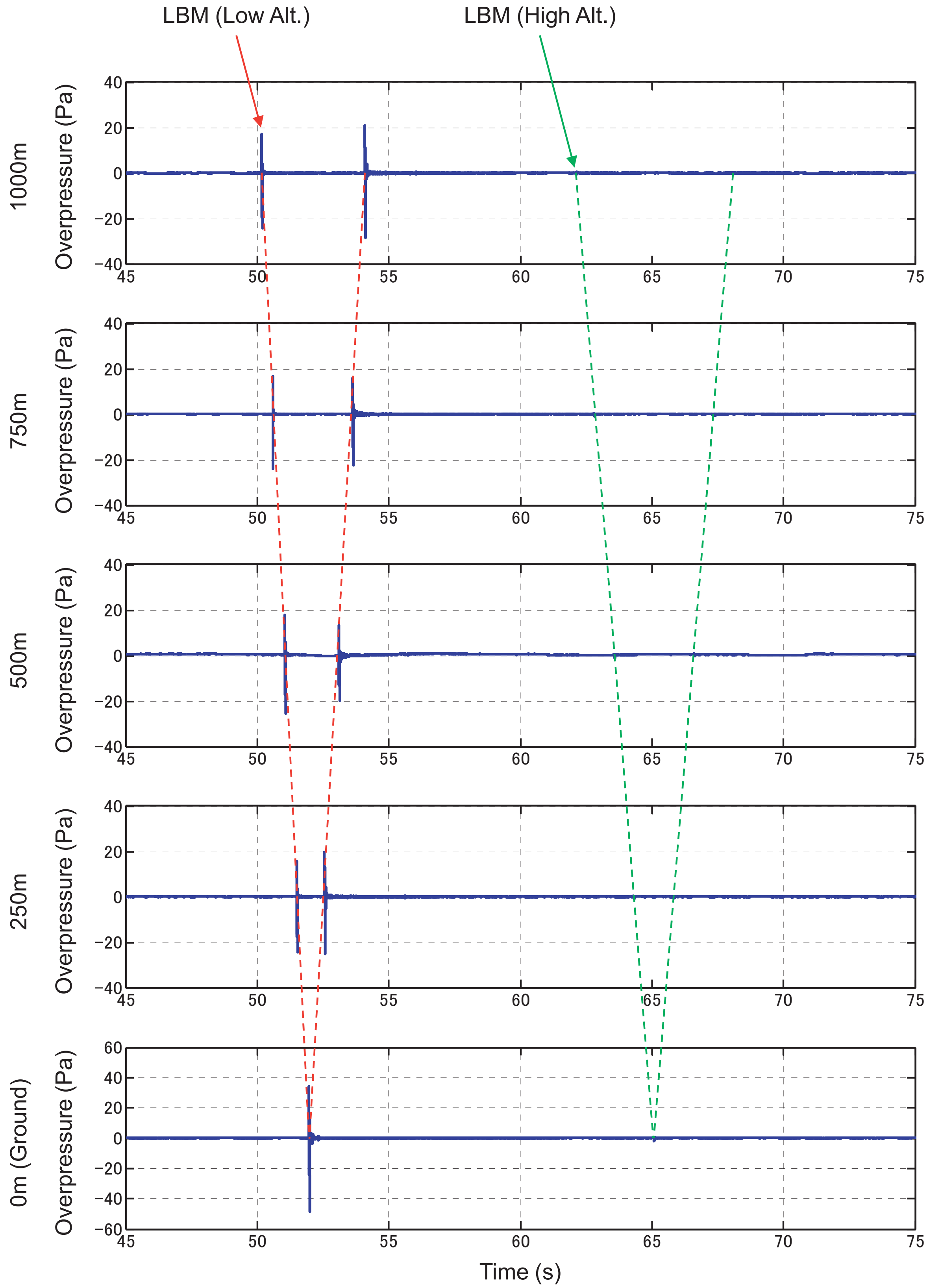

Fig. 3-18 Waveforms from LBM measured at MP1 in the second drop test

3.2.1. Aerial Measurement

Aerial measurement was successfully made by all of the five microphones at MP1. Signatures of sonic booms generated at the lower altitude and directly recorded by the microphones are shown in Fig. 3-19. Unlike the first drop test, aerial waveforms seem to be distorted to a certain extent. It is inferred that atmospheric condition was unsteady (in space and/or time) up to a relatively high altitude at the time of the second test [2]. Also different from the first test is that no "bumps" are found after the front and rear shocks in the 1000 m data.

All signatures from all different paths are shown in Fig. 3-20 through Fig. 3-29.

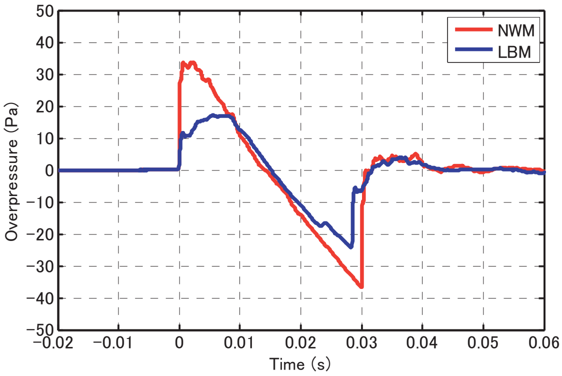

(a) 1000 m, Ch 1

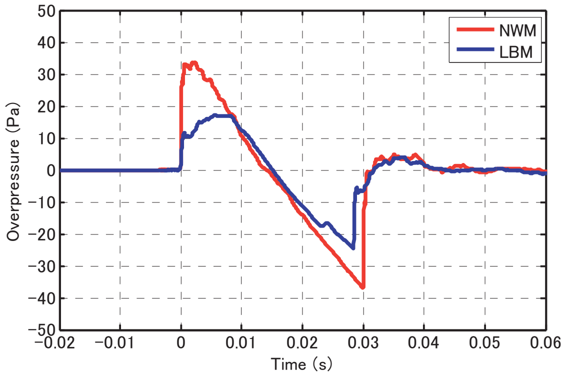

(b) 1000 m, Ch 2

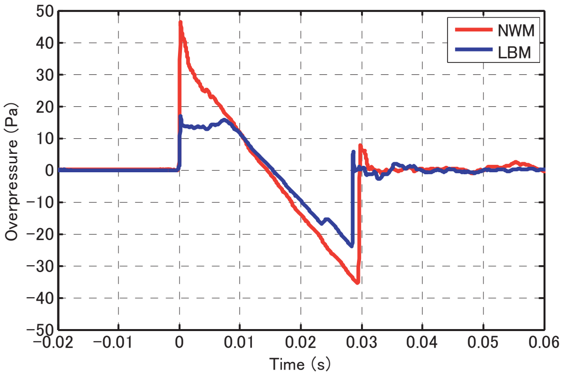

(c) 750 m, Ch 1

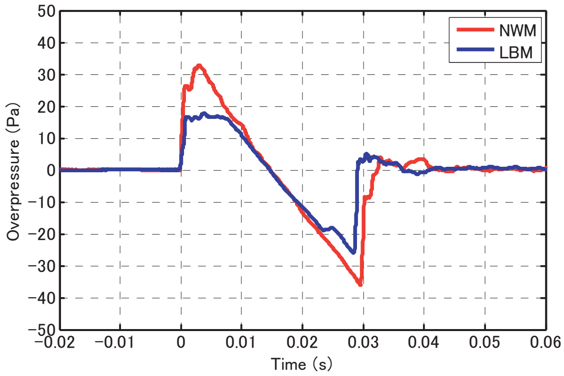

(d) 500 m, Ch 1

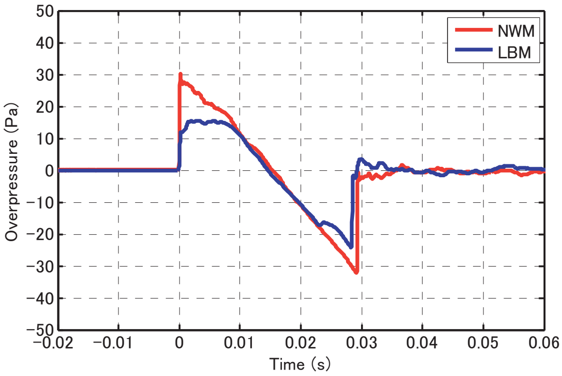

(e) 250 m, Ch 1

Fig. 3-19 NWM and LBM aerial data in second drop test

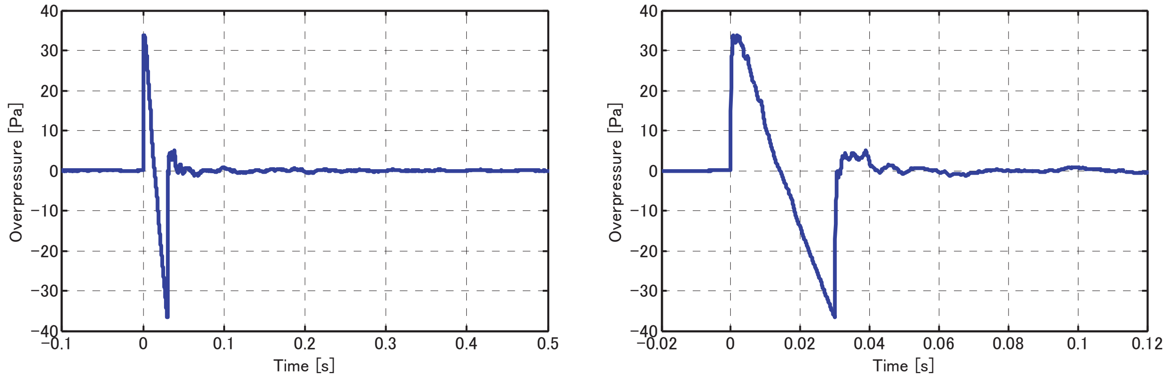

(a) Low Altitude, Direct

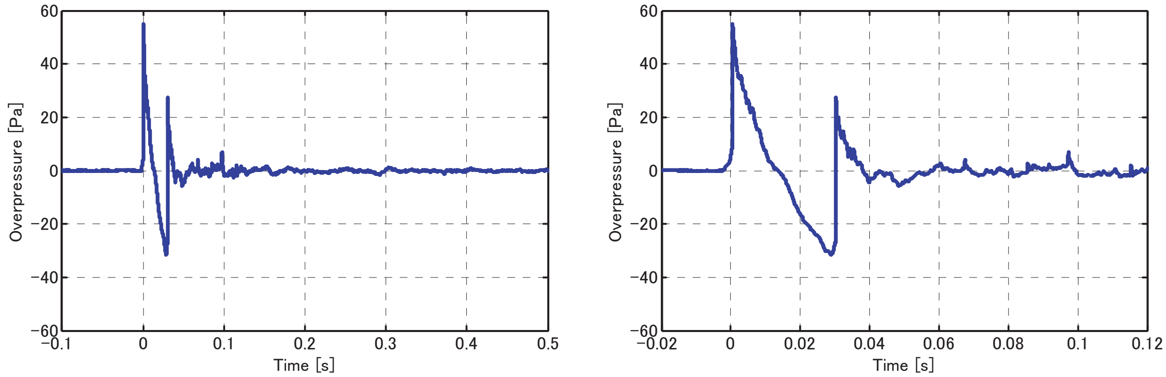

(b) Low Altitude, Reflected

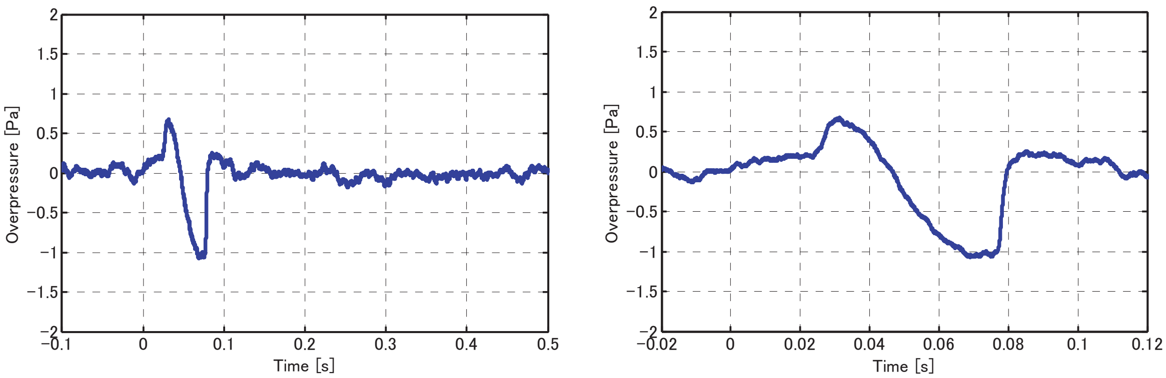

(c) High Altitude, Direct

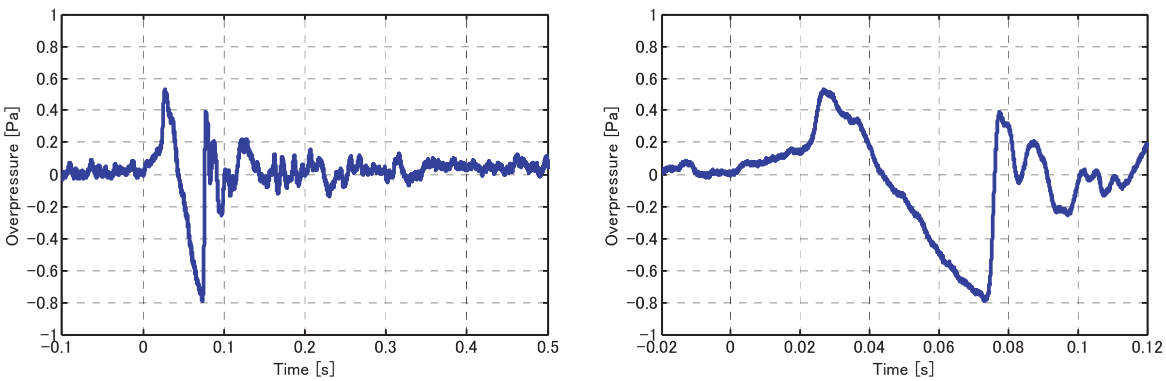

(d) High Altitude, Reflected

Fig. 3-20 Sonic booms in second drop test (MP1, Aerial 1000m Ch1, NWM)

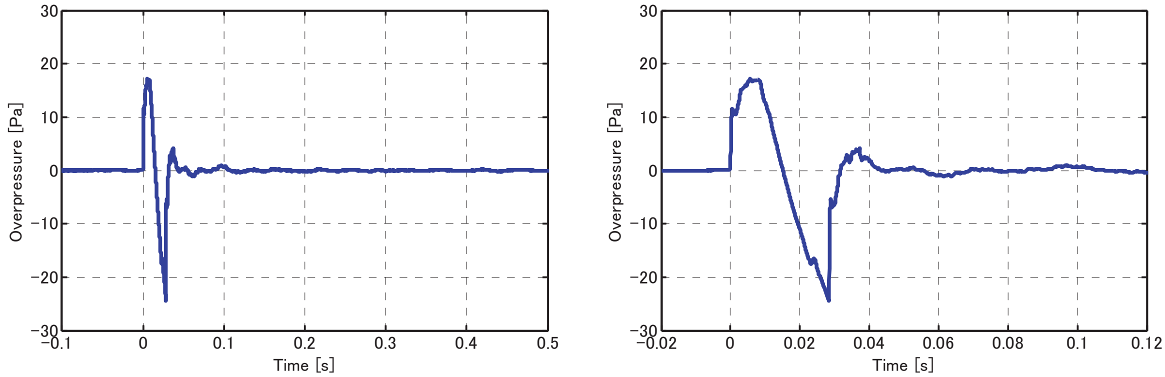

(a) Low Altitude, Direct

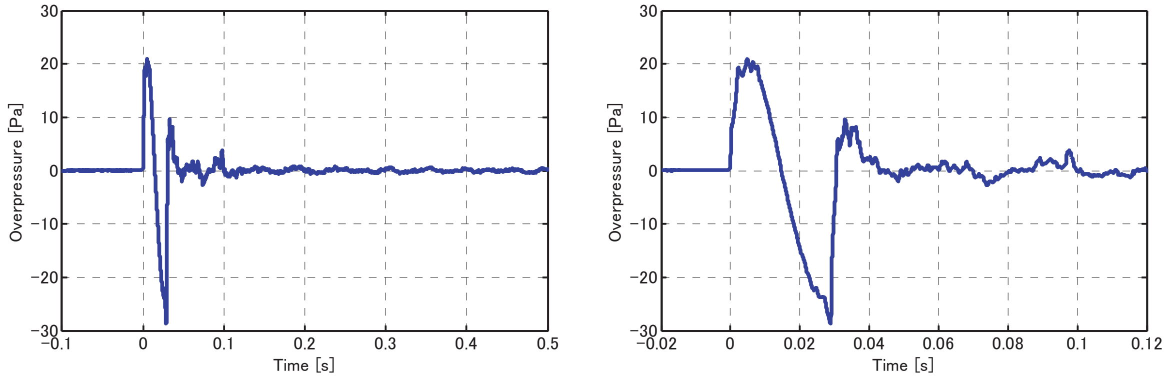

(b) Low Altitude, Reflected

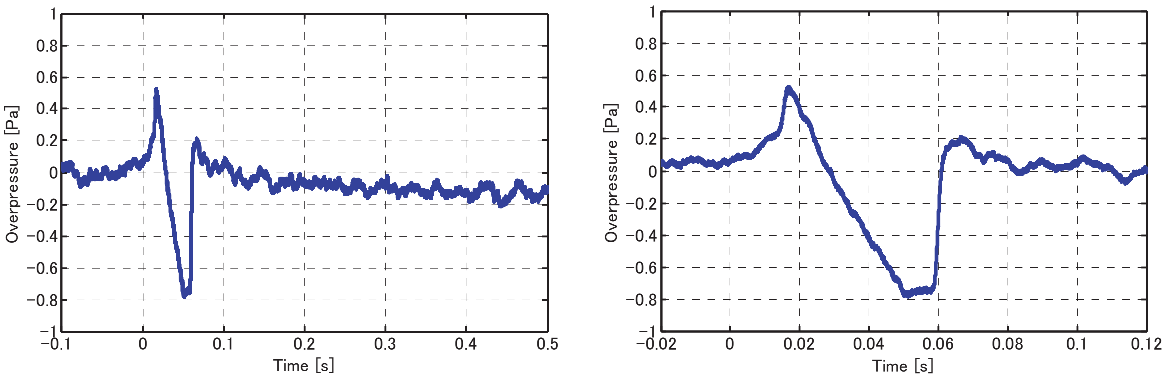

(c) High Altitude, Direct

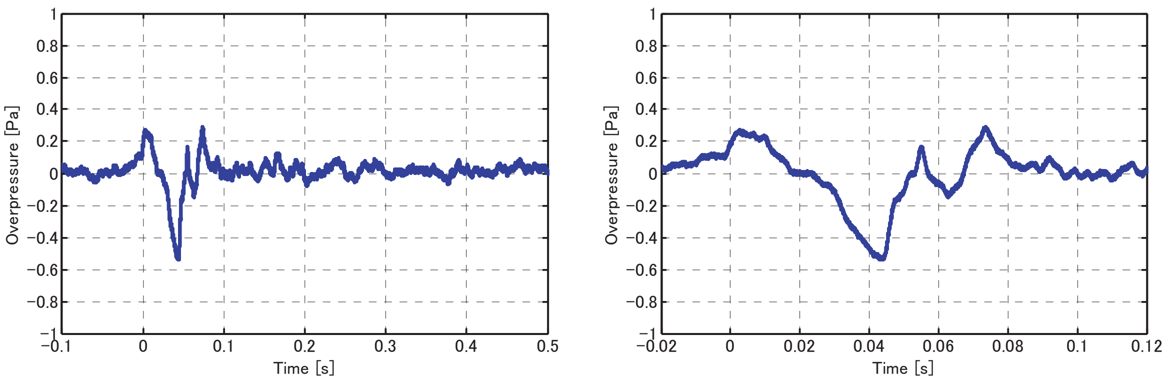

(d) High Altitude, Reflected

Fig. 3-21 Sonic booms in second drop test (MP1, Aerial 1000m Ch1, LBM)

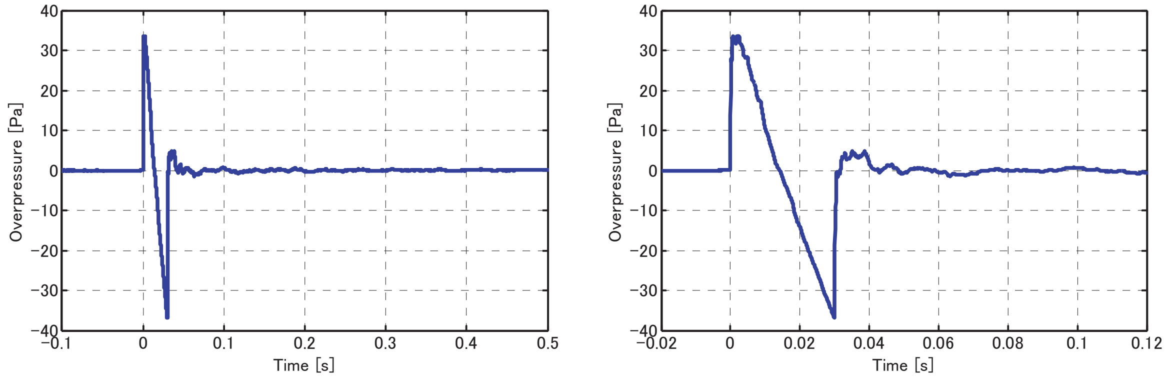

(a) Low Altitude, Direct

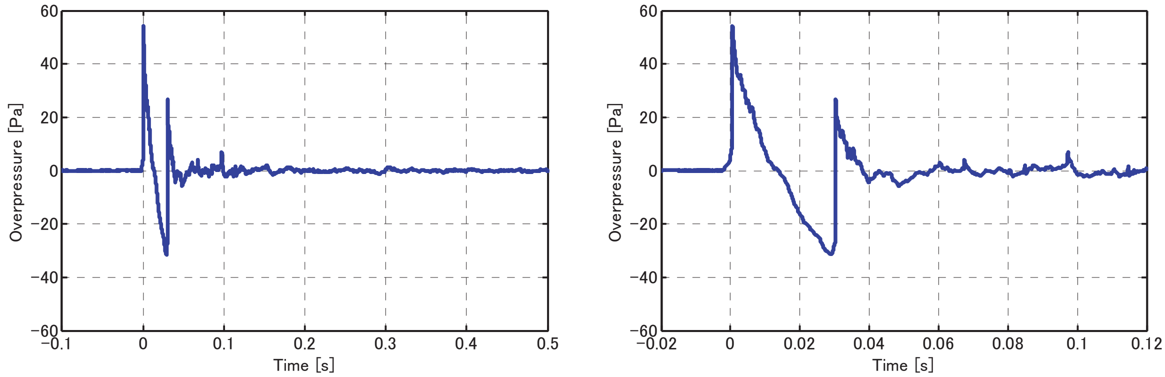

(b) Low Altitude, Reflected

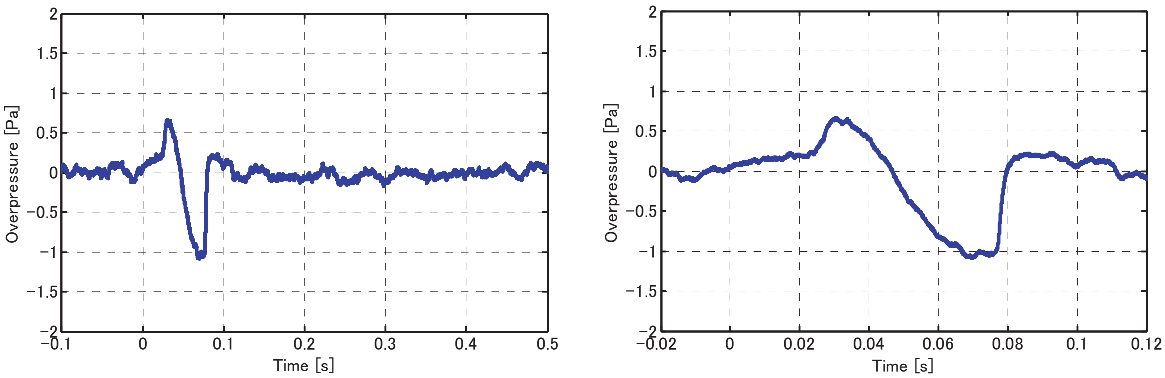

(c) High Altitude, Direct

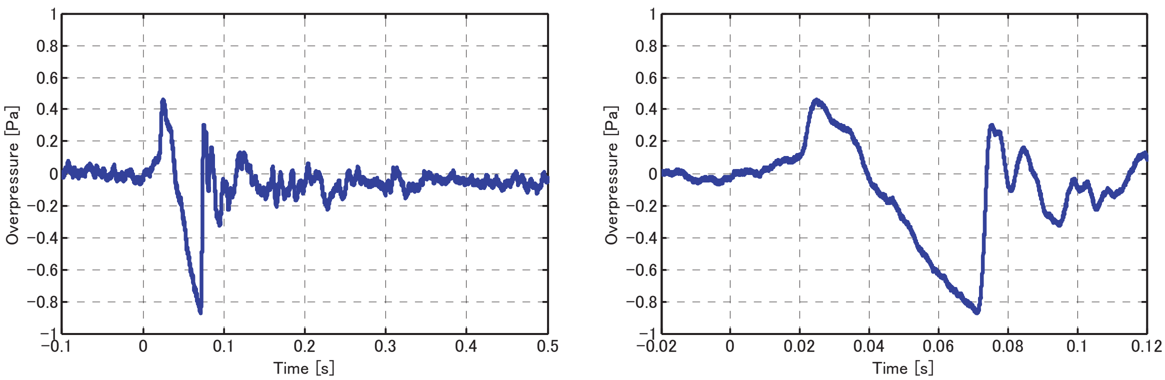

(d) High Altitude, Reflected

Fig. 3-22 Sonic booms in second drop test (MP1, Aerial 1000m Ch2, NWM)

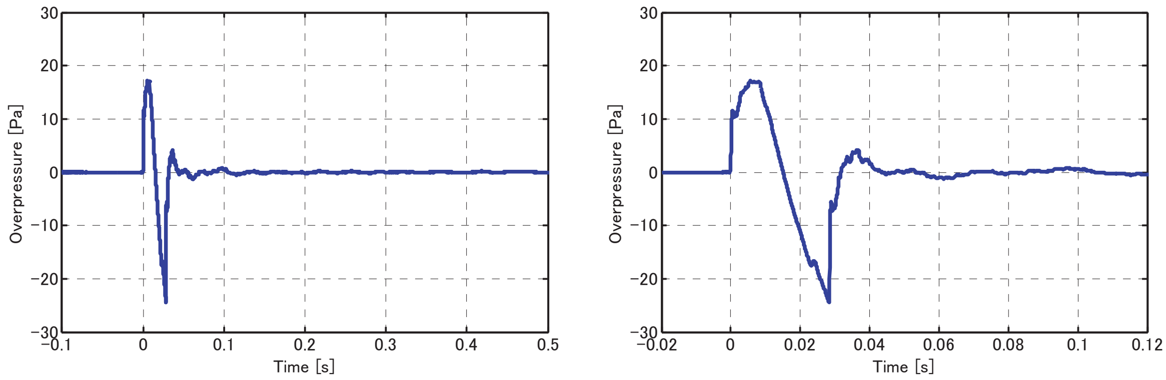

(a) Low Altitude, Direct

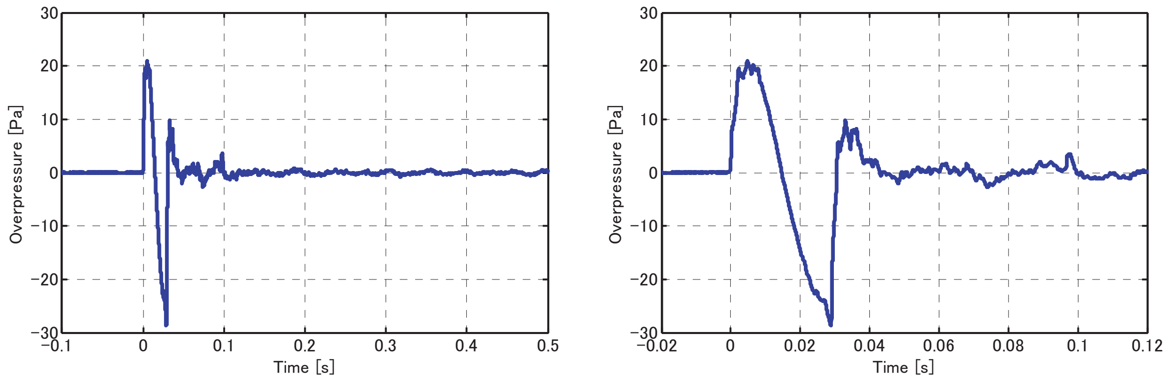

(b) Low Altitude, Reflected

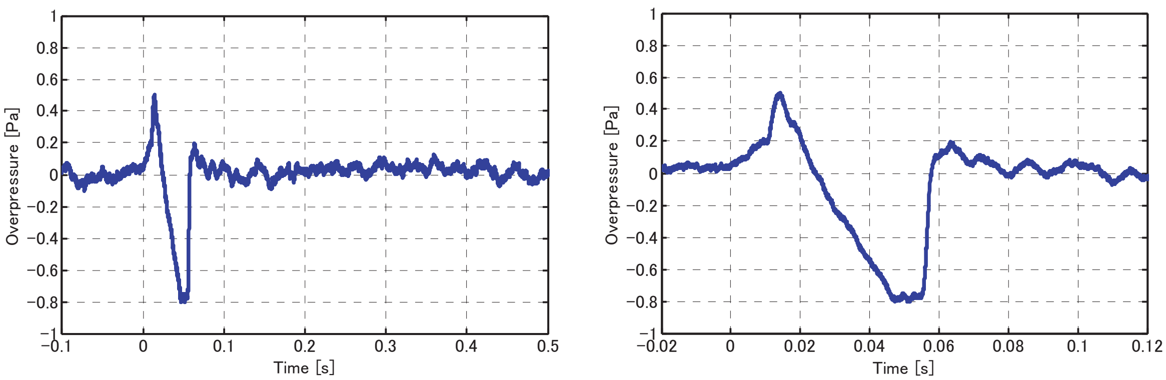

(c) High Altitude, Direct

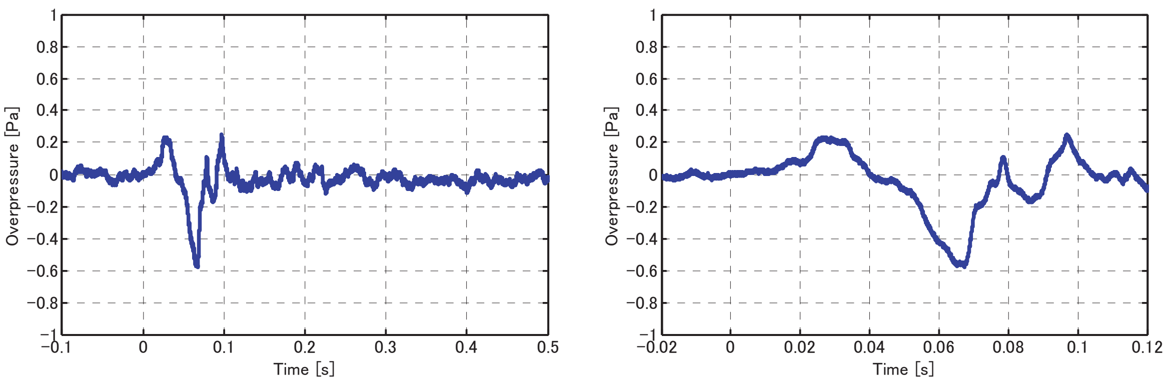

(d) High Altitude, Reflected

Fig. 3-23 Sonic booms in second drop test (MP1, Aerial 1000m Ch2, LBM)

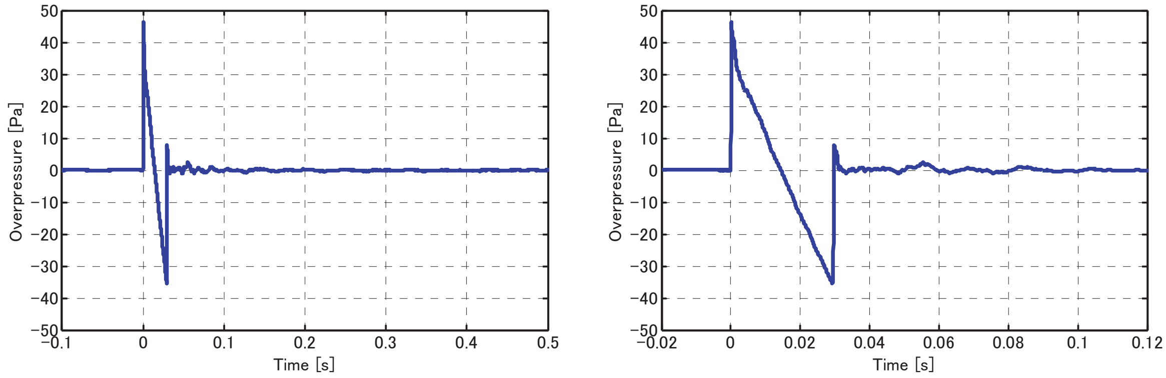

(a) Low Altitude, Direct

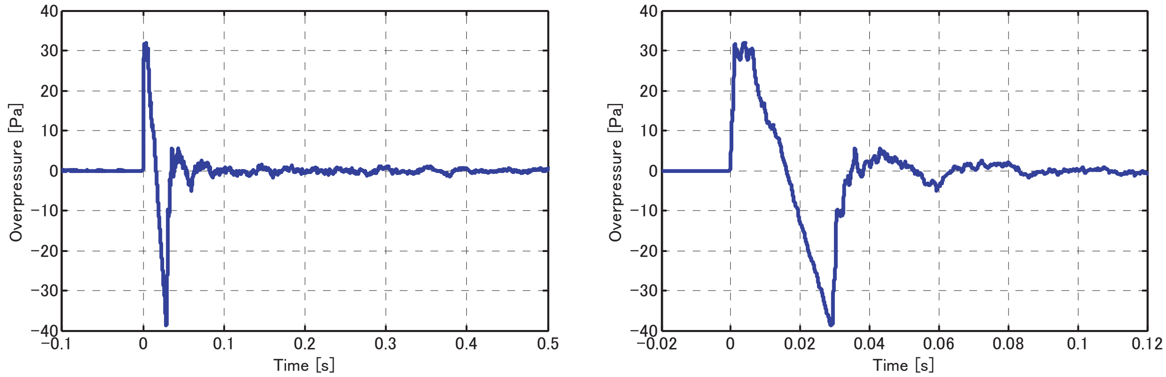

(b) Low Altitude, Reflected

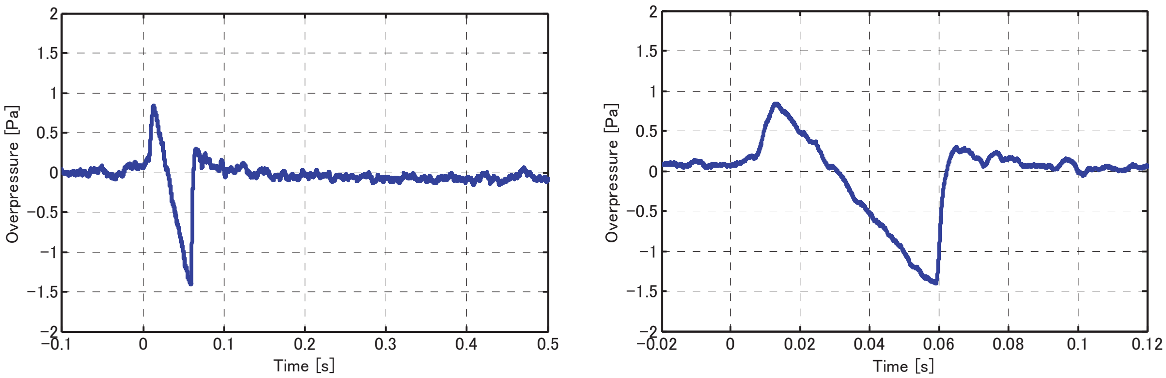

(c) High Altitude, Direct

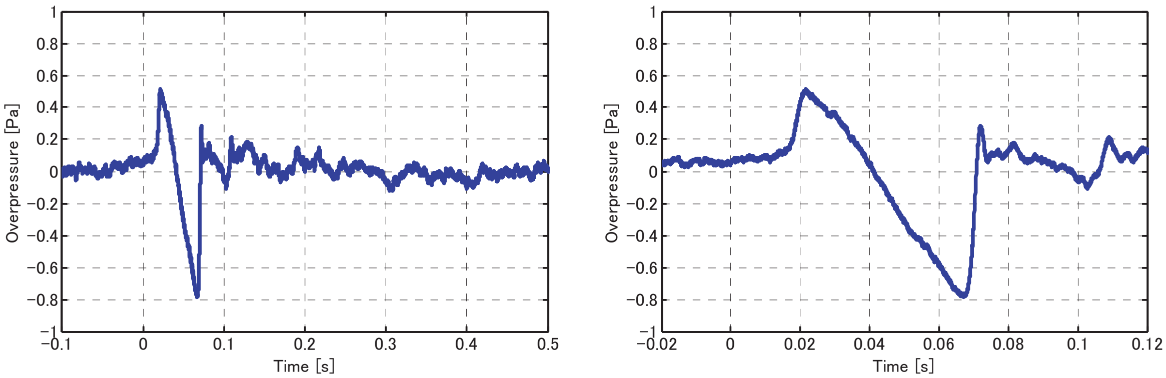

(d) High Altitude, Reflected

Fig. 3-24 Sonic booms in second drop test (MP1, Aerial 750m Ch1, NWM)

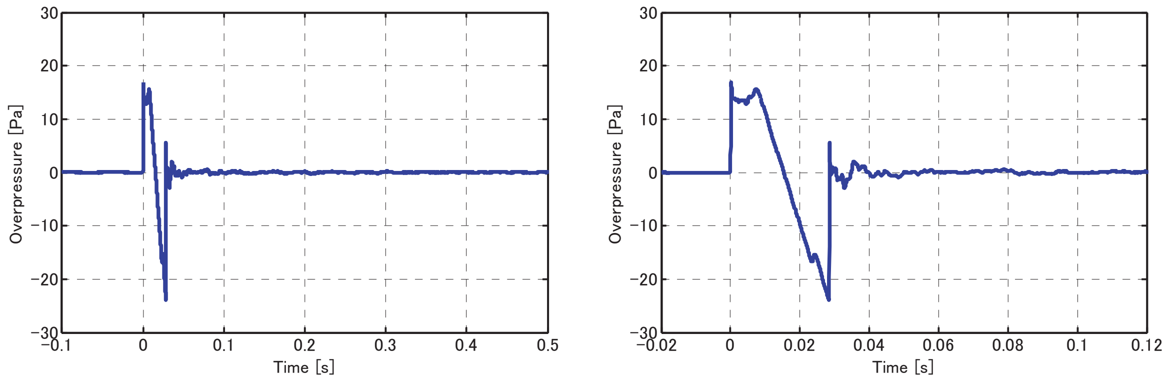

(a) Low Altitude, Direct

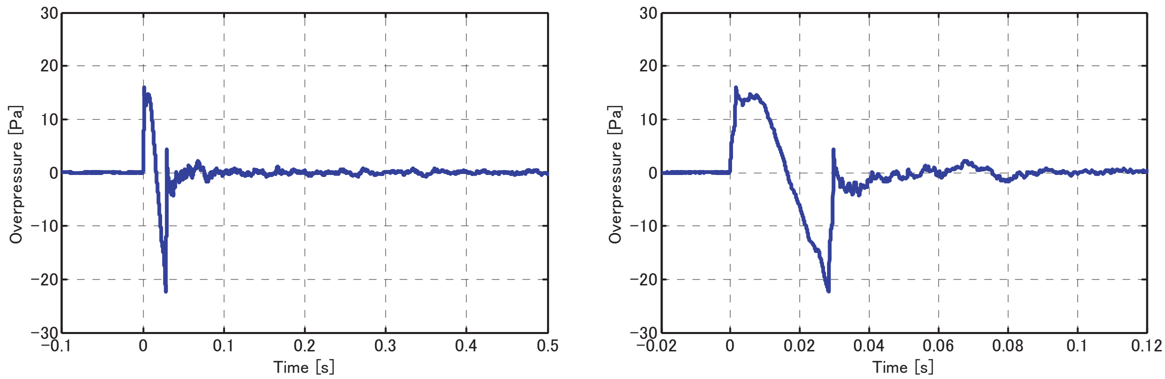

(b) Low Altitude, Reflected

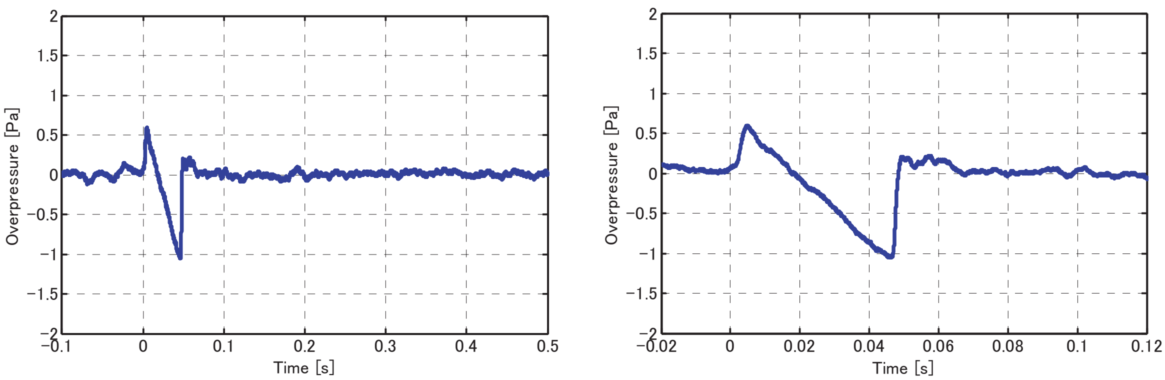

(c) High Altitude, Direct

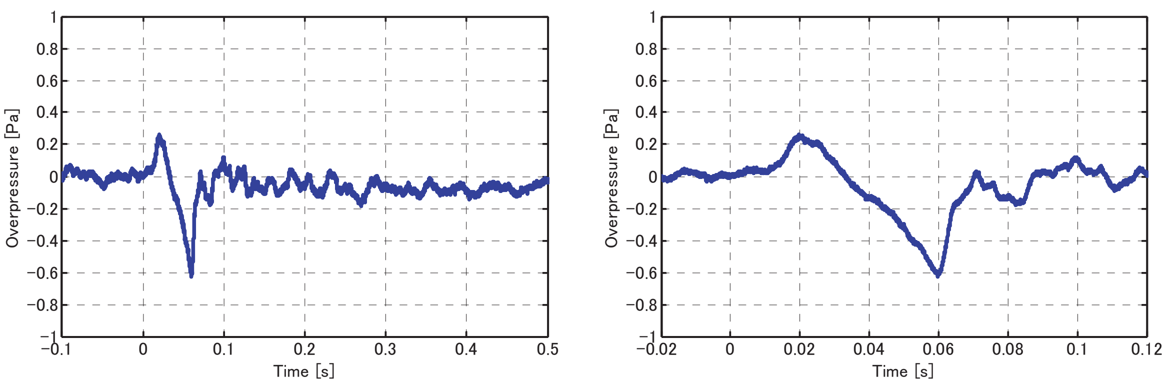

(d) High Altitude, Reflected

Fig. 3-25 Sonic booms in second drop test (MP1, Aerial 750m Ch1, LBM)

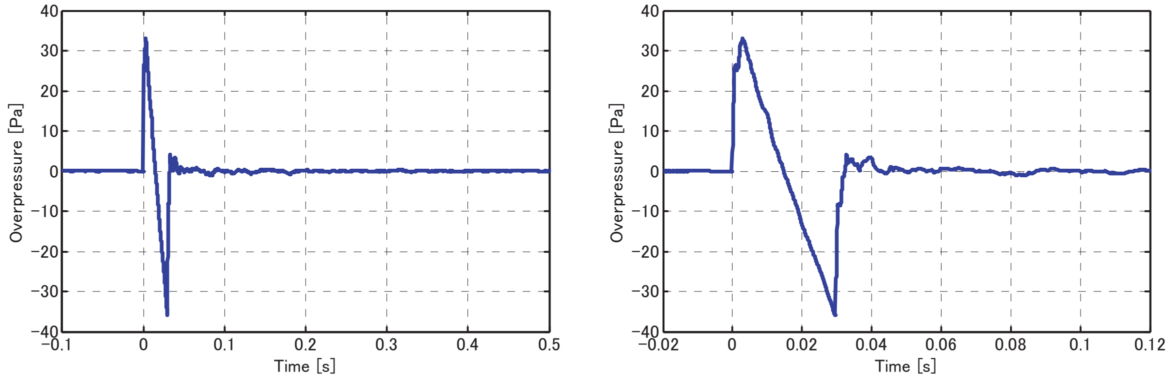

(a) Low Altitude, Direct

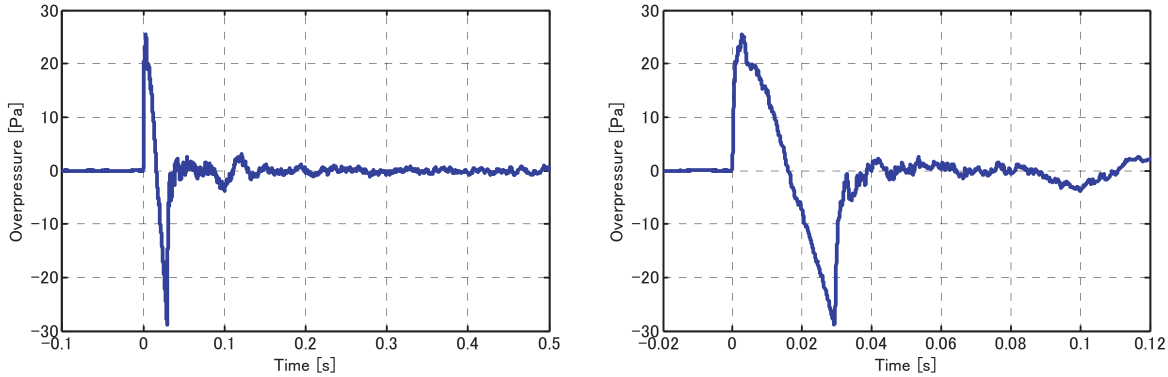

(b) Low Altitude, Reflected

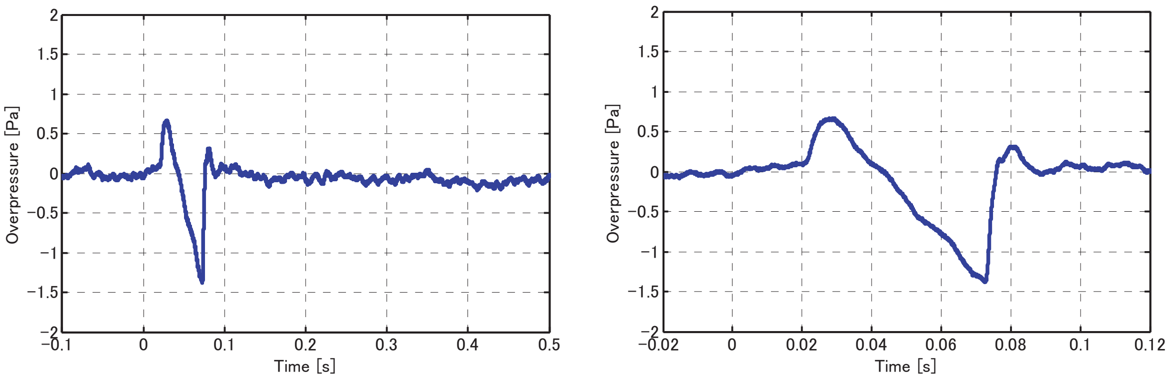

(c) High Altitude, Direct

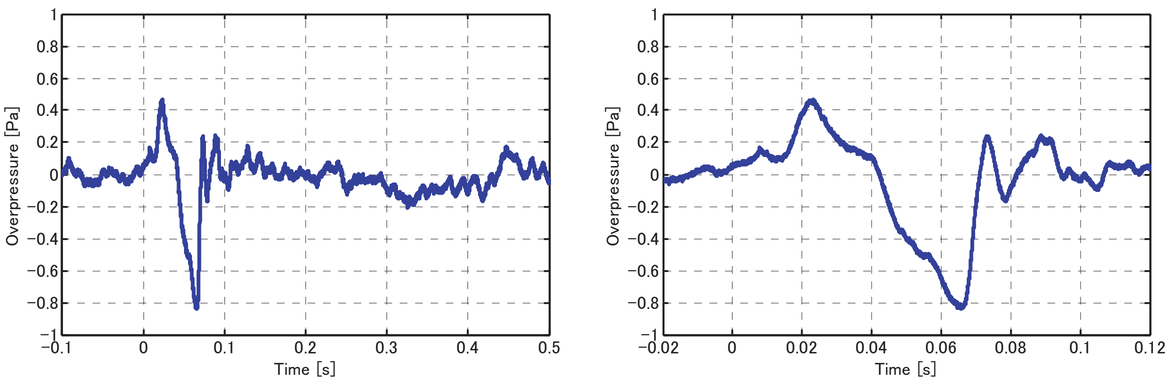

(d) High Altitude, Reflected

Fig. 3-26 Sonic booms in second drop test (MP1, Aerial 500m Ch1, NWM)

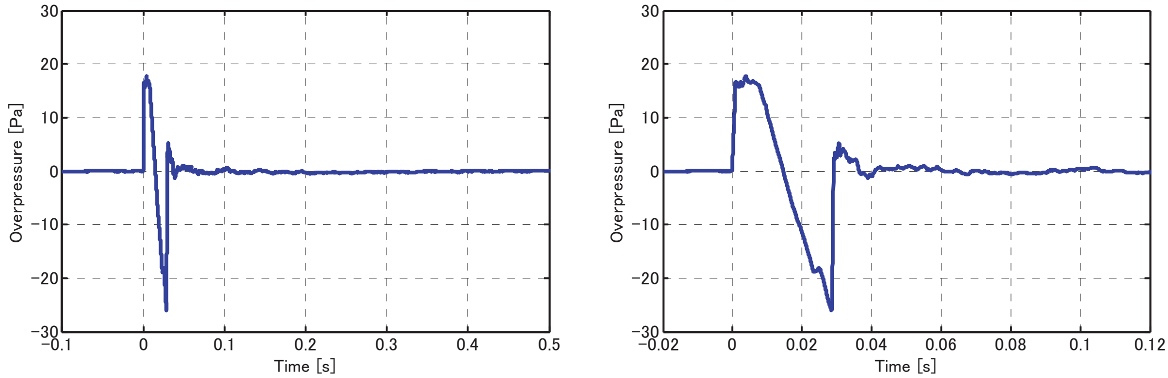

(a) Low Altitude, Direct

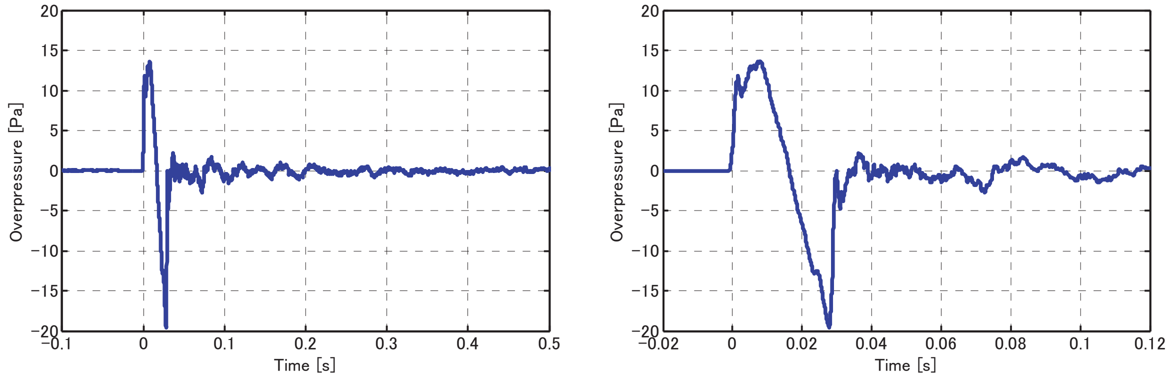

(b) Low Altitude, Reflected

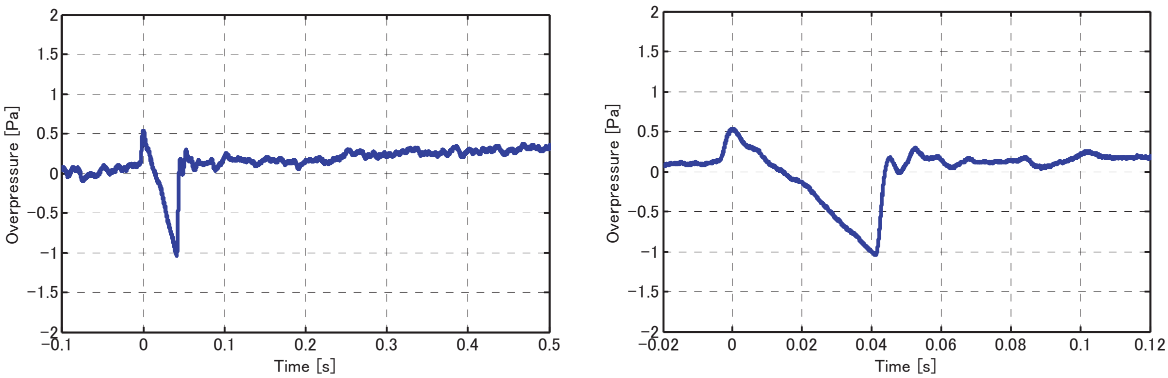

(c) High Altitude, Direct

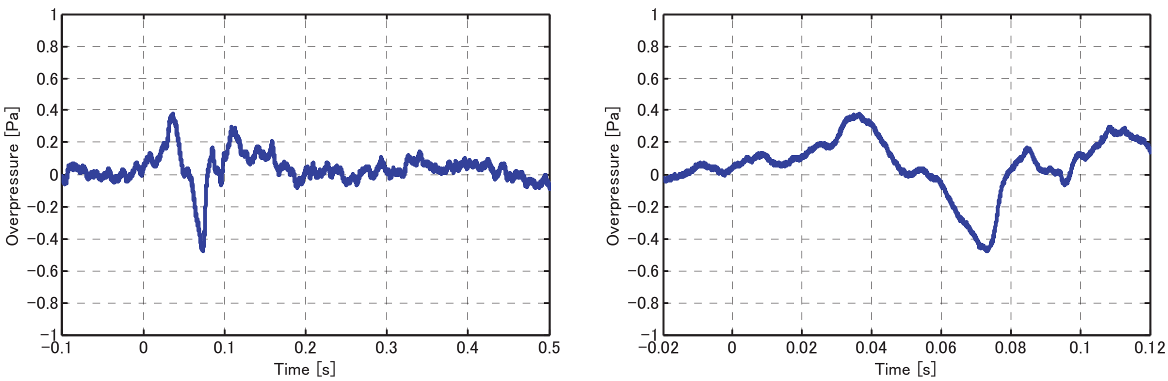

(d) High Altitude, Reflected

Fig. 3-27 Sonic booms in second drop test (MP1, Aerial 500m Ch1, LBM)

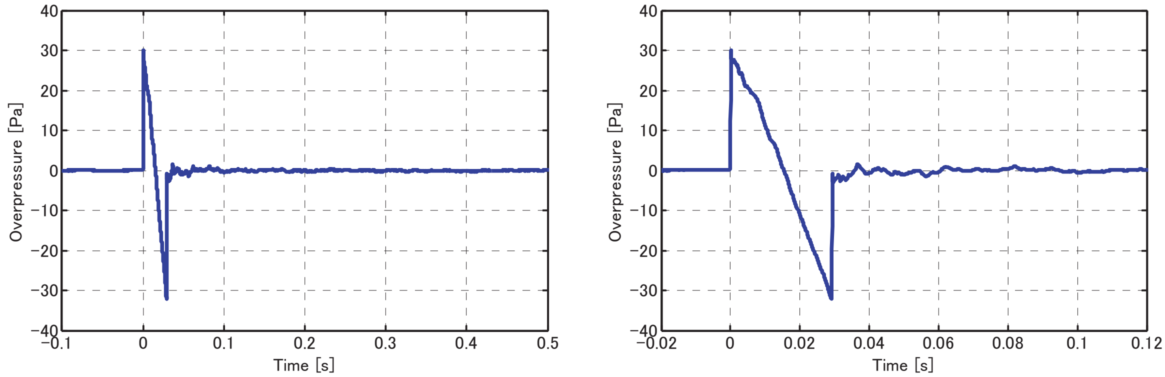

(a) Low Altitude, Direct

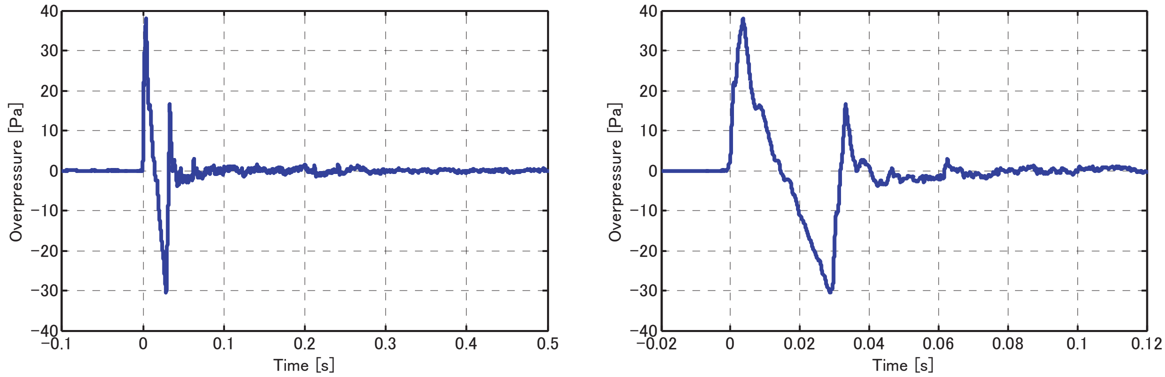

(b) Low Altitude, Reflected

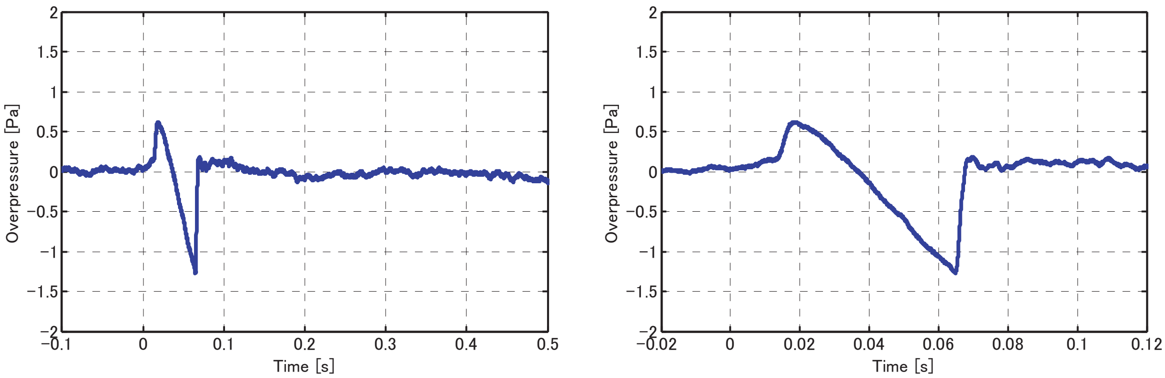

(c) High Altitude, Direct

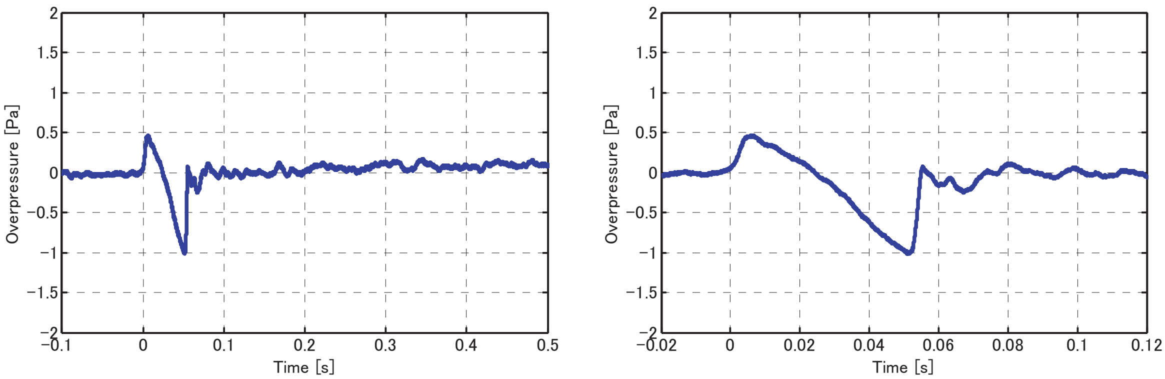

(d) High Altitude, Reflected

Fig. 3-28 Sonic booms in second drop test (MP1, Aerial 250m Ch1, NWM)

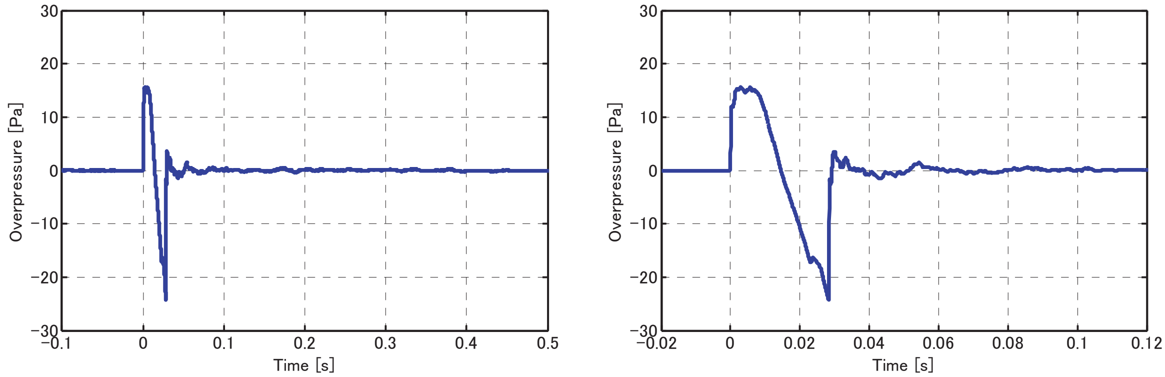

(a) Low Altitude, Direct

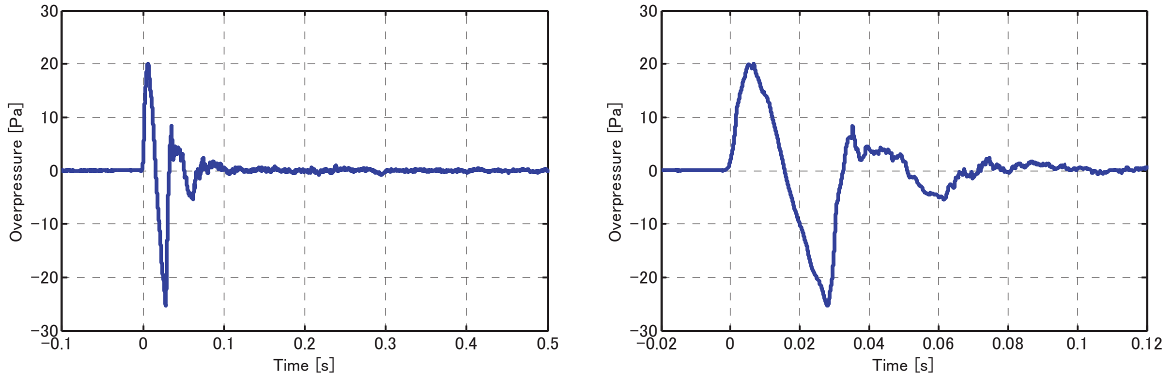

(b) Low Altitude, Reflected

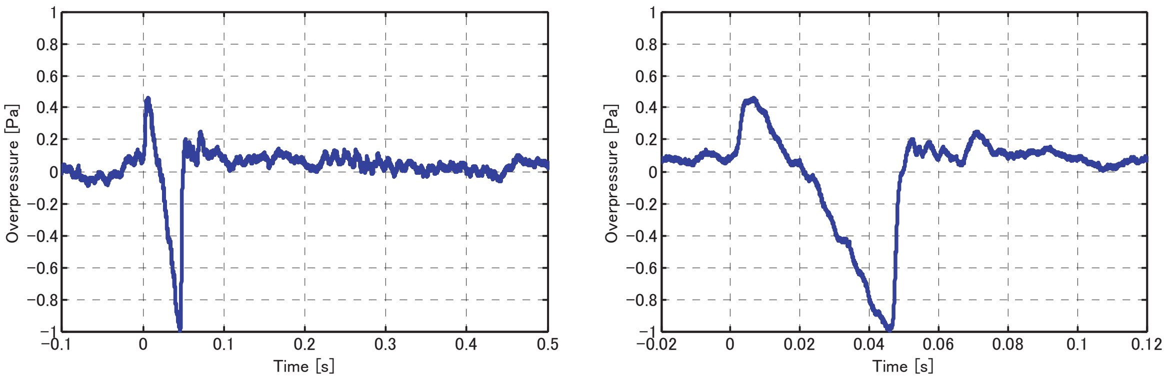

(c) High Altitude, Direct

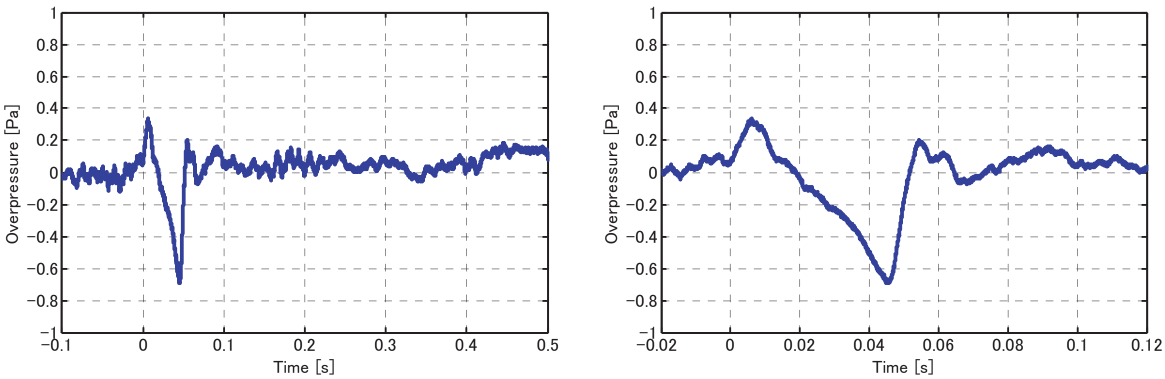

(d) High Altitude, Reflected

Fig. 3-29 Sonic booms in second drop test (MP1, Aerial 250m Ch1, LBM)

3.2.2. Ground Measurement

As shown in Fig. 3-30, ten microphones were located on the ground, 3 to 5 m apart from each other, except channels 7 and 8, which were installed with about 0.7 m of interval. Microphones 7 through 10 were not in the flush-mount setup, but laid on wooden boards. These microphones had been originally planned to be used as part of the aerial measurement systems at MP2 and MP3. The blue box in the top-left corner of Fig. 3-30 is the house used for the indoor measurement, whose picture is shown in Fig. 2-4. The other two blue boxes are also small houses (storage and sauna). The rough direction of sonic boom propagation is indicated by the green arrow in Fig. 3-30.

The ground waveforms of the target sonic booms produced at the lower altitude are shown in Fig. 3-31. Although the shapes of the aerial signatures in the second drop test have somewhat deformed, probably due to turbulence in the higher altitude region (Fig. 3-19), it could be said that the ground signatures are more distorted. However, the discrepancy between NWM and LBM waveforms both in their magnitudes and shapes are still clearly recognized.

Similarly to the first drop test, the manner of change in waveform shapes are not the same over the microphones. For example, Ch 3 data has peaky shapes after the shocks, while Ch 8 data (especially NWM data) have rounded shapes. On the other hand, the distortion pattern of the two waveforms measured by the same microphone with roughly a minute of interval look similar. Thus, it could be said that 5 to 20 m of difference in space has more effects on the ways of waveform distortion than one minute of difference in time. However, from only the data in D-SEND#1, it cannot be concluded that this observation is universal. Both of the drop tests in D-SEND#1 were conducted in calm atmospheric conditions, which were required from the view point of operating the stratospheric balloon for bringing the drop bodies and the blimps for sonic boom measurement.

All signatures of sonic booms came along different propagation paths to the ground microphones are shown in Fig. 3-32 through Fig. 3-51.

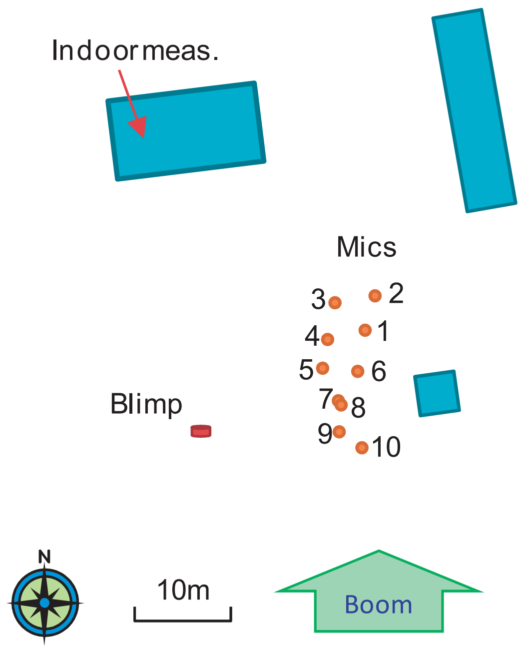

Fig. 3-30 Ground transducer arrangement at MP1 in second drop test

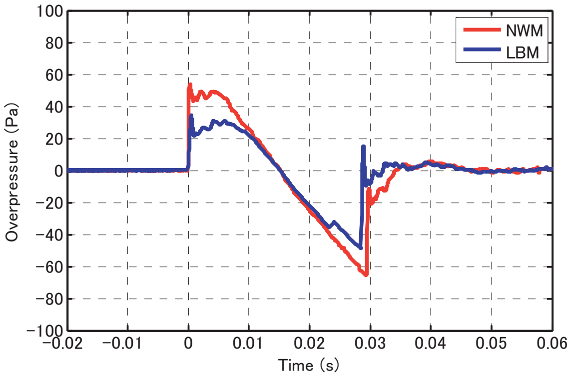

(a) Ch 1

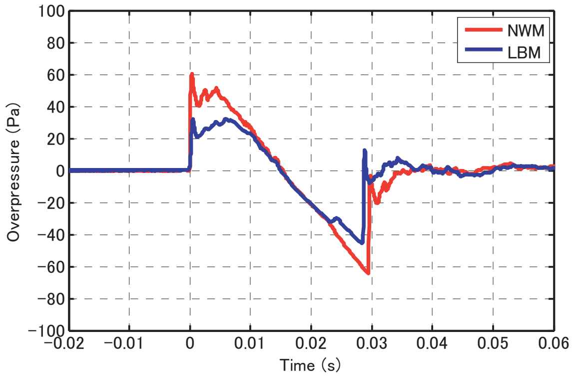

(b) Ch 2

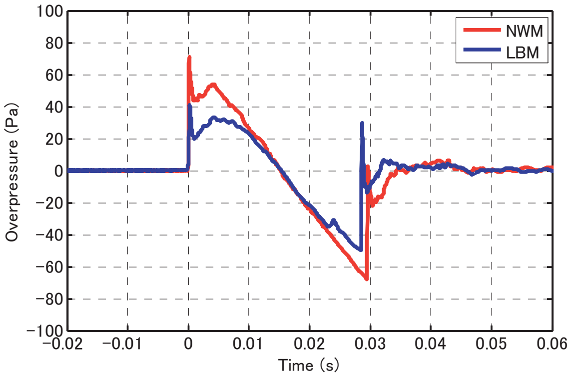

(c) Ch 3

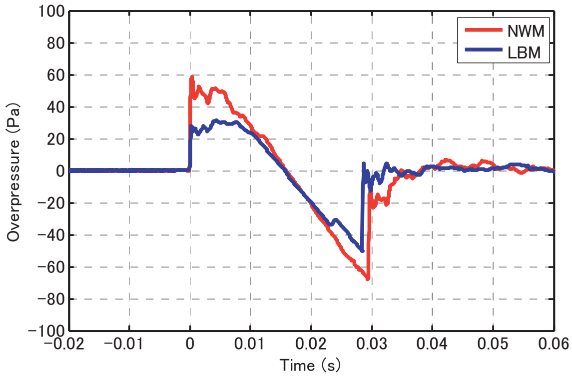

(d) Ch 4

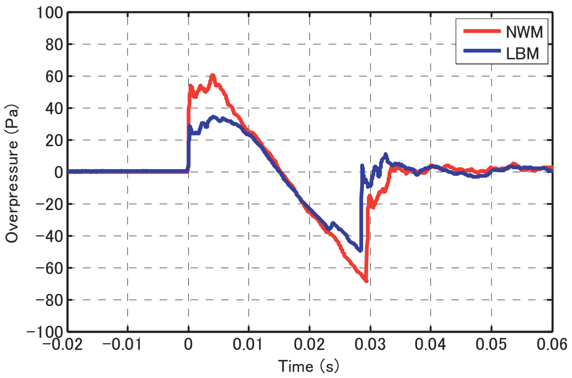

(e) Ch 5

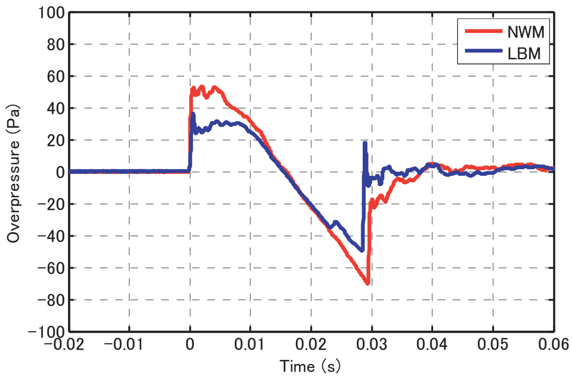

(f) Ch 6

Fig. 3-31 NWM and LBM ground data in second drop test (MP1) (1/2)

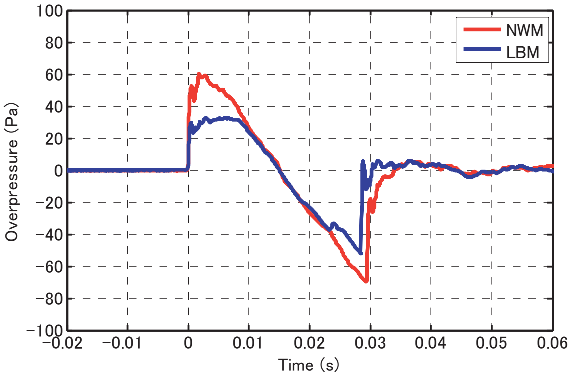

(g) Ch 7

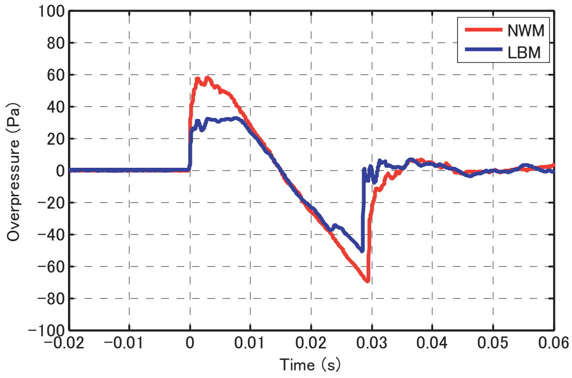

(h) Ch 8

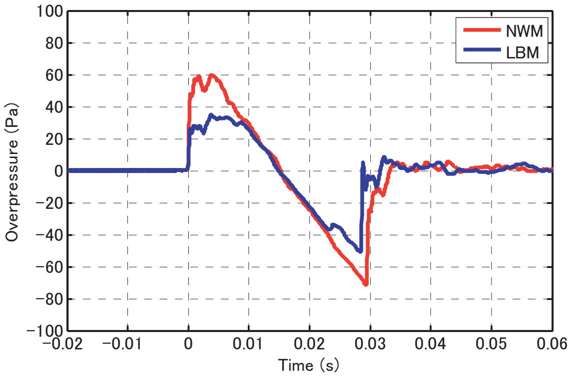

(i) Ch 9

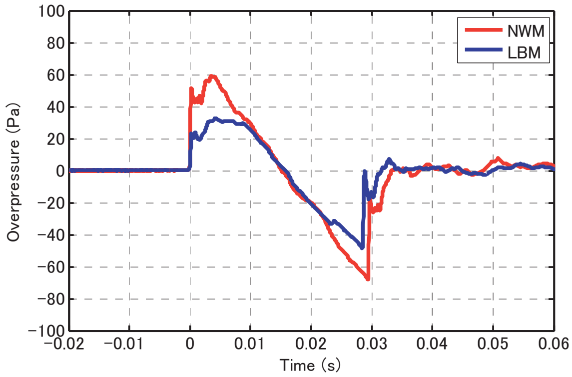

(j) Ch 10

Fig. 3-31 NWM and LBM ground data in second drop test (MP1) (2/2)

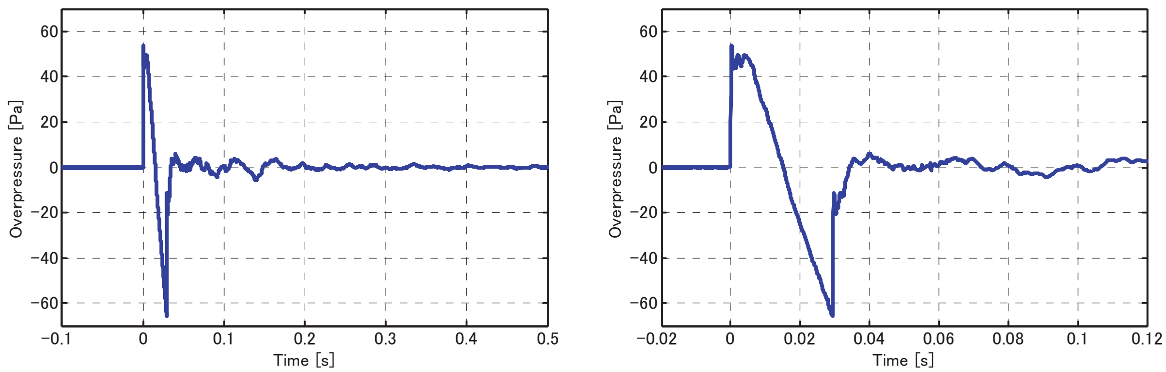

(a) Low Altitude

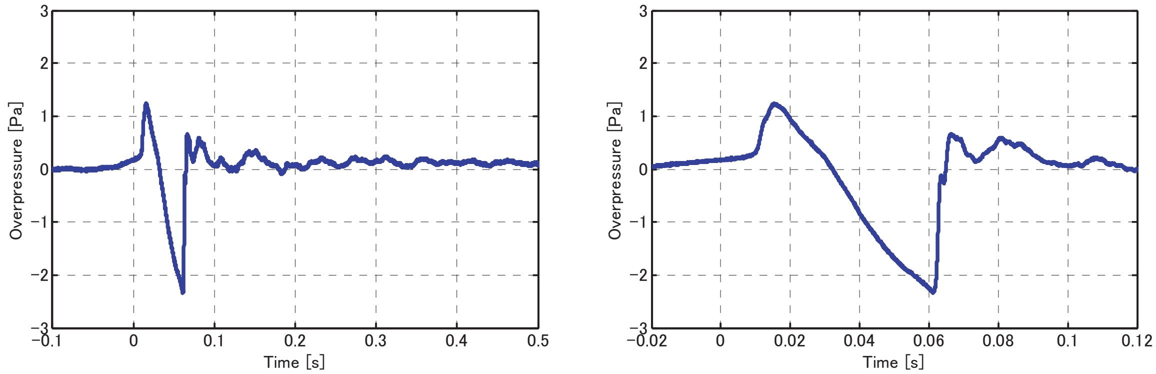

(b) High Altitude

Fig. 3-32 Sonic booms in second drop test (MP1, Ground Ch1, NWM)

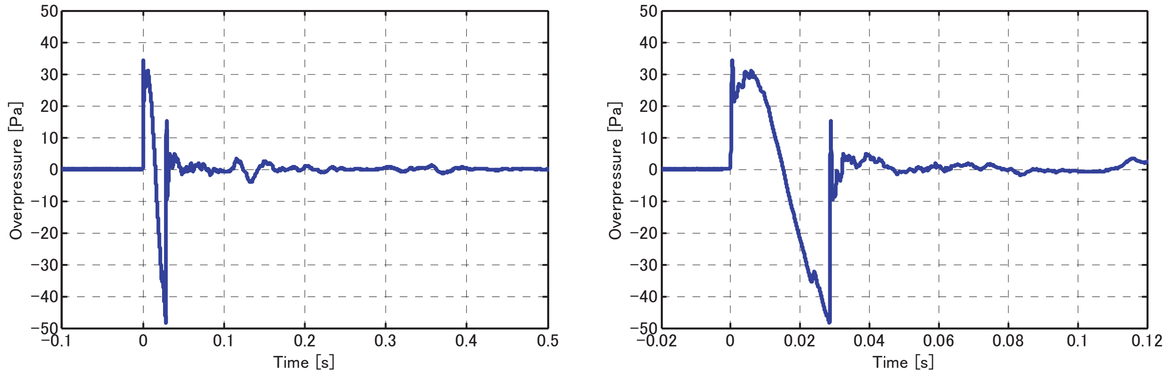

(a) Low Altitude

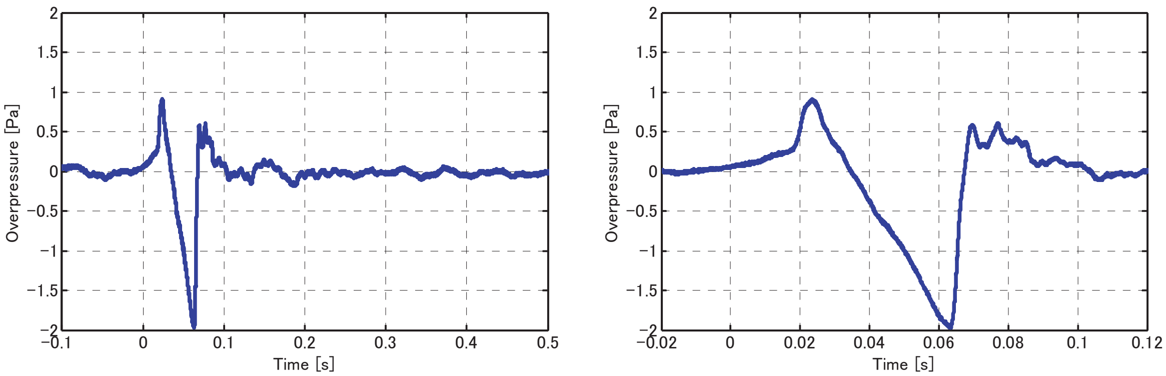

(b) High Altitude

Fig. 3-33 Sonic booms in second drop test (MP1, Ground Ch1, LBM)

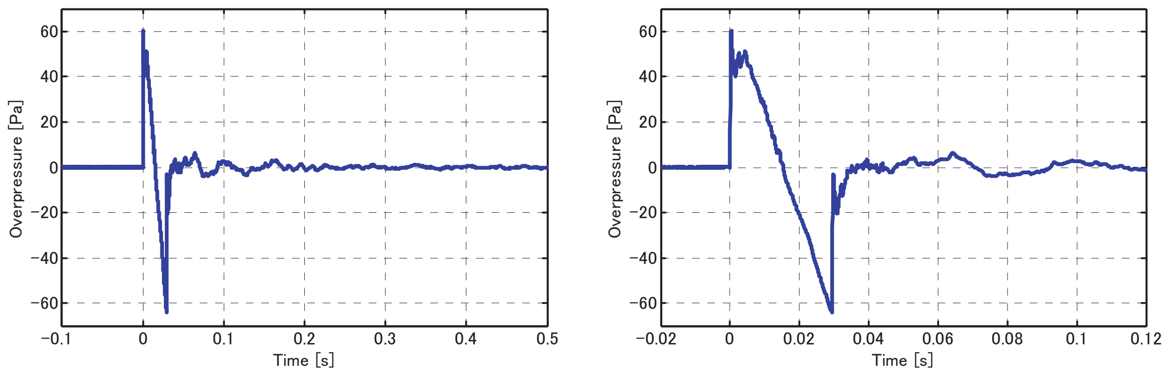

(a) Low Altitude

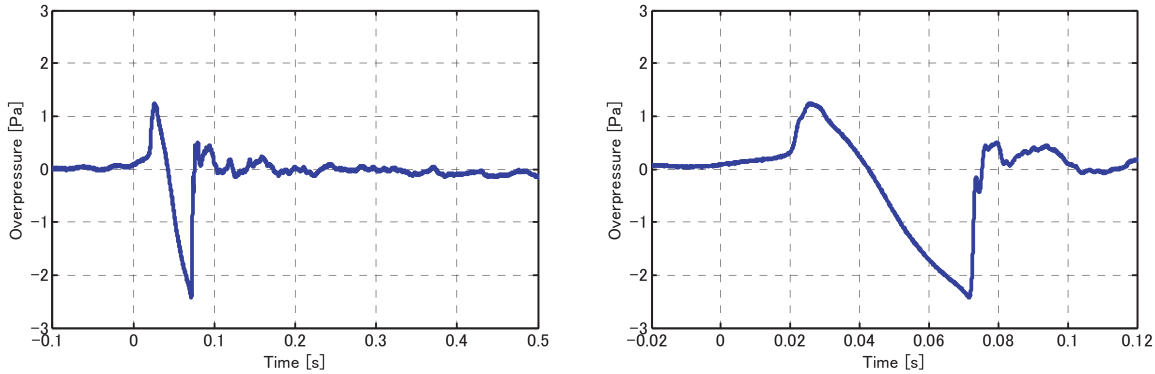

(b) High Altitude

Fig. 3-34 Sonic booms in second drop test (MP1, Ground Ch2, NWM)

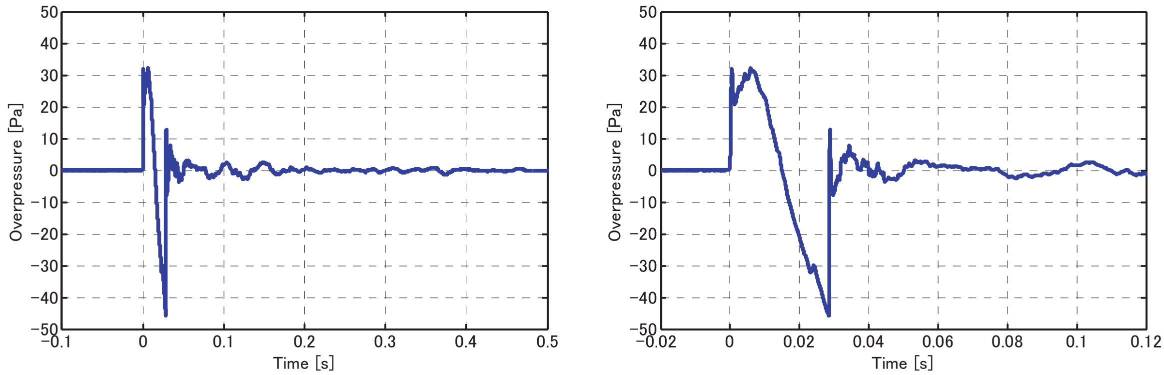

(a) Low Altitude

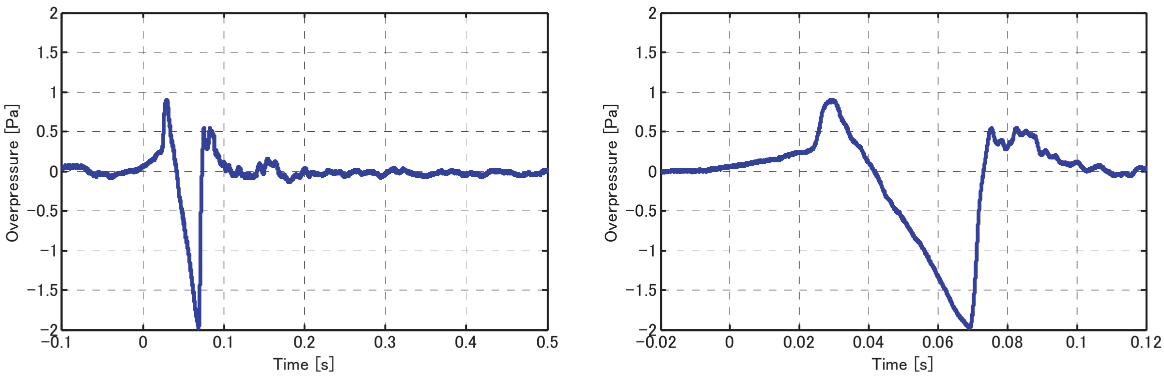

(b) High Altitude

Fig. 3-35 Sonic booms in second drop test (MP1, Ground Ch2, LBM)

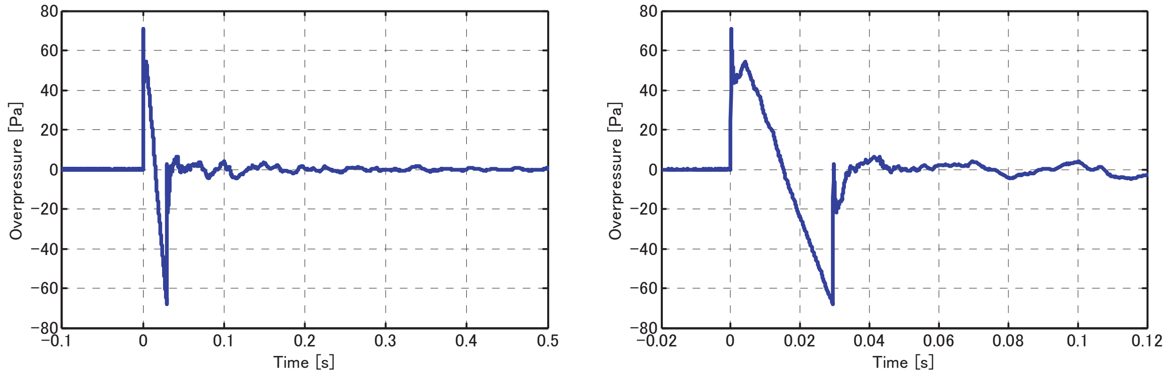

(a) Low Altitude

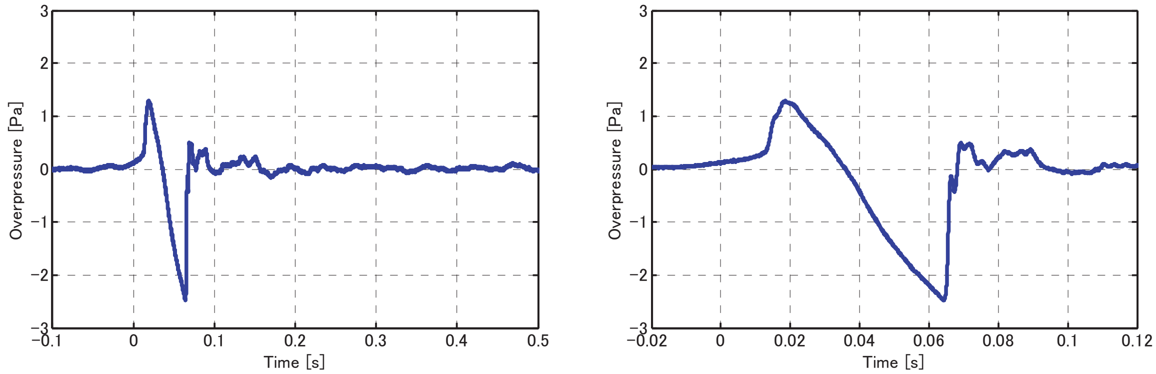

(b) High Altitude

Fig. 3-36 Sonic booms in second drop test (MP1, Ground Ch3, NWM)

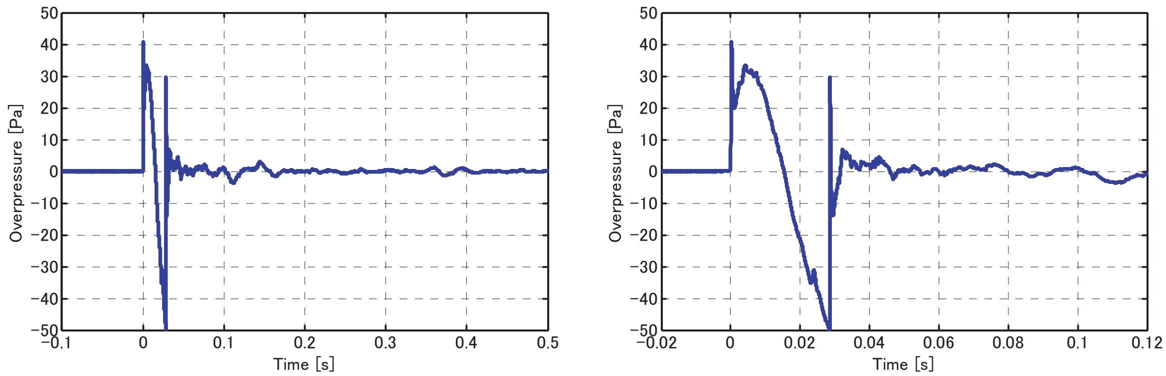

(a) Low Altitude

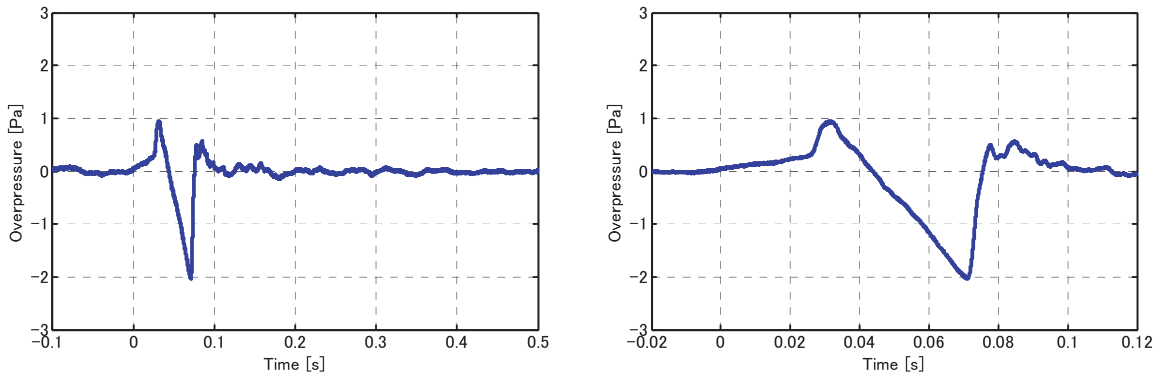

(b) High Altitude

Fig. 3-37 Sonic booms in second drop test (MP1, Ground Ch3, LBM)

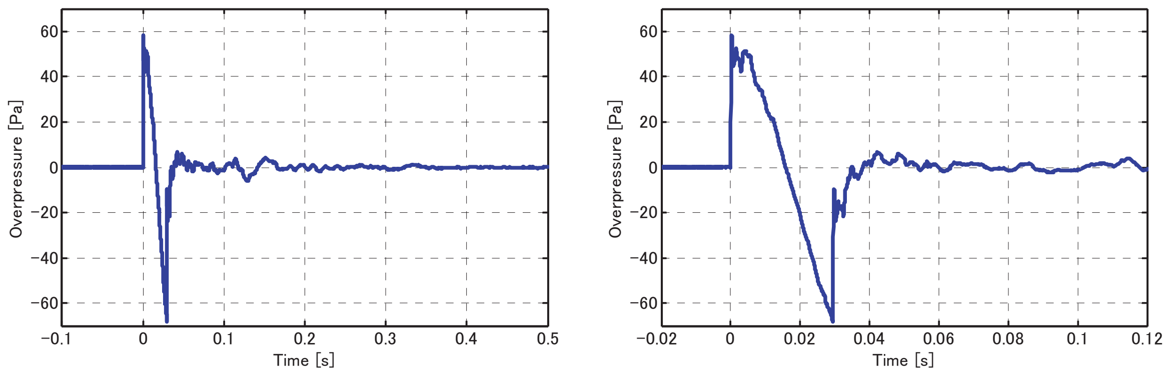

(a) Low Altitude

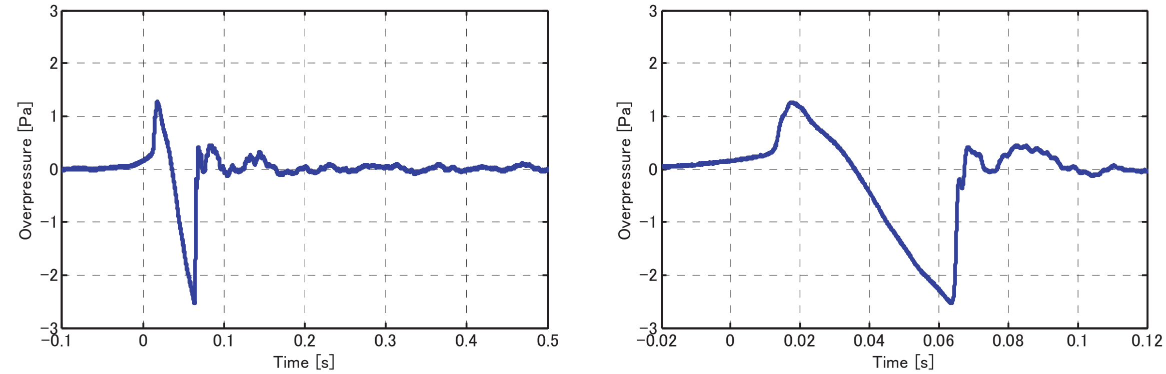

(b) High Altitude

Fig. 3-38 Sonic booms in second drop test (MP1, Ground Ch4, NWM)

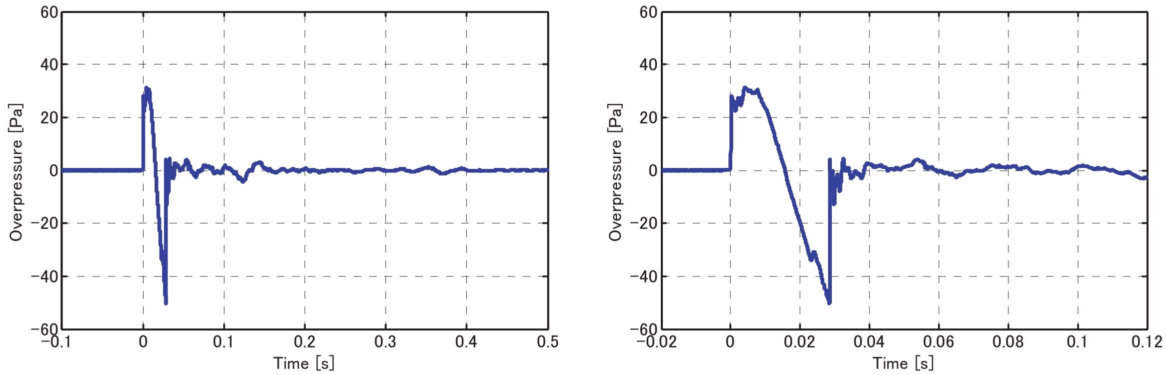

(a) Low Altitude

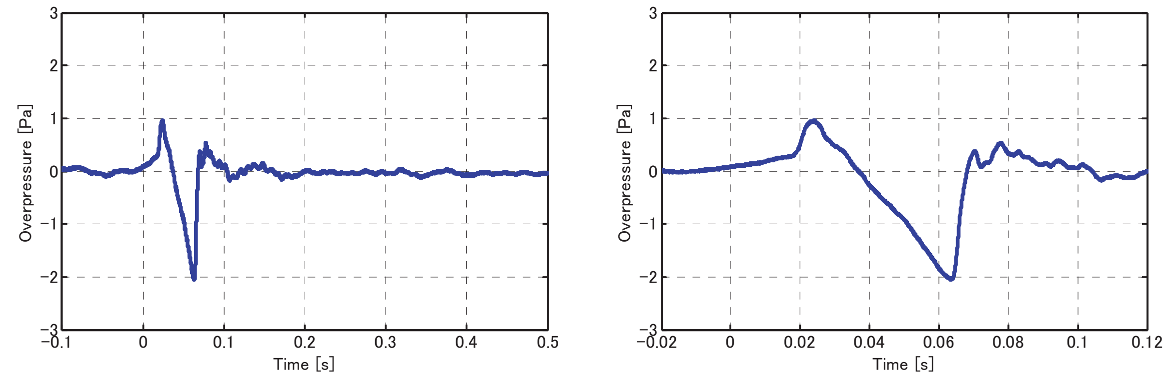

(b) High Altitude

Fig. 3-39 Sonic booms in second drop test (MP1, Ground Ch4, LBM)

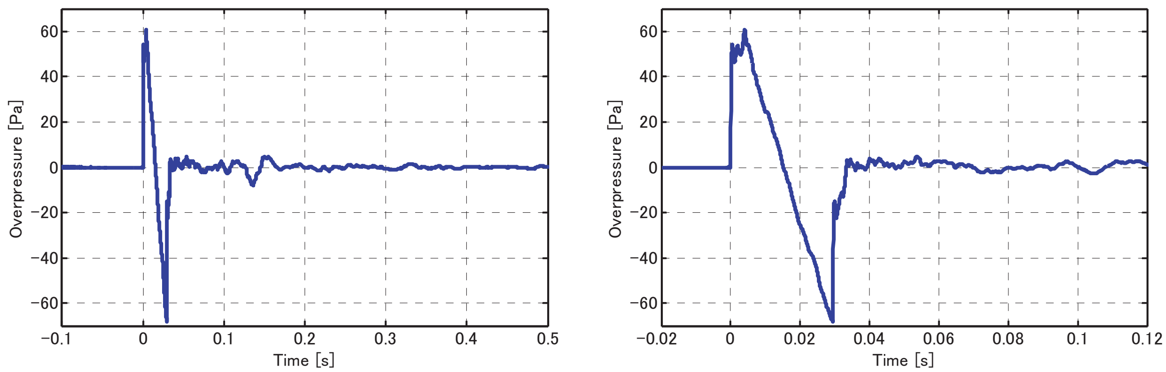

(a) Low Altitude

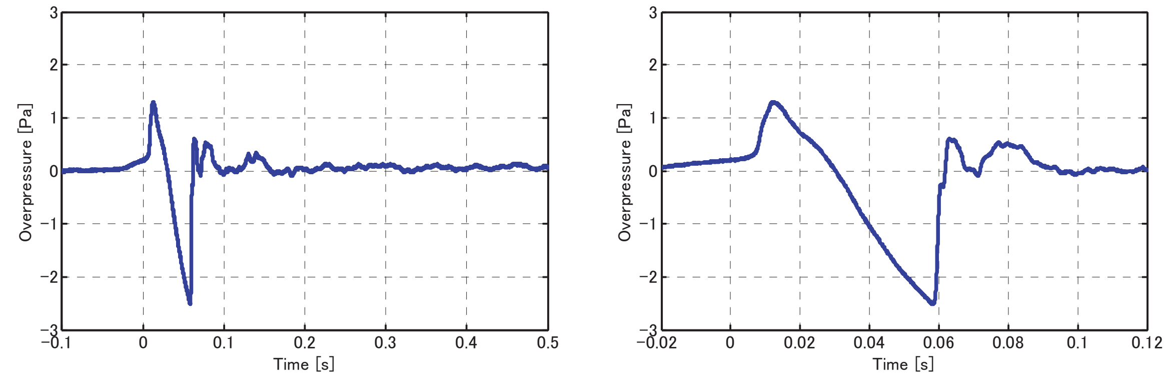

(b) High Altitude

Fig. 3-40 Sonic booms in second drop test (MP1, Ground Ch5, NWM)

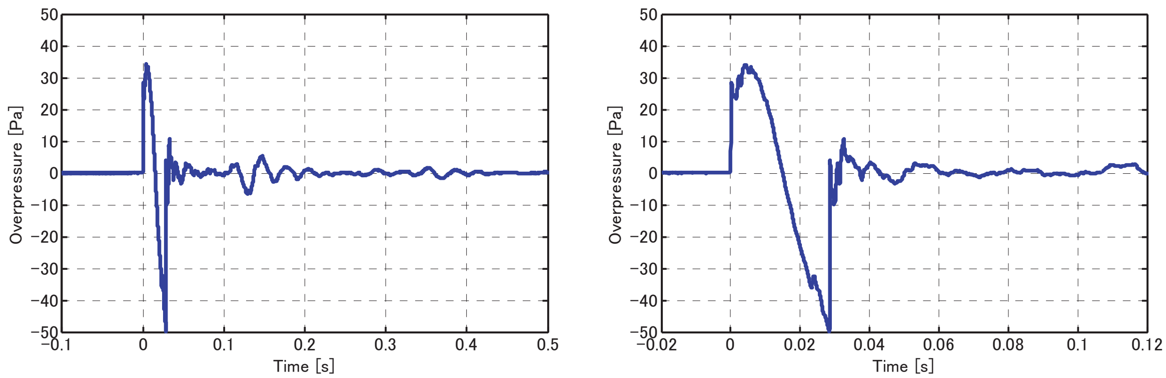

(a) Low Altitude

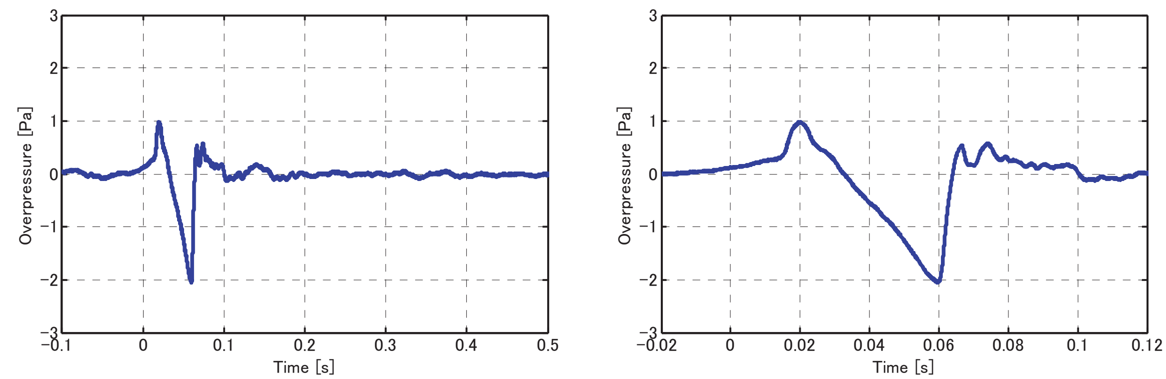

(b) High Altitude

Fig. 3-41 Sonic booms in second drop test (MP1, Ground Ch5, LBM)

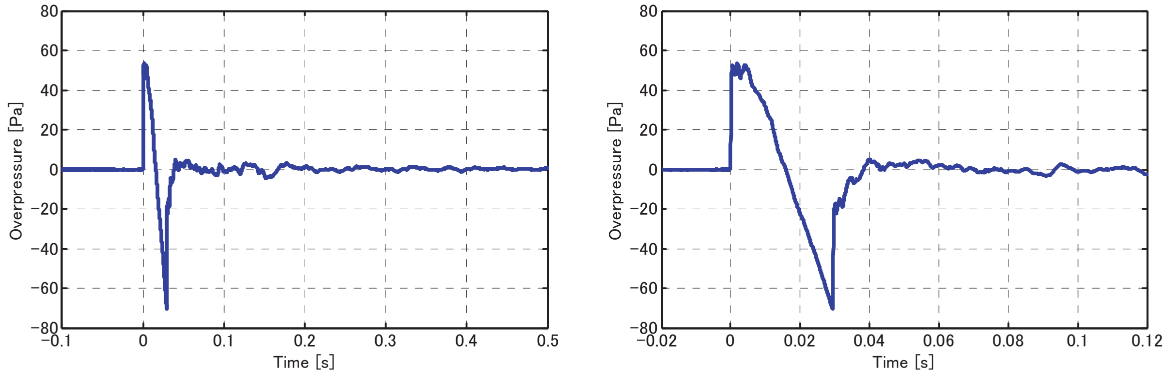

(a) Low Altitude

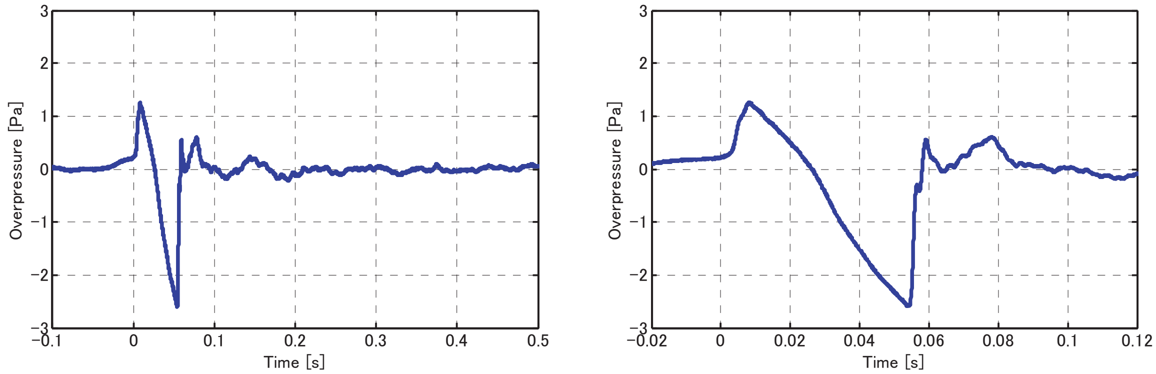

(b) High Altitude

Fig. 3-42 Sonic booms in second drop test (MP1, Ground Ch6, NWM)

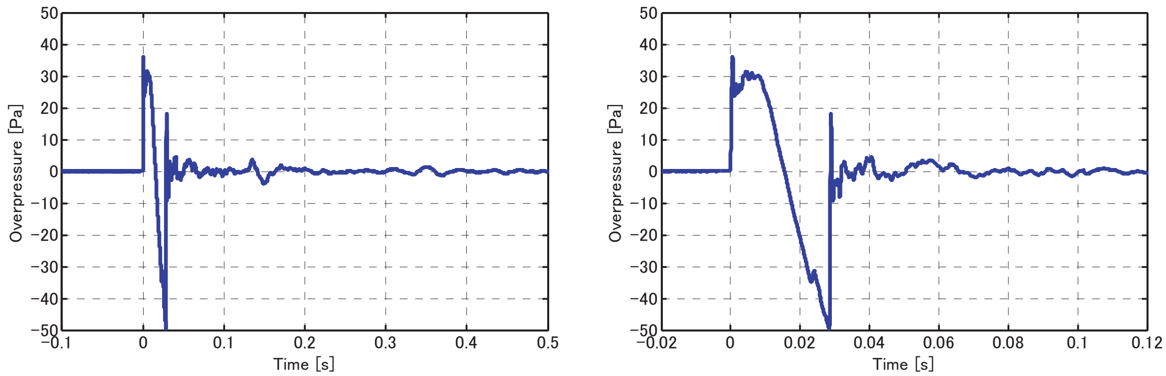

(a) Low Altitude

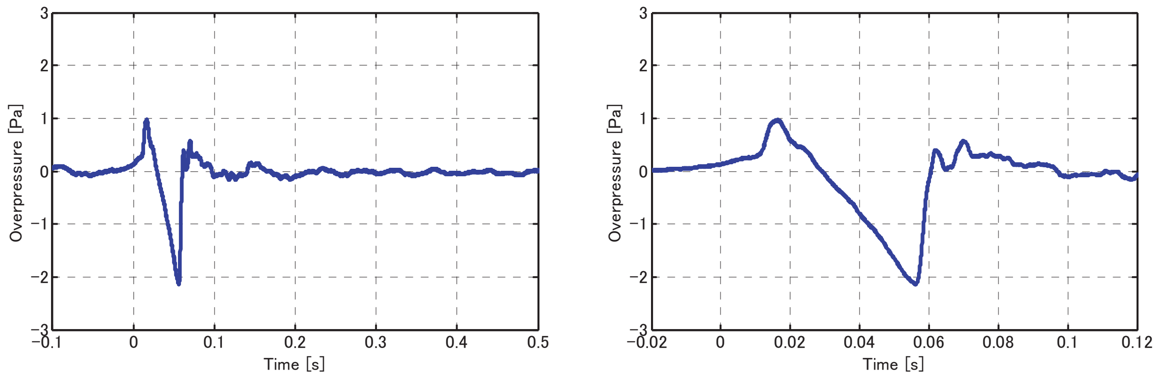

(b) High Altitude

Fig. 3-43 Sonic booms in second drop test (MP1, Ground Ch6, LBM)

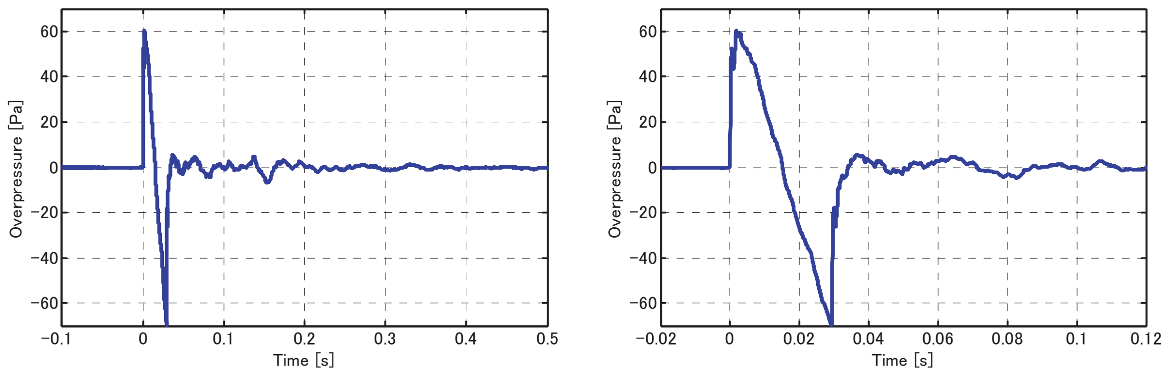

(a) Low Altitude

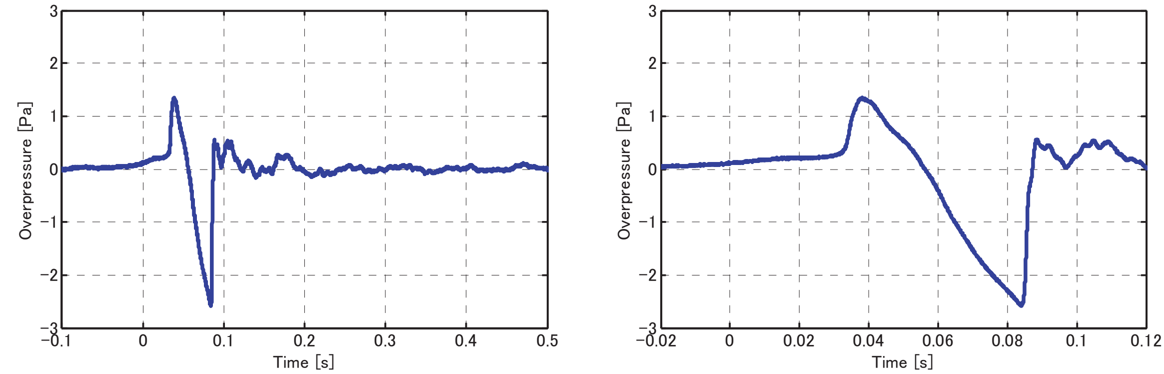

(b) High Altitude

Fig. 3-44 Sonic booms in second drop test (MP1, Ground Ch7, NWM)

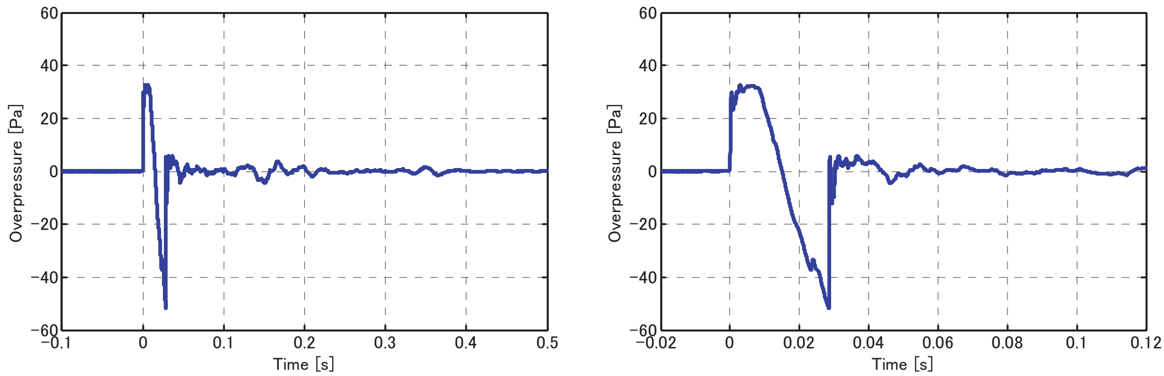

(a) Low Altitude

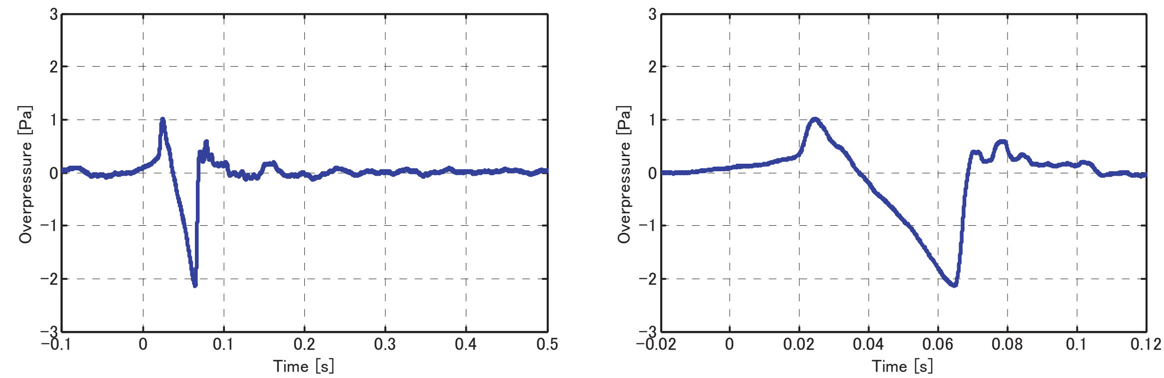

(b) High Altitude

Fig. 3-45 Sonic booms in second drop test (MP1, Ground Ch7, LBM)

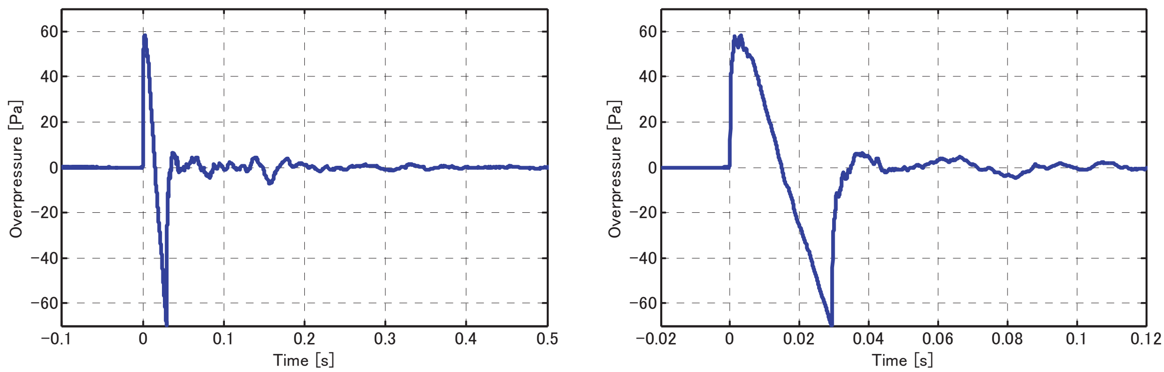

(a) Low Altitude

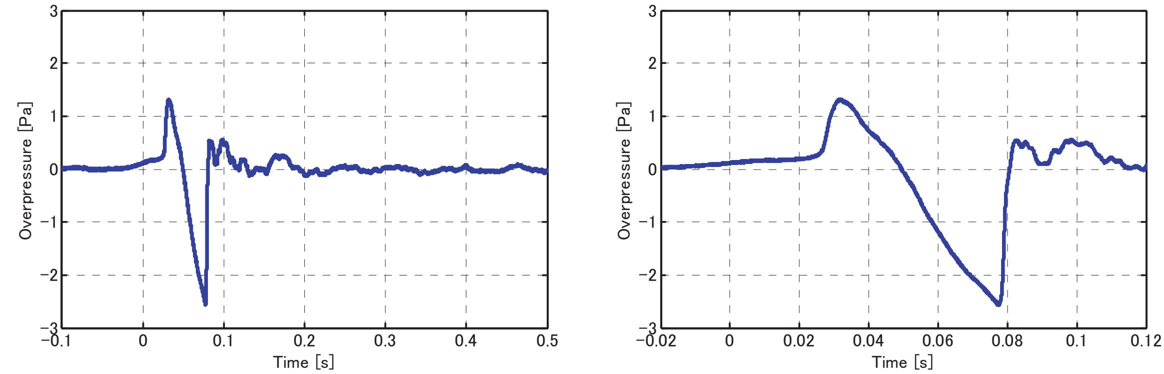

(b) High Altitude

Fig. 3-46 Sonic booms in second drop test (MP1, Ground Ch8, NWM)

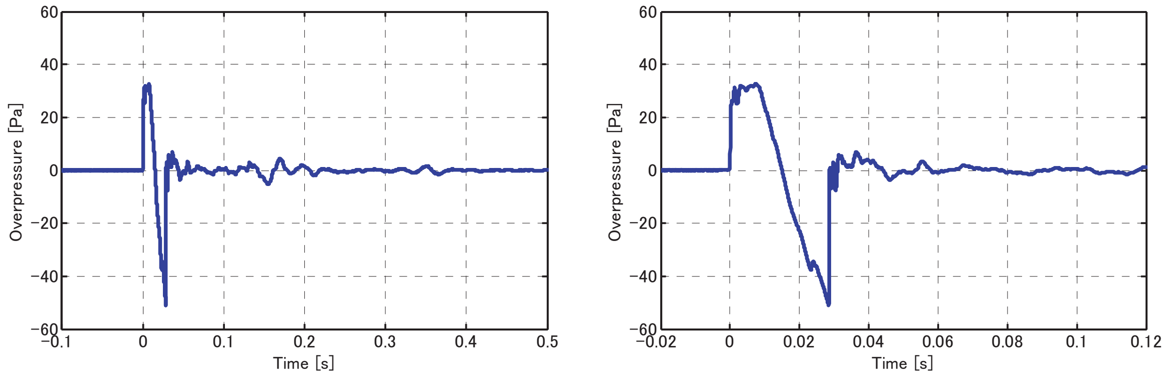

(a) Low Altitude

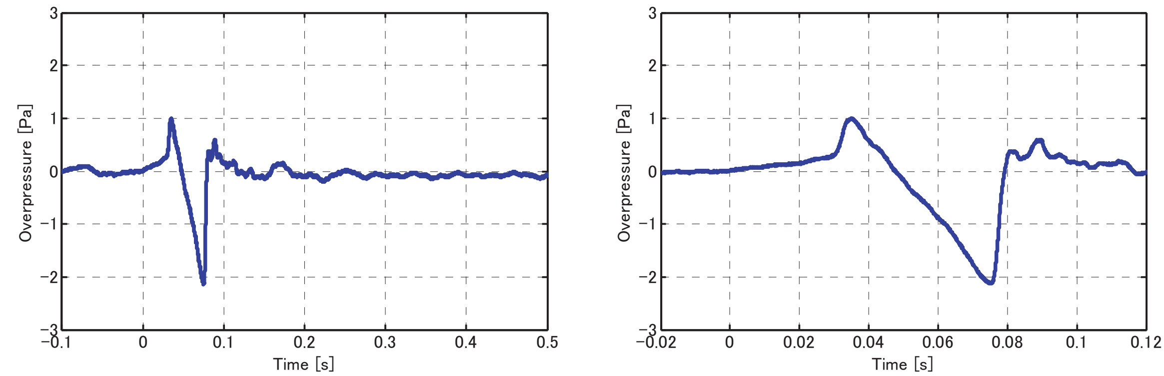

(b) High Altitude

Fig. 3-47 Sonic booms in second drop test (MP1, Ground Ch8, LBM)

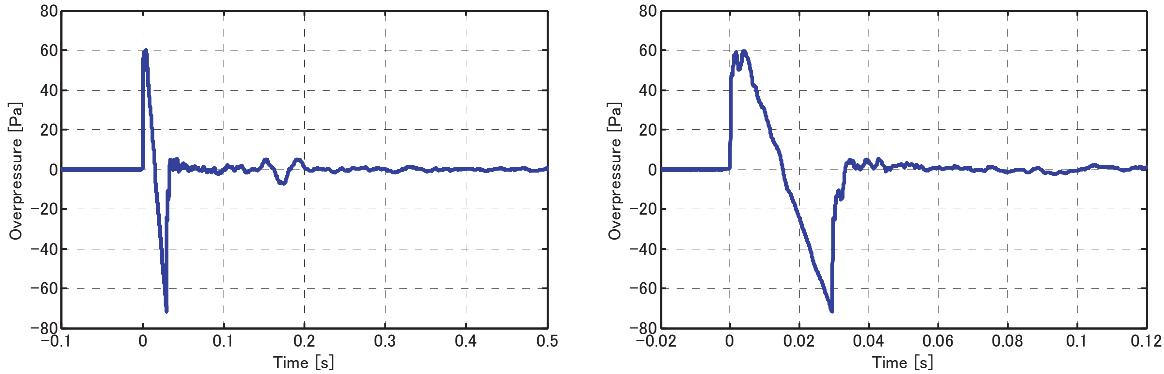

(a) Low Altitude

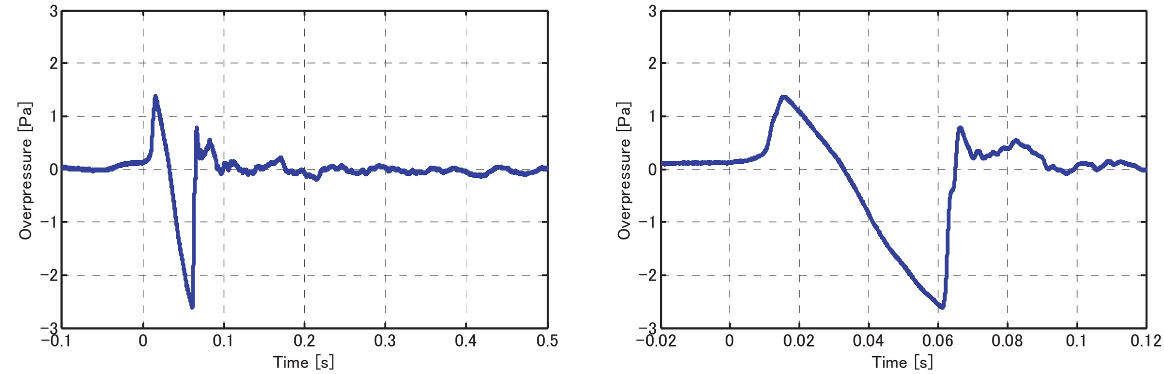

(b) High Altitude

Fig. 3-48 Sonic booms in second drop test (MP1, Ground Ch9, NWM)

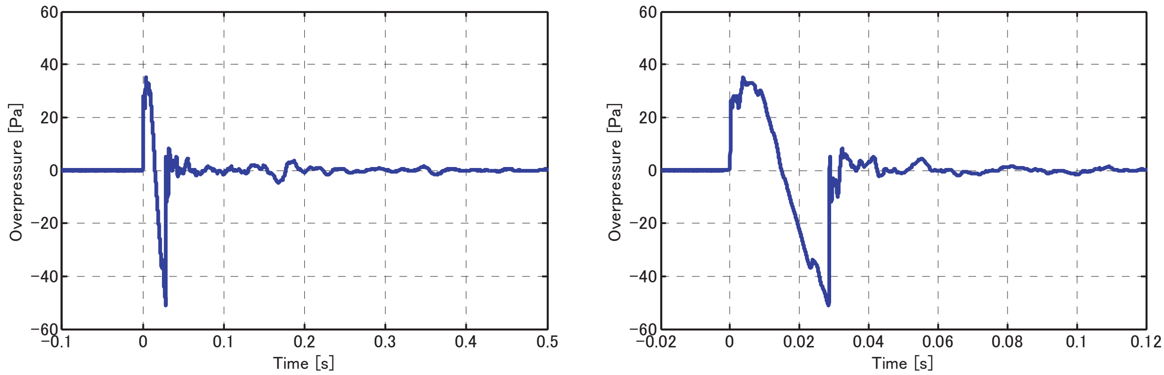

(a) Low Altitude

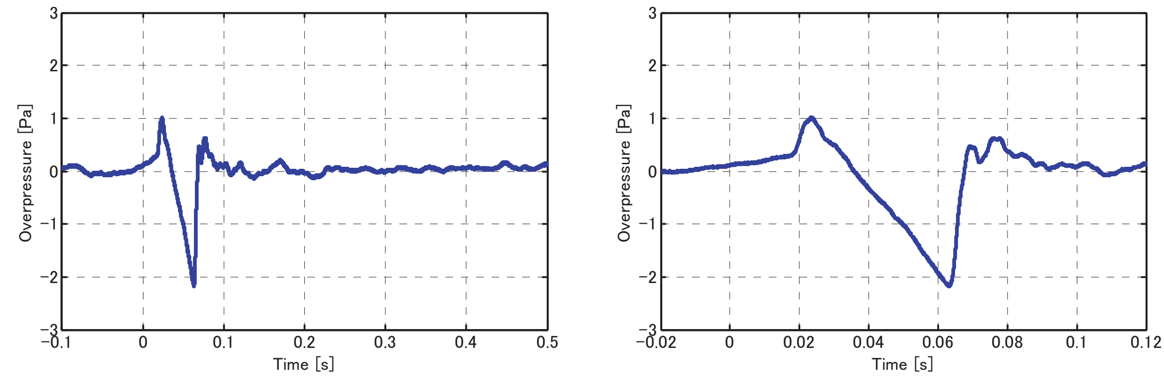

(b) High Altitude

Fig. 3-49 Sonic booms in second drop test (MP1, Ground Ch9, LBM)

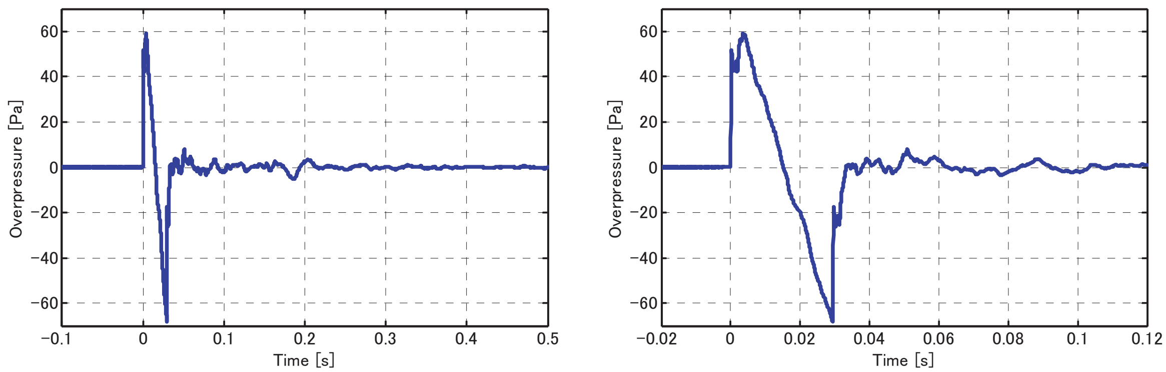

(a) Low Altitude

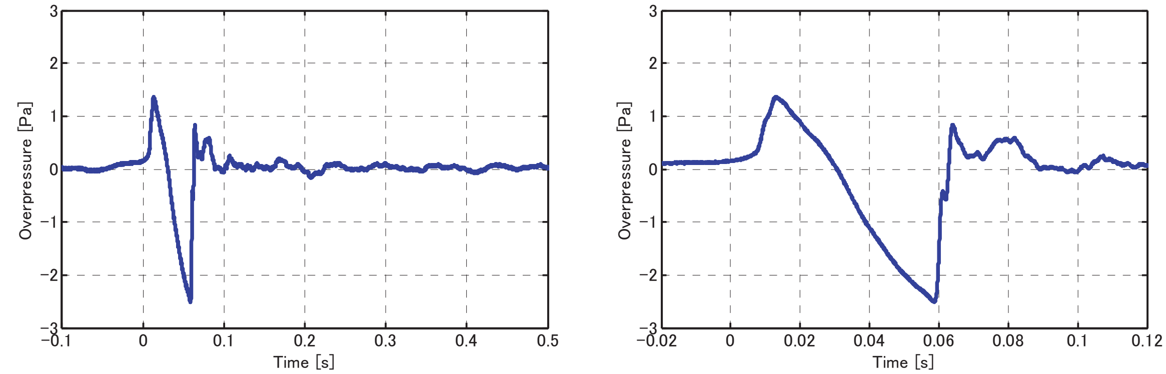

(b) High Altitude

Fig. 3-50 Sonic booms in second drop test (MP1, Ground Ch10, NWM)

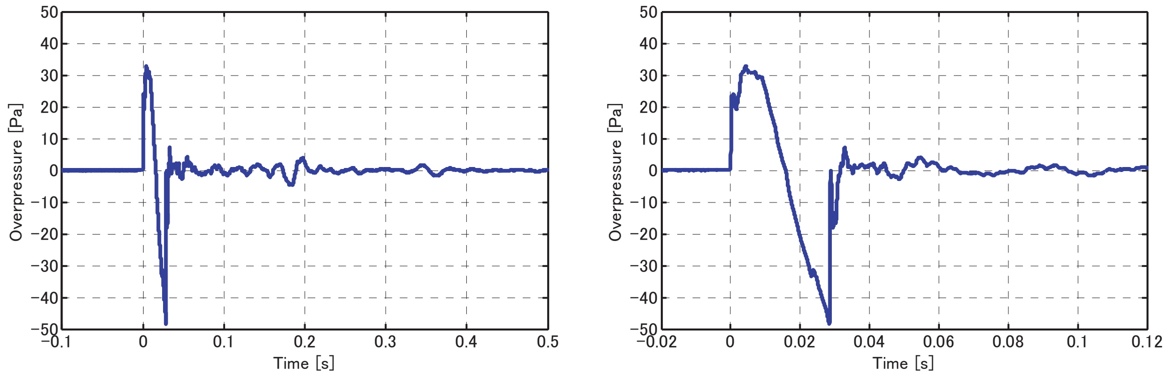

(a) Low Altitude

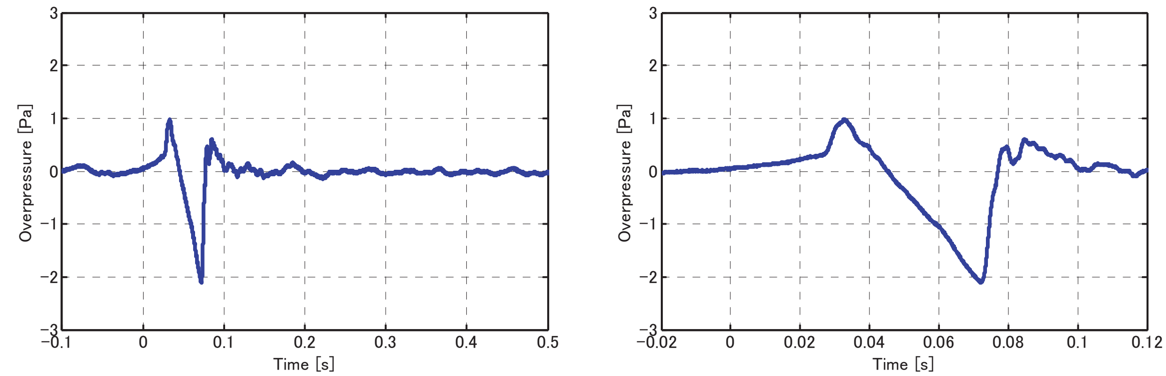

(b) High Altitude

Fig. 3-51 Sonic booms in second drop test (MP1, Ground Ch10, LBM)

3.2.3. Indoor Measurement

Indoor measurement was also made inside a 15 by 8 m house at MP1 as described in Sec 2.5, and data were successfully collected in the second test. Three microphones were located in a room as shown in Fig. 3-52. Ch 1 and Ch 3 were placed close to (about 0.01 m away from) window glasses indicated by blue panels in Fig. 3-52. Note that there were several more window sashes installed on the same walls, although they are not shown in Fig. 3-52. Roughly approximated direction of sonic boom propagation is also indicated in this figure by the green arrow.

Measured waveforms of sonic booms generated at the lower altitudes are shown in Fig. 3-53. Inside the house, shapes of the pressure waveforms look quite different from those outdoors. Indoor signatures are not N-shape or flat-top. Rather, they look like sinusoids decaying with time. Pressure fluctuation continues much longer indoors due to echoes and reverberation. Please notice that the range of the time axes in Fig. 3-53 are longer than the similar figures in this report (e.g., Fig. 3-31).

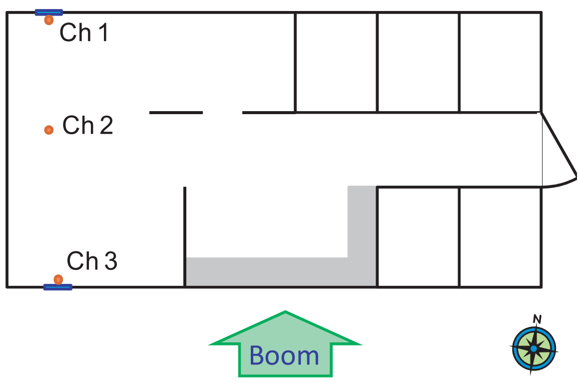

Fig. 3-52 Indoor microphone configuration

In the Ch 3 data, small and rapid (high-frequency) pressure fluctuation of window rattles is superposed on the sinusoidal waveforms. Although rattling noises are not clearly recognized in Ch 1 and Ch 2 by looking at the waveforms in Fig. 3-53, they are obviously noticed by listening to the recorded data.

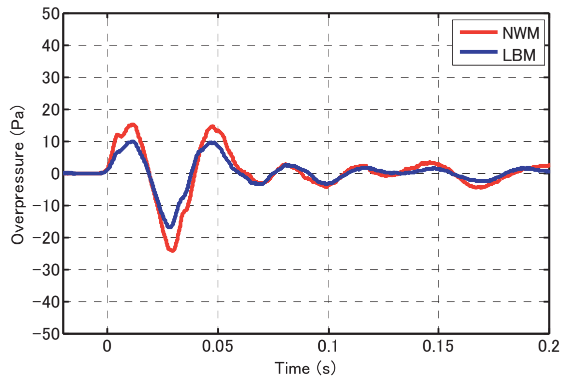

(a) Ch 1

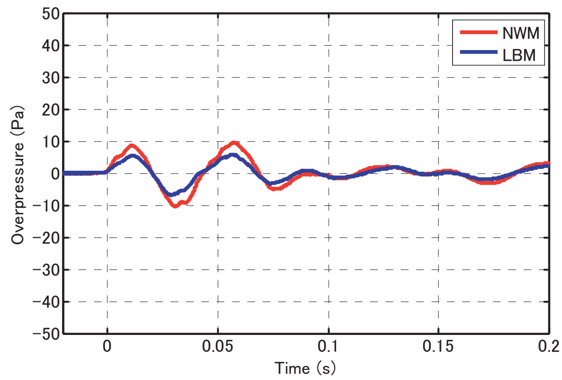

(b) Ch 2

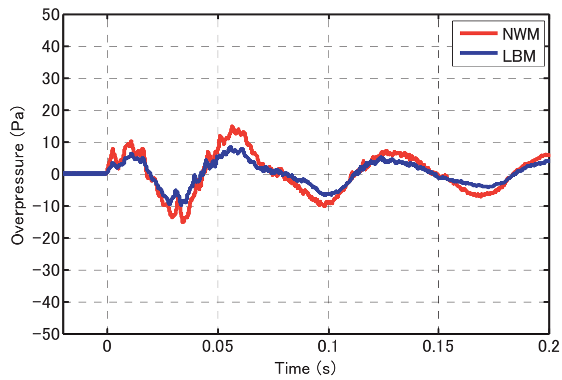

(c) Ch 3

Fig. 3-53 NWM and LBM indoor data in second drop test (MP1)

It is interesting that the overall shapes of the signatures from NWM and LBM considerably resemble each other, while those outdoors have clear discrepancy. However, magnitudes of the LBM signatures are still smaller than NWM. Also, by looking at Fig. 3-53 (c) and by listening to the recorded data, it is felt that rattling noise is not as loud for LBM. Although detailed investigation, such as calculating loudness and other psychoacoustic metrics and possibly conducting subjective evaluation tests, is necessary, the intuitive observation above would imply that positive effects are expected indoors as well from sonic boom shaping.

When comparing the data among different channels, non-uniform pressure distribution is found over the room. Although Ch 1 is located near the wall on the back side of the house with respect to the sonic boom propagation direction, the magnitude is the largest among the three channels. This is probably related to the acoustic modes in the room, and also to the diffraction around the house. While it cannot be said that the pressure magnitude is always higher in the back side of the house, it could be concluded that the magnitude of the pressure depends on the position in a room.

All the indoor waveforms are shown in Fig. 3-54 through Fig. 3-59.

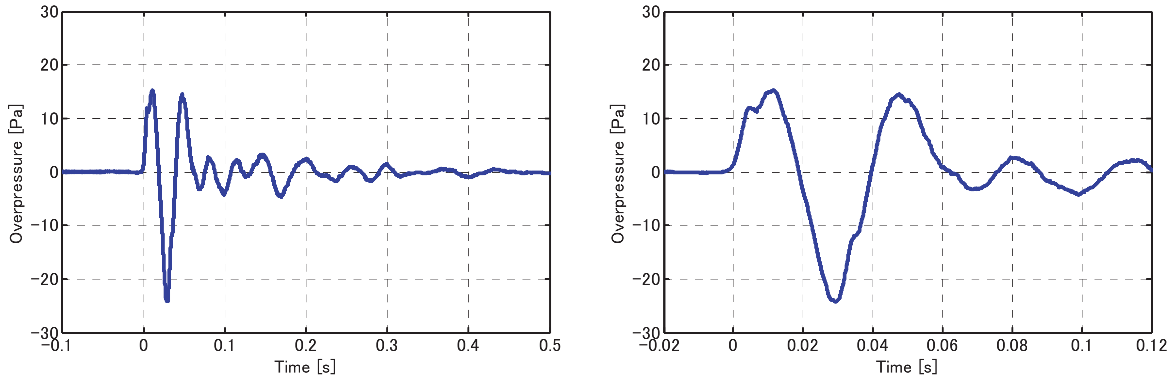

(a) Low Altitude

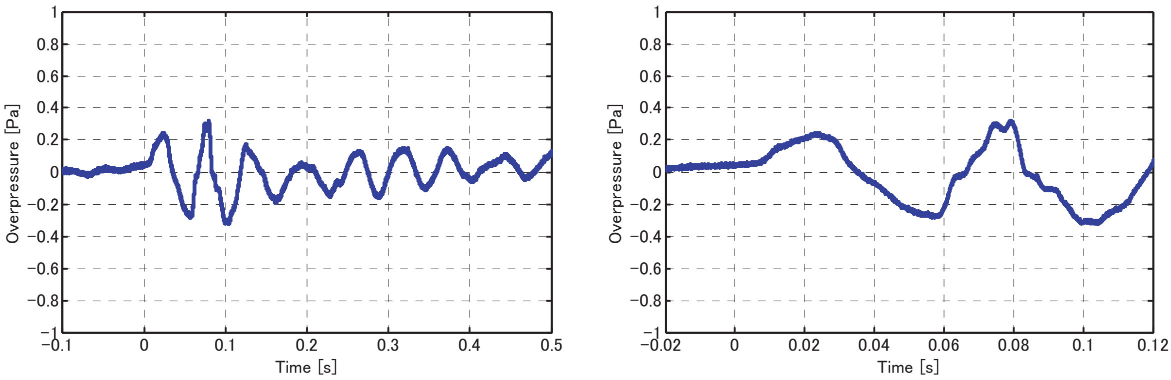

(b) High Altitude

Fig. 3-54 Sonic booms in second drop test (MP1, Indoor Ch1, NWM)

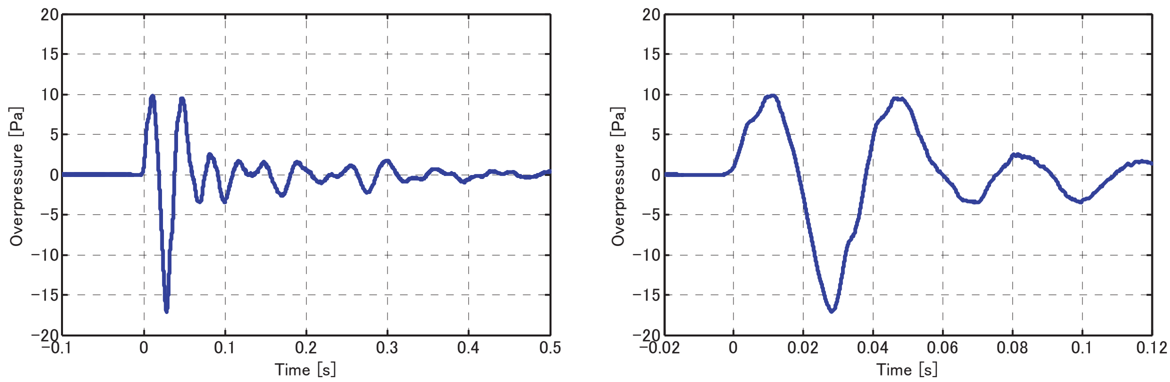

(a) Low Altitude

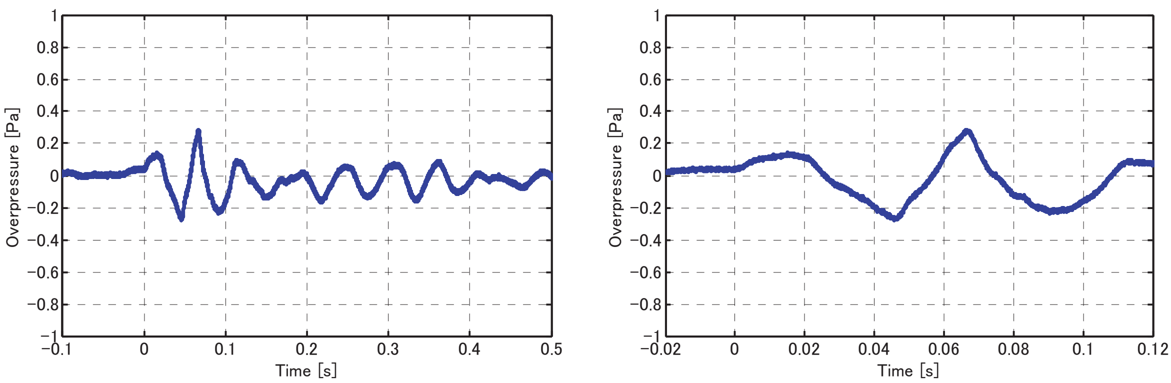

(b) High Altitude

Fig. 3-55 Sonic booms in second drop test (MP1, Indoor Ch1, LBM)

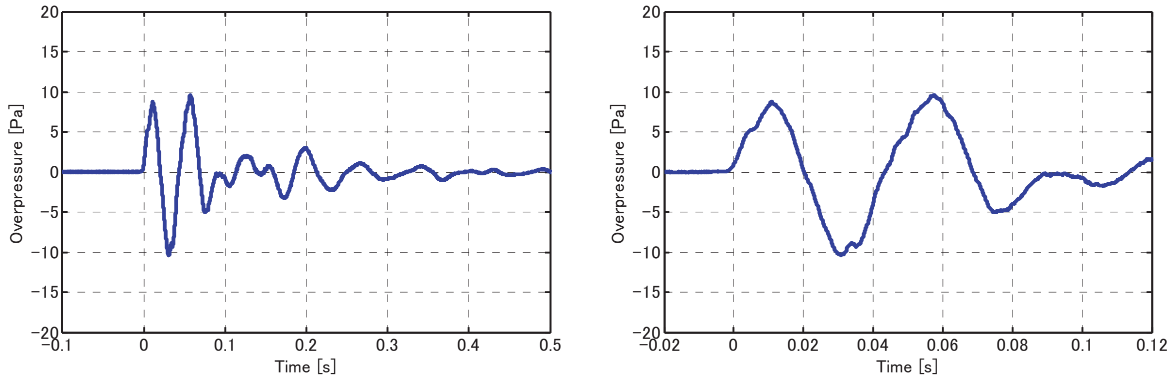

(a) Low Altitude

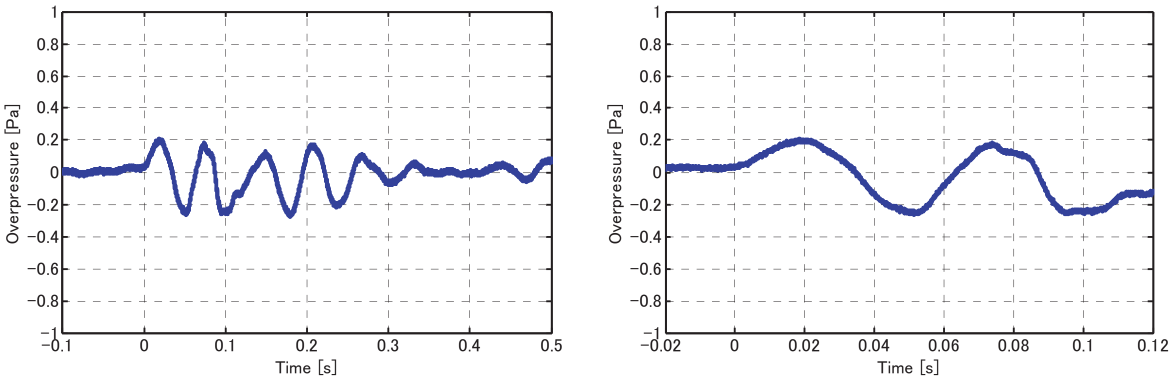

(b) High Altitude

Fig. 3-56 Sonic booms in second drop test (MP1, Indoor Ch2, NWM)

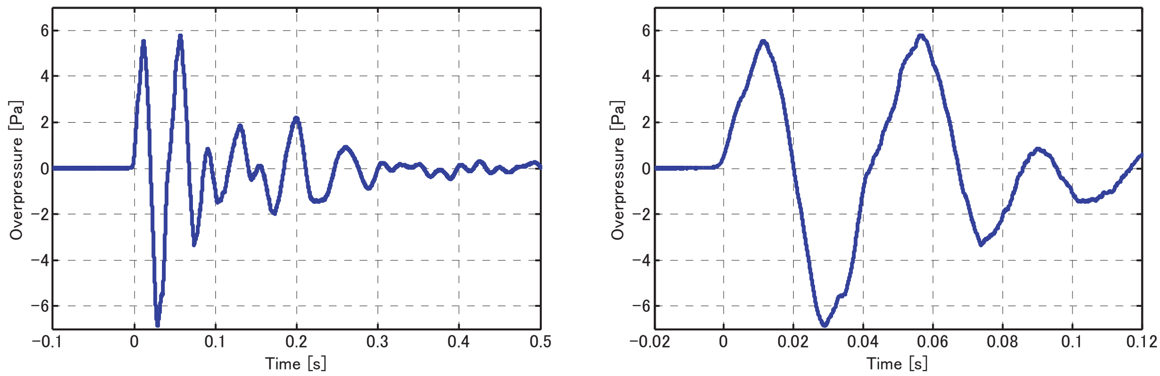

(a) Low Altitude

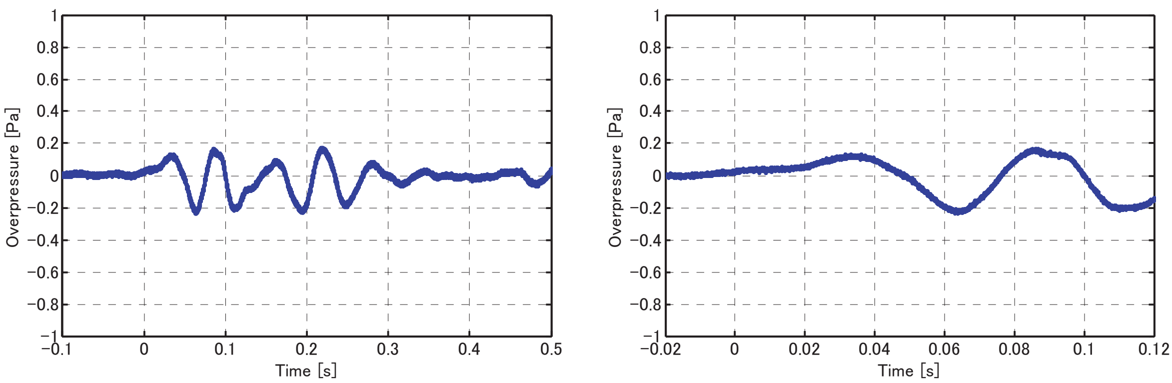

(b) High Altitude

Fig. 3-57 Sonic booms in second drop test (MP1, Indoor Ch2, LBM)

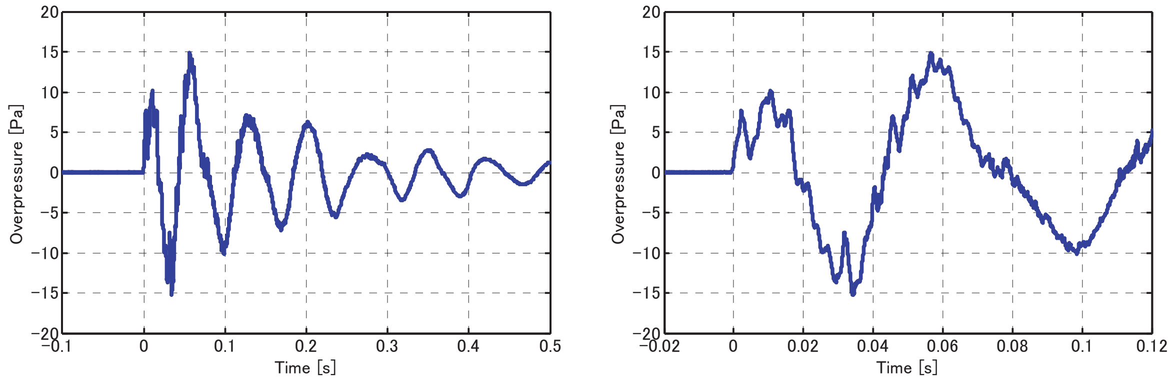

(a) Low Altitude

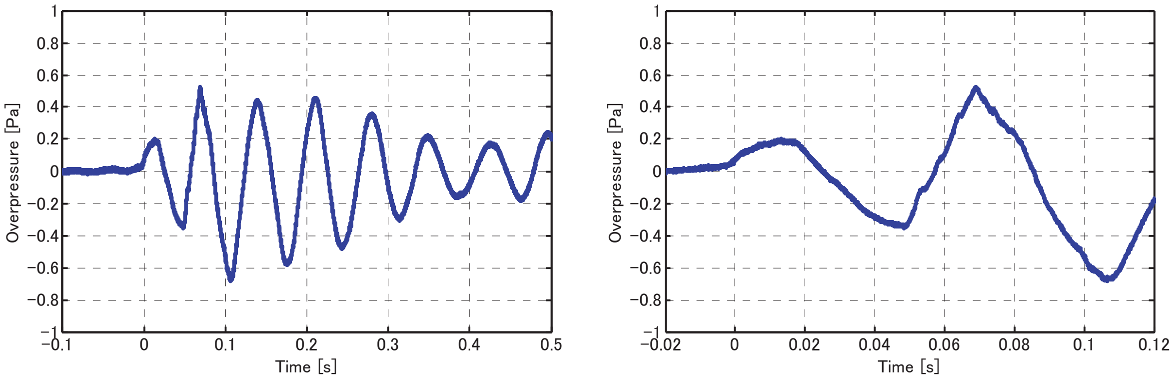

(b) High Altitude

Fig. 3-58 Sonic booms in second drop test (MP1, Indoor Ch3, NWM)

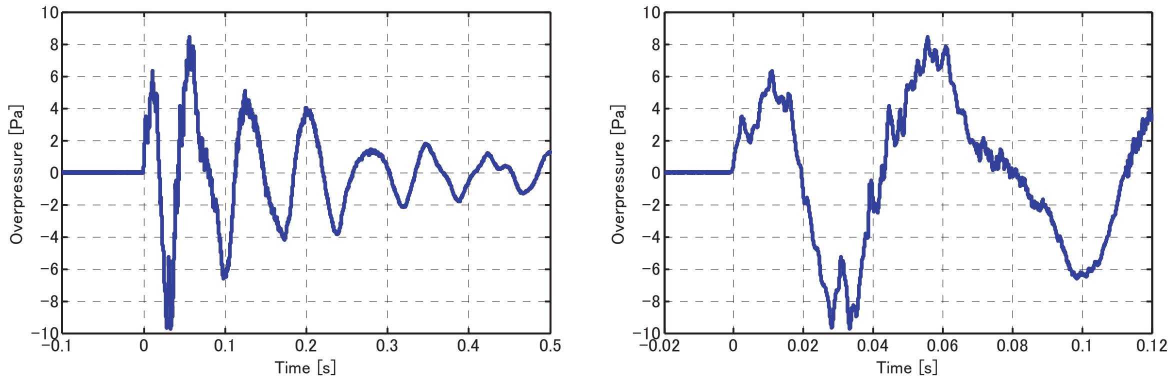

(a) Low Altitude

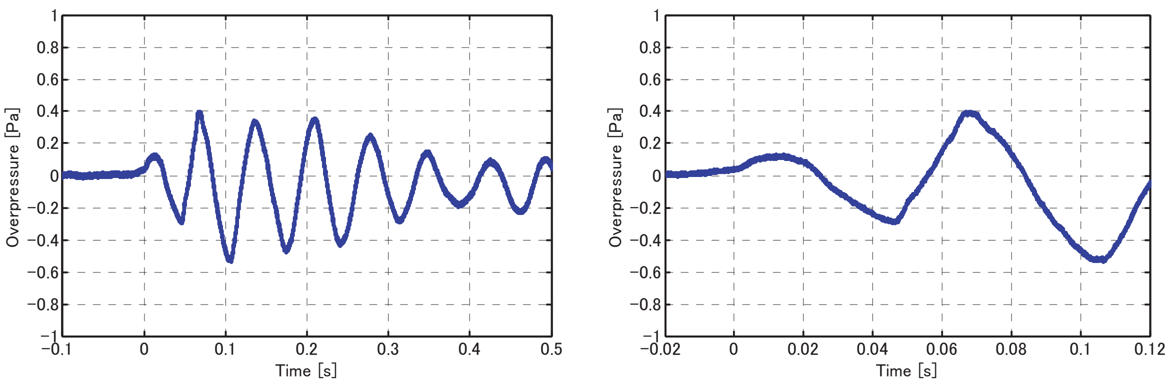

(b) High Altitude

Fig. 3-59 Sonic booms in second drop test (MP1, Indoor Ch3, LBM)

3.3. Second Drop Test (Esrange)

As stated in Sec 2.6.2, two microphones were setup on the balloon launch pad of Esrange Space Center. These microphones were laid directly on the gravelly ground surface (not on boards).

3.3.1. Ground Measurement

At Esrange, each microphone captured only one signature for each drop body. All the four signatures are shown in Fig. 3-60 through Fig. 3-64. In Fig. 3-60, great difference in magnitude is found between NWM and LBM waveforms. The maximum value is about six times larger in NWM than LBM. This difference could be explained by considering sonic boom focusing. Preceding sonic boom propagation analysis conducted right before the second drop test suggested that two sonic booms generated at different altitudes could arrive at Esrange almost at the same time, resulting in focusing. Judging from the high level of magnitude and shapes of the waves, it is considered that focusing occurred at the microphone position for NWM. For LBM, no clear evidence of focusing is found. However, in the left panels of Fig. 3-62 and Fig. 3-64, it seems two sonic boom waveforms arrived at the microphone in quick succession. This implies that it was close to focusing. One possible reason why focusing occurred only for NWM is the one minute difference in time of release from the balloon. This lead to a change in separation position, resulting in diverse paths and lengths of propagation.

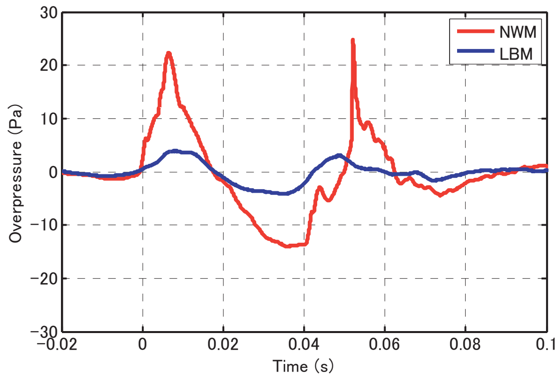

(a) Ch 1

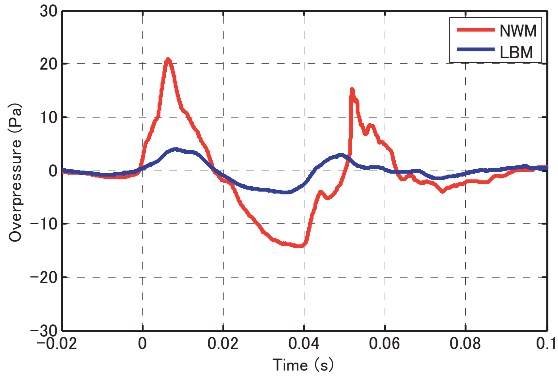

(b) Ch 2

Fig. 3-60 NWM and LBM ground data in second drop test (Esrange)

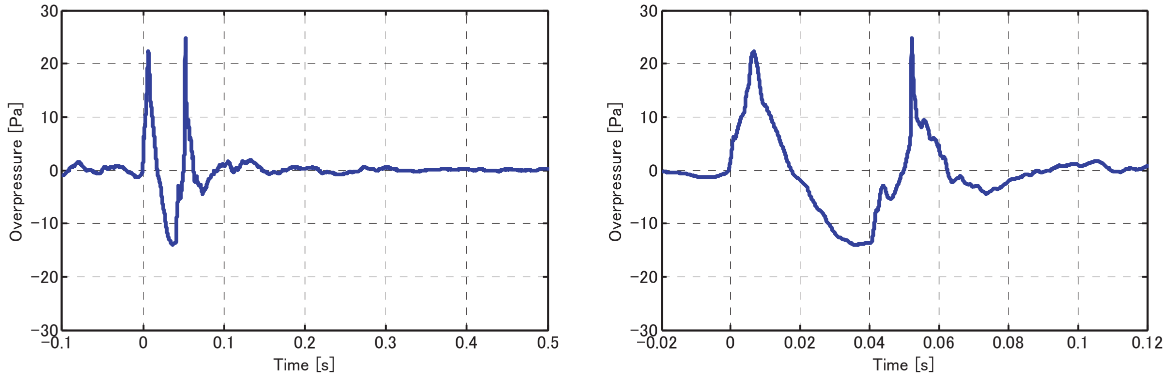

Fig. 3-61 Sonic booms in second drop test (Esrange, Ground Ch1, NWM)

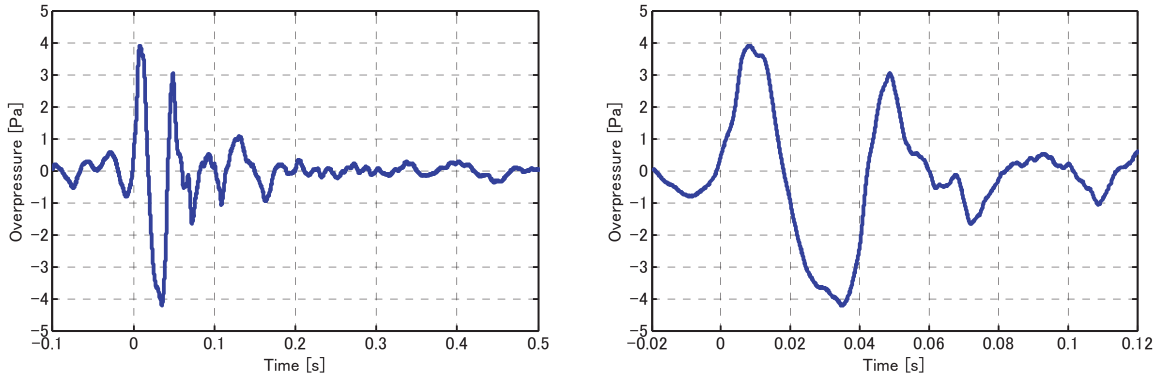

Fig. 3-62 Sonic booms in second drop test (Esrange, Ground Ch1, LBM)

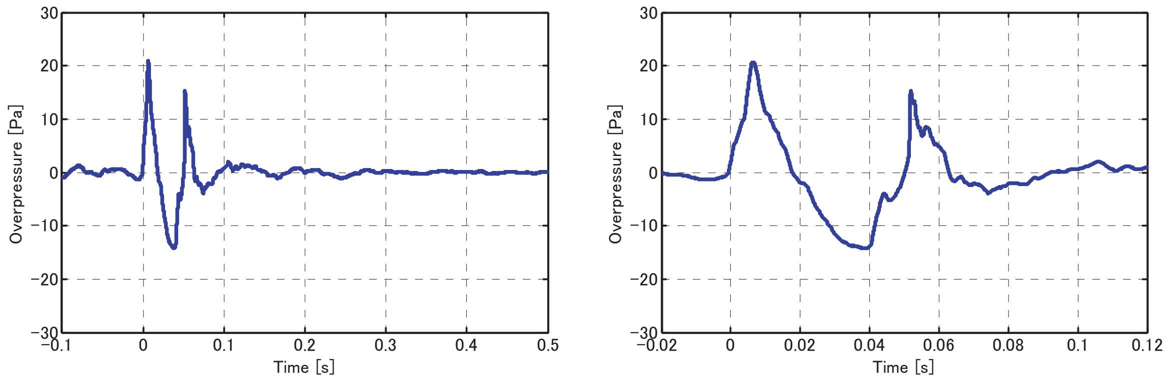

Fig. 3-63 Sonic booms in second drop test (Esrange, Ground Ch2, NWM)

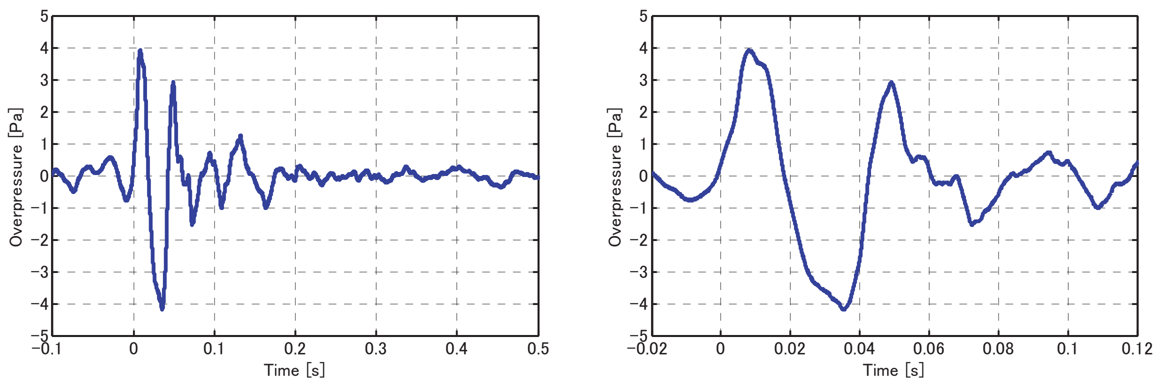

Fig. 3-64 Sonic booms in second drop test (Esrange, Ground Ch2, LBM)

4. SUMMARY

In D-SEND#1, sonic booms from two types of drop bodies were successfully measured above the ground up to 1 km, on the ground surface, and inside a house. Recorded sonic boom signatures of the two types of bodies are in good agreement with the designed ones and show significant differences from each other in both the maximum overpressure and wave shapes. This demonstrated the possibility of validating low-boom aircraft design concept and techniques by using a scaled model, as planned in D-SEND#2.

REFERENCES

1) M. Honda, "Flight results of D-SEND#1 drop test using stratospheric balloon," *Proc. 8th International Conference on Flow Dynamics*, Sendai, Japan, 2011.
2) I.E. Garrick and D.J. Maglieri, "Variability of sonic boom pressure signatures associated with atmospheric conditions," NASA TM-X-73023, 1967.
3) Y. Naka, Y. Makino, and S. Shindo, "Flight test for airborne blimp boom acquisition (ABBA) system check (ABBA Test #1)," JAXA RM-10-012, 2010. (in Japanese)
4) B.M. Sullivan, P. Davies, K.K. Hodgdon, J.A. Salamone III, and A. Pilon, "Realism assessment of sonic boom simulators," *Noise Control Eng. J.* 56 (2), pp. 141-157, 2008.